Maritime transportation of LOHCs

A greenhouse gas footprint and economic assessment of importing renewable H_2 from Portugal to the Netherlands, using liquid organic hydrogen carriers

By João Godinho

TÉCNICO LISBOA

Universiteit Utrecht

CERENA Centro de Recursos Naturais e Ambiente

Universiteit Utrecht

Master thesis submitted to the Faculty of Geosciences of Utrecht University in partial fulfilment of the requirements for the degree of

Master of Science
in **Energy Science**

A greenhouse gas footprint and economic assessment of importing renewable H_2 from Portugal to the Netherlands, using liquid organic hydrogen carriers

By João Godinho

Student Number: 6247083
Course Code: GEO4-2523
Supervisors:
Ph.D. José Granjo, CERENA-IST, Lisbon
Ph.D. Ric Hoefnagels, UU, Utrecht
Second Reader: Ph.D. Agneev Mukherjee, UU, Utrecht

November 2021

Abstract

This research was conducted to quantify the economic and GHG impact of importing green H_2 from Sines, Portugal, to Rotterdam, in the Netherlands. The H_2 to be transported was stored within two-way LOHCs – specifically, the toluene-methylcyclohexane (TOL-MCH) and the dibenzyltoluene-perhydro-dibenzyltoluene (DBT-PDBT) systems – and the transportation was assumed to be handled by chemical/oil tankers. H_2 has been highly regarded as one of the most important energy carriers of the coming decades (Detz et al., 2019; European Commission, 2018, 2020a), and is projected to have a substantial contribution towards mitigating the inherent intermittence in energy production via RES. This is a crucial step to achieve decarbonization goals of several industries, such as the feedstock industry, process heating, build environment, transportation, etc. (Port of Rotterdam, 2020). This research was further motivated by the bilateral agreement between the Portuguese and Dutch governments to establish a supply chain of green H_2 (2020). Moreover, this research complements the study conducted by Carvalho (2021), which optimized the hydrogenation and dehydrogenation processes of the mentioned LOHC systems, for an annual delivery of 50 kt of H_2. The necessary data to compute the results was gathered through literature review and interviews with experts from the respective fields. Overall, the results were assessed based on the impact of completing one roundtrip between Sines and Rotterdam, for the years 2030, 2040 and 2050. Following, these values were extrapolated to match the yearly requirements. The findings from this study concluded that transporting DBT-PDBT, while using small tankers – with a capacity of 27,300 DWT – is the most financially viable option. Accordingly, the results attested that transporting H_2 stored in DBT from Sines to Rotterdam, would increment the supply chain in 0.30 €/kg-H_2 in 2030, increasing to 0.34 €/kg-H_2 in 2040, and finally to 0.38 €/kg-H_2 in 2050. When added to the costs concerning the production of H_2 and the LOHC conversion processes, a total supply chain cost of 4.28 €/kg-H_2 can be expected, for 2030. For 2040, this value is slightly lower, at 4.16 €/kg-H_2, and for 2050, it is projected to reach roughly 3.17 €/kg-H_2. The respective GHG impact was projected to be 2.471 kg-CO_2/GJ-H_2 (LHV) in 2030 decreasing to 1.309 kg-CO_2/GJ-H_2 (LHV) in 2040, and 0.461 kg-CO_2/GJ-H_2 (LHV) in 2050. Comparing with conventional steam methane reforming, the projected LOHC supply chain allows for savings of 96.0% in 2030, increasing to 99.0% in 2050.

Keywords: LOHC, toluene, dibenzyltoluene, supply chain, green H_2.

Acknowledgements

This thesis encompasses my work during the final nine months of my MSc degree in Energy Science. I consider it to be the epitome of my experience at the University of Utrecht, and the most satisfying piece to finish another important academic step. Firstly, I would like to extend my appreciation to my supervisor from UU, Ph.D. Ric Hoefnagels, and my host supervisor, from CERENA-IST, Ph.D. José Granjo. Throughout these nine months, both have provided me with all the support and guidance to successfully conduct this research. I am very thankful for their round-the-clock availability and insightfulness. Furthermore, it was extremely rewarding to be able to establish a good and, I dare to say, fun working relationship, regardless of the remote conditions that were externally imposed, due to COVID-19. I would also like to share my gratitude with every contact that helped contributing to complement my research, specifically Ph.D. Agneev Mukherjee, from UU, Professors Henrique Matos and Rui Castro, from IST, Coen Ponsioen from Vopak and Didier de Beaumont from the Port of Amsterdam. On a personal level, my deepest appreciation goes to my loving family, who unconditionally have and will always support me beyond what anyone could ask for. Lastly, and most importantly, I would like to thank my girlfriend and life partner Sofia. Having joined me in this academic endeavour abroad, she has almost quite literally been by my side for the entirety of this period of my life. I am not able to imagine how this process could have been smoother if not for her daily encouragement and relentless uplifting. To the reader, I hope to provide valuable and insightful information with this thesis.

Table of Contents

List of Tables

List of Figures

List of Acronyms

BAU – Business-as-usual

CCS – Carbon Capture and Storage

CCU – Carbon Capture and Utilization

DBT – Dibenzyltoluene

DWT – Deadweight tonnage

ETS – Emissions Trading System

GHG – Greenhouse Gas

GT – Gross Tonnage

GWP – Global Warming Potential

HZ – Hydrographic Zero

IMO – International Maritime Organization

LCA – Life Cycle Assessment

LHV – Low Heating Value

LNG – Liquefied Natural Gas

LOHC – Liquid Organic Hydrogen Carrier

MCH – Methylcyclohexane

NG – Natural Gas

NM – Nautical miles

PDBT – Perhydro-dibenzyltoluene

RES – Renewable Energy Sources

SMR – Steam Methane Reforming

TOL – Toluene

ZILS – Sines Industrial and Logistical Zone

CO_2 – Carbon dioxide

H_2 – Hydrogen

NH_3 – Ammonia

1. Introduction

1.1. Societal background

As climate change progresses, it is ever more pivotal to mitigate its consequences and refrain from its causing behaviours. Increasing global population growth – and the consequential drive of anthropogenic greenhouse gas (GHG) emissions from the combustion of fossil fuels, agriculture and forestry – which is one of the prime triggers leading to climate change, has also driven global energy demands to unprecedented levels (McDonald et al., 2011; Satterthwaite, 2009). This expansion has led to several studies alluding to the key role that fossil fuels will lead throughout this century (Arutyunov & Lisichkin, 2017; Dogan & Erol, 2019; Durand, 2018). To halt the rapid accumulation of GHG in the atmosphere resulting from human activities, several parties, including the European Commission (EC), signed the Paris Agreement in 2015. As a universally agreed goal, it was set a target to decrease CO_2 emissions by 40% in 2030 compared to 1990 (Foran, 2016). Although Abas et al. (2015) agrees that fossil fuel production rates are expected to rise until 2055, it also states that an energy mix including fossil fuels, hydrogen (H_2), biofuels, and renewable energy sources should become the main priority worldwide. To successfully comply with the targets put forward by the Paris Agreement, the EC has established a minimum of 32% renewable energy share in 2030. Furthermore, in September 2020, the Commission proposed a more ambitious target to reduce GHG emissions by 55% compared to 1990, although it has not yet updated the relevant policy sub-targets (EuropeanCouncil, 2018).

Following the Paris Agreement, the EC released the European Green Deal in 2019, where a set of targets to achieve by 2030 was established, among which is the deployment of fully scalable clean or low carbon H_2 technologies (2019). As a complement of the Green Deal, the Commission also released a Hydrogen Strategy Roadmap (HSR) (2020a), stating the transversal impacts that low carbon H_2 could have on sectors like industry, transport, power, and the built environment, i.e. residential and work place buildings. The use of H_2 as a feedstock, fuel, energy carrier, and energy storage medium has the potential to, not only help the decarbonisation in applications where electrification is challenging, but it also has tremendous potential to reduce the intermittence and spatial constraints of renewable energy systems (further explained in sub-section 1.3). From projections made in 2018, H_2 is expected to substantially increase its share in the European energy mix, from nearly 2% to around 13-14% by 2050, serving as a vital integrative solution to achieve the targeted carbon neutrality.

Nonetheless, from the current H_2 production inside the EU, over 90% of it is performed using mainly natural gas and coal, resulting in roughly 70 to 100 Mt of CO_2 annually (European Commission, 2018). To tackle this issue, however, the EU has outlined a strategic approach, involving stakeholders from different sectors to reach an ambitious goal of 80 GW of H_2 electrolyser capacity in 2030 – the plan includes 40 GW capacity within the EU and another 40 GW being imported from neighbouring countries. Furthermore, as a platform for concrete project planning and stakeholder engagement, the European Clean Hydrogen Alliance (2020b) was founded, bridging relationships between industry players, national and local public authorities and other stakeholders. All these efforts complement the Green Deal, as H_2 has been identified as one of the key strategic value chains by the Strategic Forum on Important Projects of Common European Interest (IPCEI).

1.2. Domestic and imported hydrogen in the Netherlands

In 2019, TNO released a report (Detz et al., 2019) on the future role of H_2 in the Netherlands. By compiling the results of multiple scenarios performed using different projection models, it was estimated that the total consumption of H_2 in the Netherlands in 2015 was around 100 PJ/yr. It also states that this H_2 is almost entirely produced within the Netherlands, with its large majority being produced by reforming of natural gas, and as by-product of steam cracking of naphtha and in chlorine production. The most conservative scenarios state that H_2 technologies will be negligible until 2050, only reaching a scalable level in the second half of the century – like with the example of the Sky scenario (Shell, 2018). Conversely, two scenarios (Benndorf et al., 2014; Gigler & Marcel, 2018) consider a much higher demand for H_2 in 2050, of roughly 1,700 and 1,900 PJ/yr, respectively, which can be explained since these studies considered using H_2 in significant amounts to convert CO_2 into carbon-based products, such as methane, kerosene and diesel. Overall, H_2 demand is expected to reach, on average, 900 to 1,100 PJ/yr in 2050, with applications in several sectors: in the build environment, H_2 has the potential to replace all the natural gas usage for heat, with an expected average demand of 34 PJ/yr; the power sector is expected to benefit from the increasing H_2 market, with possible applications for it to be used in cogeneration plants, gas turbines and fuel cells to produce electricity. Estimations range from 95 to 380 PJ/yr, with the latter resulting from a higher capacity of renewables and the respective need to store excess energy. In the transport sector, fuel-cell electric vehicles are projected to boost the sector's H_2 demand to 160 PJ/yr. Finally, in the industry sector, H_2 is projected to supply 254 PJ/yr for energetic and non-energetic applications.

Within the context of the Strategic Forum on IPCEI, a project partnering Portugal and the Netherlands was formally accepted to produce 465 kt of green H_2 annually from competitive sources of solar and wind energies. Green H_2 is defined as being produced with electricity generated from renewable sources – Lanphen (2019) provides a more detailed explanation of the term, also mentioning grey H_2 (from natural gas) and blue H_2 (from natural gas with carbon capture and storage or CCS). This project is detailed in the Roadmap and Action Plan for Hydrogen in Portugal (2019) and directly responds to the Energy and Climate Plans of both countries (DGEG, 2019; Parliament et al., 2019). Following the official decommissioning of the coal-fired power plant in Sines, Portugal (Céu, 2021), the plan is to install a 1 GW electrolyser unit for green H_2 production. This shift opens multiple opportunities: Sines is located on the Atlantic coast of Portugal, and it contains one of the main deep-water ports in Europe, favouring the potential transportation of H_2 and other energy carriers. Furthermore, there is the potential of optimising the existing electricity and gas grids (produced electricity can be transferred to the grid, and pure H_2 can be blended with natural gas and injected into the gas grid); also, using the existing transport infrastructure, there is the possibility to establish a refuelling station for H_2 fuelled vehicles. In the Netherlands, green H_2 technologies and infrastructure are also expected to develop and be a focus to several sectors, such as heavy-duty transportation, and electricity, where H_2 is expected to play a major role in renewable energy storage (Parliament et al., 2019). In September of 2020, the Dutch government announced a Memorandum of Understanding (2020) between the two countries, reinforcing the importance of a synergetic connection towards accomplishing their respective 2030 hydrogen plans. This reiterates how relevant it is to develop a strategic import-export value chain, to ensure the production and transportation of green H_2 from Portugal to the Netherlands. The goal will be to transport the produced green H_2 from the port of Sines to the port of Rotterdam via maritime transportation (Government of Netherlands, 2020). Further details regarding the demand for H_2 specifically for the port of Rotterdam is given in sub-section 2.3.2. This project will increase the supply of H_2 in the Netherlands, which is expected to provide a considerable amount of energy within the available projections for the energy mix in 2050. Liquid organic hydrogen carriers (LOHCs), explained in more detail in sub-section 1.4.1, could be a promising option for imported H_2.

1.3. Knowledge gaps

Despite having reached a bilateral agreement, neither Portugal nor the Netherlands mention LOHCs as a potential solution for the export or import of green H_2 via maritime transportation in their respective National Plans for Energy and Climate (2019; 2019). In fact, no specific outlines for H_2 export have been disclosed whatsoever, and neither which medium would potentially be preferred. At a European level, the Green Deal (2019) and the HSR (2020a) also do not mention LOHCs specifically, but both emphasise the importance of boosting energy storage capacity. The former states that mitigating the underlined intermittence of electricity from solar PV and wind is crucial for energy security and independence. In the HSR, the ability of H_2 to serve as a vector for renewable energy storage is referred to, as it favours a more long-term, large-scale, and flexible storage capacity. Furthermore, following the aftermath of the COVID-19 pandemic crisis, it also states that securing investments to increase RES production and the supply, storage, and transport of green H_2 will undoubtedly contribute to a faster recovery. Initiatives like the European Clean Hydrogen Alliance (2020b) will also help to encompass all available storage technologies and shine a light on potential new solutions and applications for current technologies.

Within this framework, the EU has financially contributed to several related projects, such as the HySTOC (2018) project, which will demonstrate the distribution of high purity H_2 through a DBT-PDBT LOHC-based storage system, to a H_2 refuelling station, in Finland. Studies have shown that using LOHCs could lead to transportation costs reductions of up to 80% compared to standard compressed H_2 gas, due to their higher storage capacity. Additionally, Hydrogenious LOHC Technologies GmbH, which is one of the five stakeholders involved in the HySTOC project, has mentioned that transporting LOHCs is only feasible if these are transported from one single point to another single point – making it a potential LOHC for the aforementioned IPCEI project (European Commission, 2020c). Contrarily, Eypasch (2017), which considered DBT in its research – despite stating that N-Ethylcarbazole (NEC) is the most researched LOHC –, mentions that most LOHCs can sustain a liquid state under ambient conditions and have similar physical properties to diesel, making them easy to handle, safe and eligible to be used in existing diesel distribution infrastructure.

Due to its comparingly higher similarities to diesel fuel and lower levels of toxicity, NEC has been more widely researched and has been considered in a study by Teichman et al. (2012) for the medium (1,000 km) and long-range (5,000 km) transportation of green H_2 by sea. The study provides a direct comparison between transporting LOHCs and liquefied H_2, through a currently established maritime route from Canada to Germany (Gretz et al., 1990). Overall, the study found the LOHCs to be a considerably cheaper option for transportation compared to liquified H_2, for both medium- and long-distance. Nonetheless, it is noteworthy that important aspects of the supply chain are left out from their research. It only encompasses the direct transportation costs, disregarding the associated costs both at the export and the import terminals. Aside from this, the research assumed fixed levels of H_2 export, and only accounted for electricity generated through hydropower.

In the research conducted by Lanphen (2019), a detailed overview of the techno-economic aspects of importing H_2 is given. The study compares the import of H_2 either in gaseous or liquid state, as well carried either by ammonia (NH_3) and methylcyclohexane (MCH). The argument for choosing the TOL-MCH system is that both organic compounds can be stored in similar conditions to petroleum products and use the existing supply chain infrastructure. Furthermore, it indicates its longevity over long distances and long periods of time, and MCH is the reaction product of H_2 and toluene, making it recyclable. Lanphen analyses every step of the supply chain, from its production and conversion to the respective medium, to the export and import terminals, as well as the bridging transportation. At the export terminal, it mentions that MCH can be stored in oil tanks.

Regarding transportation, it uses chemical or oil tankers, which contain a carrying capacity of around 20,000 to 442,000 tonnes. More details about the maritime transportation of liquid bulk, using tankers, is given below in sub-section 1.4.2. Finally, at the import terminal, Lanphen suggests MCH is dehydrogenated using the patented dehydrogenation process developed by Chiyoda Corporation (2013). The considered route is between Brazil and the port of Rotterdam in the Netherlands. It concludes that, overall, ammonia is the cheapest option to transport H_2, followed by MCH, liquid, and finally gaseous H_2. Compared to the other options, the associated costs at the import terminal for MCH are considerably higher, which can be explained by the high investment costs and energy consumption of the dehydrogenation process. When assessing the impact of different export locations, the research concluded that MCH has minimal cost variations from short- (1,000 km) to long-range (20,000 km) distances, similarly to ammonia and liquified H_2. Furthermore, MCH is also reported to have negligible variations in cost across different demand levels, making it highly competitive for high demand levels and much cheaper than gaseous or liquified H_2 for low demand levels (and on par with ammonia). Still, a few aspects are missing from this study, such as the levelized cost of electricity (LCOE) when producing green H_2 from different sources and future carbon tariffs, which directly and indirectly affect the final delivery costs of H_2.

1.4. Supply-chain background

This sub-section provides an outline of the composition of the supply chain. Firstly, a deeper analysis is presented regarding LOHCs and both the historical and potential future applications of these products. Secondly, emphasis is given to the sea transportation of liquid bulk, and how it currently operates. Finally, sub-sections 1.4.3. and 1.4.4. briefly describe the ports of Sines and Rotterdam.

1.4.1. Liquid Organic Hydrogen Carriers (LOHCs)

According to the International Renewable Energy Agency (IRENA), from 2009 to 2017, PV module prices have decreased around 81%, whilst wind turbine prices have dropped by nearly half, on average (Sugawara & Nikaido, 2014). However, solar and wind energies suffer from high intermittency levels (Lanphen, 2019). Furthermore, it has also been referred that the supply of renewable energy is spatially asynchronous since demand is not geographically related to production sites, resulting in possible energy curtailments (Eypasch et al., 2017; Tso et al., 2019). In the case of off-grid applications, this issue could also lead to energy shortages when demand is much higher than supply, dramatically increasing energy prices, as recently observed in Texas, USA (Krauss et al., 2021). As the global installed capacity of renewables is expected to increase, energy markets and stakeholders have been developing several short and long-term energy storage technologies.

Currently, there are several available energy storage solutions. The most mature technologies are pumped-storage hydroelectricity and compressed air energy storage, but both are geographically restricted due to requisites in the construction location (Tso et al., 2019). Regarding batteries, even though some breakthroughs are anticipated to reduce the costs of storing energy (Zhang et al., 2018), the respective current capacity is suitable only for short-term applications and frequency control. Some studies claim that it is economically unfeasible to develop batteries to a utility scale due to their relatively low gravimetric energy density and low efficiency for long-term energy storage (Aakko-Saksa et al., 2018). Lastly, Dehghani-Sanji et al. (2019) has also emphasised that large-scale or grid-scale battery (>50MW) supply chains create several environmental pollutants such as hazardous waste, GHG emissions and toxic gases.

To overcome the problem of intermittent renewable electricity supply, it is necessary to deploy technologies that allow for more efficient energy storage in the long-term and are easily transportable and not spatially constrained. In the last few years, using H_2 to distribute and store energy has shown to be a suitable and competitive solution (Lanphen, 2019). Regardless, in terms of energy density by volume, H_2 underperforms compared to hydrocarbon fuels such as gasoline (Dawood et al., 2020). For these reasons, H_2 can only be used for storage or transportation purposes when compressed, liquefied, or attached to a carrier. The first two options present some difficulties – the low density of H_2 only allows storage as a gas at pressures of around 350-700 bar with ca. 1.0 kWh/L volumetric energy content; and its low boiling point is extremely low (-253 °C), with liquefied H_2 containing ~2.5 kWh/L (Brynolf et al., 2018; Tso et al., 2019). As an alternative, H_2 can also be stored in numerous metal and chemical hydrides, as shown in Figure 1. Both are performed through chemical bonds and have a considerably stronger physical bond when compared to molecular hydrogen adsorption (Andersson & Grönkvist, 2019). These stronger bonds imply a high capacity for H_2 absorption for the former, even if performed at ambient temperature and pressure. Nonetheless, some have stated that solid systems hold some disadvantages, such as materials degradation after dehydrogenation, i.e., irreversibility of the process, as well as the need to build an operational infrastructure for regular use (Aakko-Saksa et al., 2018; Niermann et al., 2019).

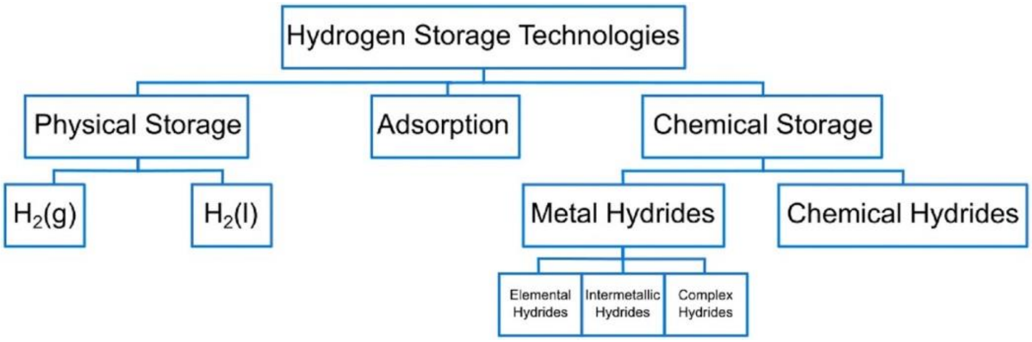

Figure 1 – H_2 storage technologies. Adapted from (Andersson & Grönkvist, 2019).

The most studied and widely used chemical hydrides for H_2 storage are ammonia, methanol, and formic acid. Ammonia is produced through a very energy-intensive process (Haber-Bosch) and can be stored as a liquid at mild conditions. Regarding methanol and formic acid, there are current applications where these are produced via green H_2 and captured CO_2 and used as fuels in a carbon-neutral cycle. Both ammonia and methanol have a higher H_2 volume density compared to liquefied or gaseous H_2 (Aakko-Saksa et al., 2018; Niermann et al., 2019; Tso et al., 2019). According to Andersson & Grönkvist (2019), these cannot be characterised as LOHC. LOHCs, also commonly referred to as two-way LOHC, are a pair of liquid organic compounds that allow for the safe, reversible and long-term storage of H_2 through catalytic hydrogenation and dehydrogenation cycles and accompanied by heat exchange (Eypasch et al., 2017; Reuß et al., 2017). Figure 2 illustrates the LOHCs concept presented by Müller et al. (2011), showing the renewable energy system and H_2 storage pairing. Recently, more research has been conducted on such combinations of renewable energy production and H_2-based storage. Some examples, such as Li et al. (2009), Sherif et al. (2005) or Agbossou et al. (2001) provide insight on integrated systems with either PV, wind, or hybrid systems and H_2 storage, respectively.

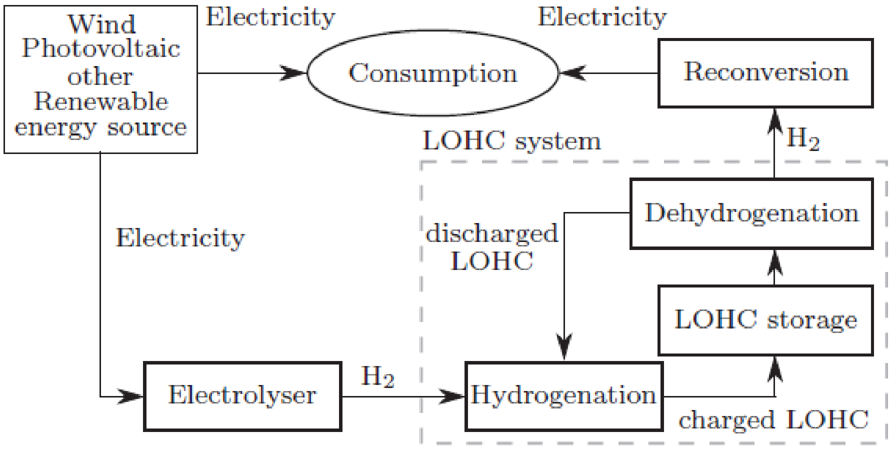

Figure 2 – LOHC storage system, using green H_2. Concept by (Müller et al., 2011); Illustration by and adapted from (Eypasch et al., 2017).

During periods of overproduction, excess electricity is used to power an electrolyser to produce H_2. The H_2 is 'loaded' into a LOHC through the hydrogenation process and stored or transported. Before final use, the LOHC carrier is dehydrogenated to release H_2, which can be used for electricity generation or in other applications.

Currently, the most widely researched LOHCs are (in dehydrogenated and hydrogenated forms, respectively): toluene-methylcyclohexane (TOL-MCH), dibenzyltoluene-perhydro-dibenzyltoluene (DBT-PDBT), and N-ethylcarbazole-dodecahydro-N-ethylcarbazole (NEC-DNEC) (Andersson & Grönkvist, 2019; Eypasch et al., 2017). The use of LOHC has been suggested for several energy applications, including gas turbines, fuel cells, and transportation (Gahleitner, 2013). Residential and commercial energy storage and heating have also been analysed, combining renewable energy generation and LOHC storage (Teichmann, Stark, et al., 2012). As further referred to in sub-section 1.5, the TOL-MCH and the DBT-PDBT systems were selected for this research. These systems, as well as their respective conversion processes, are discussed in more detail in sub-section 2.4.

1.4.2. Liquid bulk maritime transportation

As mentioned in sub-section 1.3, the maritime transportation of LOHCs is assumed to be performed using oil or chemical tankers. Currently, tankers encompass a wide range of sizes, from small tankers (which usually vary from 10,000-24,999 Deadweight Tonnage or DWT) to Ultra large crude tankers (ULCC) (with DWT between 320,000-549,999). DWT measures a ship's capacity to carry cargo (Britannica, 2019), and it is computed by considering 90% of the ship's deadweight tonnage, converted based on the densities of different petroleum products and crude oil. Figure 3 below presents the different tanker classes, displayed per size according with the AFRA scale (U.S. Energy Information Administration, 2014). As shown, the smaller classes used to transport cargos of refined petroleum products. Furthermore, these classes are commonly used for relatively shorter distances. Also, the two largest classes of tankers are exclusive for the transportation of crude oil and would require further improvements to be able to store more refined products. Finally, as mentioned in sub-sections 1.4.3. and 1.4.4, the depth of the relevant terminals is not sufficient to dock the largest two tanker classes.

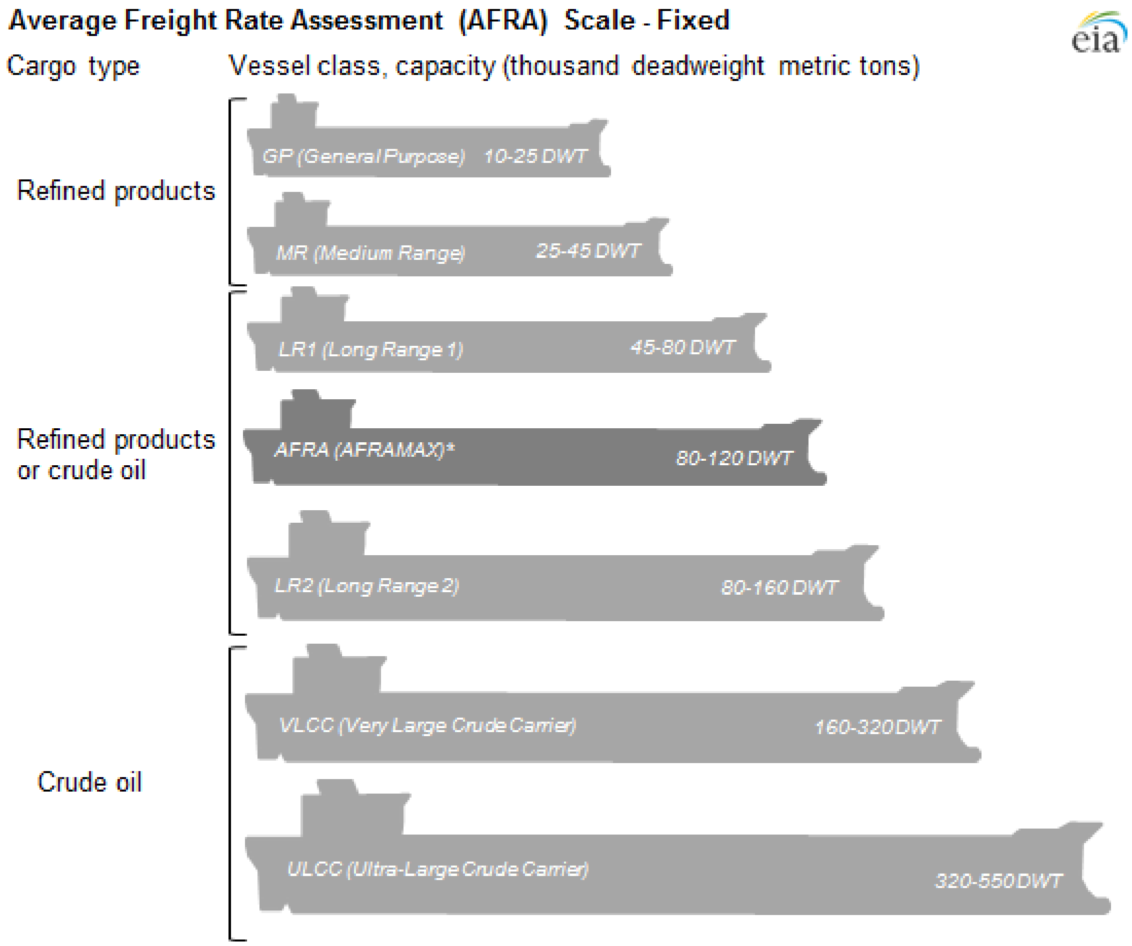

Figure 3 - Tanker classes, per DWT capacity.

1.4.3. Port of Sines

In this sub-section, a small description of the Port of Sines is provided, focusing on the characteristics that are relevant within the context of the supply chain, detailed further in sub-section 2.1. The port of Sines is a deep-water port and the main port belonging to the Iberian-Atlantic front. Its location is at approximately 58 NM or 107 km from Lisbon and crosses some of the primary international maritime routes – as shown in Figure 4 below –, making it a highly strategic location for worldwide logistics chains.

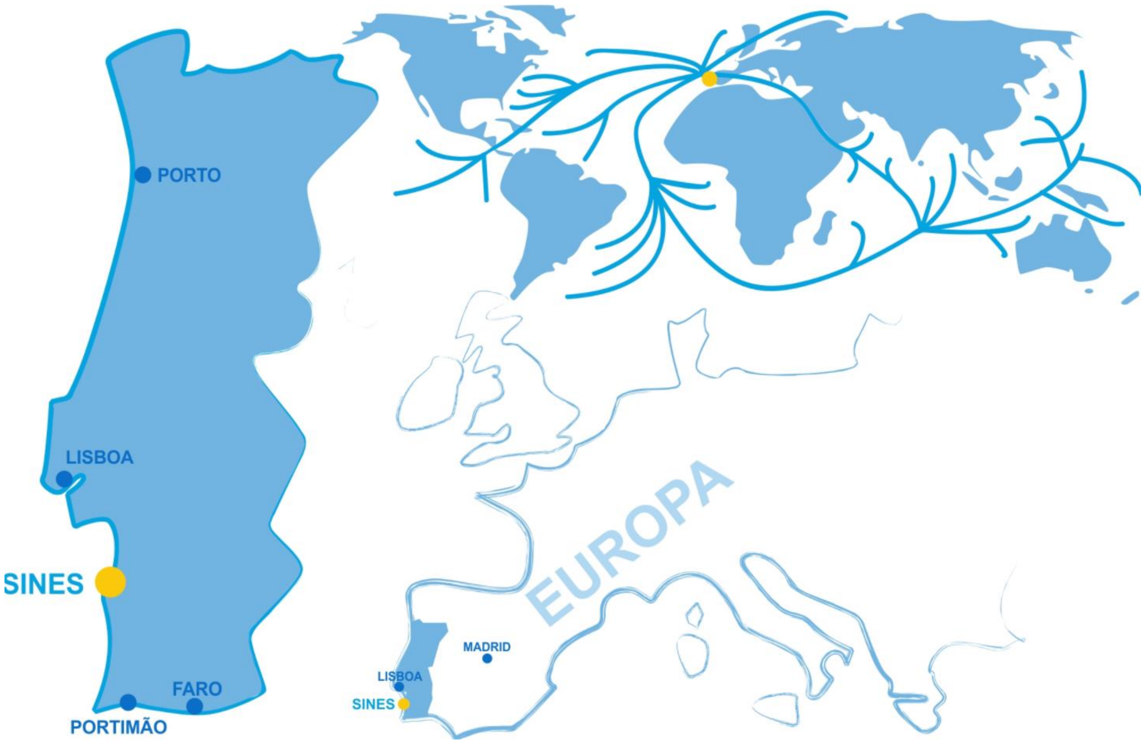

Figure 4 - Highlight of strategic geographical position of the port of Sines. (Porto de Sines, 2021c)

Currently, the port works as the main gateway for energy supply in Portugal, providing logistical services such as moving crude, oil products, natural gas and oil derivatives. The surrounding Logistics and Industrial Platform (Zona Industrial e Logística de Sines, or ZILS) covers an area of over 2,000 ha, and according to AICEP Global Parques (2021), it can potentially be expanded to around 4,000 ha. It is currently the biggest cluster for refinery and petrochemical activities in Portugal, which allows for considerable synergetic potential between the separate industries. The port contains several business-related infrastructures, as well as recreational areas, but the main terminals are the liquid bulk terminal (highlighted in green on the left bottom corner of Figure 5 presented below), the petrochemical terminal, the multi-purpose terminal, and the LNG terminal.

Figure 5 - Digital map of the port of Sines. (Domingos, 2013)

The liquid bulk terminal in the port, responsible for the logistical services that are necessary within the context of this research, contains six docking stations with natural depths of up to -28 meters/HZ. It has the capacity of docking tankers with a capacity ranging from 10,000 DWT and 350,000 DWT, and it is directly connected to the adjacent tanking area and the ZILS by a pipeline conveyor. The terminal is further equipped with a treatment station dedicated to the processing of ballast waters and residues, thus complying with the established environmental mandates. According to the port's website (2021a), the liquid bulk terminal also holds the potential for expansion, with calls for new clients to use both the tanking area as well as the ZILS. Therefore, it is assumed that sufficient storage capacity is available in the tanking area to fulfil the projected necessities of the supply chain. The ZILS is the location that was chosen to build the electrolyser referred to in sub-section 1.2.

1.4.4. Port of Rotterdam

Following the previous assessment for the port of Sines, a brief description of the characteristics for the port of Rotterdam is provided in this sub-section. The port of Rotterdam is the largest cargo seaport in Europe, and one of the largest in the world. The port holds a great amount of history, and it is located at a very important and strategic point, being surrounded by some of the largest population and industrial centres in Europe – the German Ruhr district, the London area and Paris. It is currently regulated and operated by the Port of Rotterdam Authority, who is responsible for handling shipping traffic, as well as maintaining and investing in infrastructure. The port area is comprised of over 5,300 ha of industrial sites, with a total area of roughly 10,500 ha. The total length of the port is 40 km, and around 1,500 km of pipelines operate within the port area (Ship Technology, 2019). It is a deep-water port, comparable to Sines, with the quay of the port having a 24-meter draft, capable of docking ships with over 350,000 DWT capacity. The port includes over 90 terminals, mapped in Figure 6 below, with 35 reserved exclusively for liquid bulk (highlighted in yellow in the Figure). Within the industrial area of the port, the petrochemical industry is considerably important, with six oil refineries and refinery terminals in operation. Coupled with these infrastructures, the port also includes 11 tank terminals for oil products, with a combined tank storage capacity of over 30 million cubic meters. According to insights provided from Vopak (personal communication, 2021a), sufficient storage capacity within the tank terminals would be available to fulfil the requirements inherent with this research.

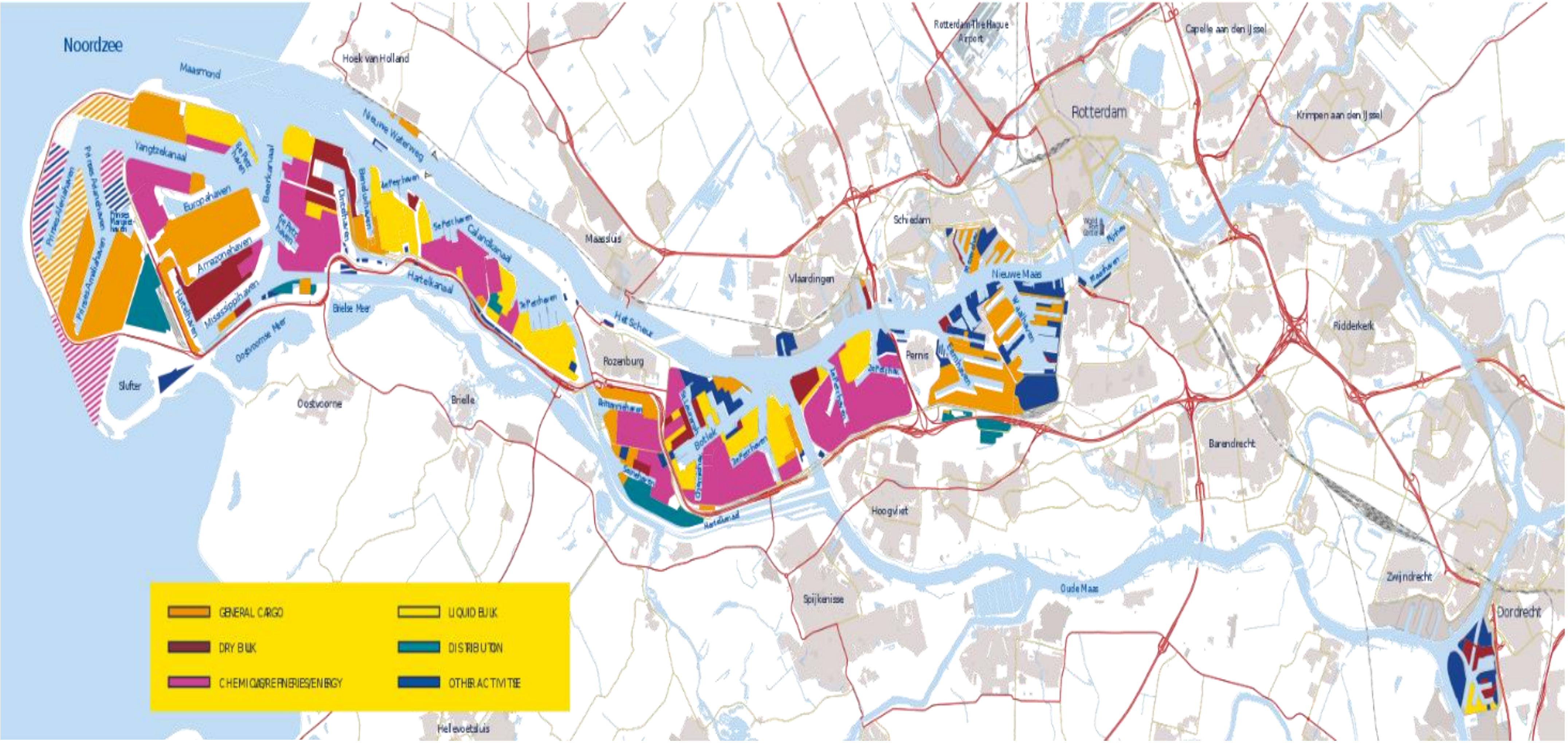

Figure 6 - Digital map of the port of Rotterdam (Mover DB, 2020)

1.5. Problem definition and research aim

This study aims to assess the economic and GHG impact of exporting green H_2 produced in Sines to the port of Rotterdam by maritime transportation, using LOHCs, and assess its future role in the Dutch energy mix. According to the report released by TNO (Detz et al., 2019), it is stated that future H_2 supply is expected to be partially composed of blue and green H_2. Figure 7 shows the trajectories of different H_2 production routes expected in the Netherlands between 2020-2050. The report argues that conventional power plants can be equipped with CCS technology for the short and medium terms. However, this would only allow for a 90% reduction in GHG emissions, which would not be enough to comply with the goals for 2050 (95-100% reduction). Hence, the only viable solutions to produce H_2 would be to perform gasification of biomass equipped with CCS or water electrolysis, using renewably generated electricity. The first option is heavily influenced by the availability of biomass and the associated costs of including CCS technology. Furthermore, the fact that population density is an ongoing issue in the Netherlands, the country does not possess much available land for biomass crop growth. This latter issue is also a deterrent to produce green H_2 since it would be highly linked to the amount of renewable energy available. The domestic potential of renewables is limited because of the lack of land available.

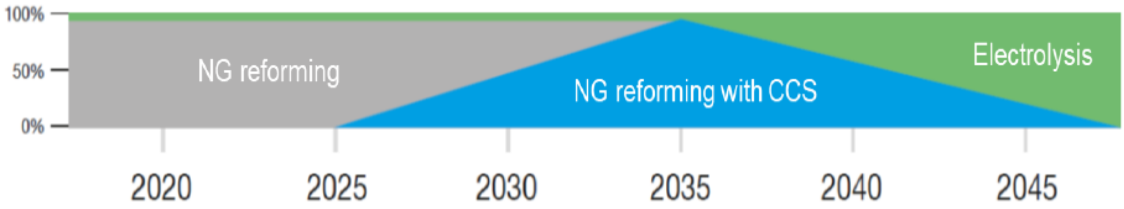

Figure 7 - Illustration of a possible trajectory of the relative shares of different H_2 production routes during a transition period. (Detz et al., 2019)

This year, Carvalho (2021) analysed the hydrogenation and dehydrogenation processes of different LOHCs within the context of the IPCEI project on H_2. The overall purpose was to optimise the operating conditions of these processes and conduct a techno-economic analysis at different scales, with operations set to start in 2030. Within the context of the research that was performed by Carvalho, much of the previously LOHCs were carefully considered, albeit some, such as methanol, do not allow for the reversibility of the process. Focusing on two-way LOHCs, previously explained in sub-section 1.4.1, Carvalho (2021) selected both the toluene-methylcyclohexane (TOL-MCH) and the dibenzyltoluene- perhydro-dibenzyltoluene (DBT-PDBT) systems, mainly because of their economic feasibility and readiness. The N-ethylcarbazole-dodecahydro-N-ethylcarbazole (NEC-DNEC) system was disregarded since it presents notable disadvantages. Firstly, NEC is mentioned as being relatively costlier that the other two compounds, due to high raw material costs. It is also characterized by having a high melting point, which makes it necessary to couple the system with resistance heaters and insulated tanks, further increasing its total costs. Lastly, the research states that NEC suffers from decomposition, unlike DBT, when exposed at dehydrogenation temperatures in the presence of a catalyst. Sub-sections 2.4.1. and 2.4.2. focus specifically on the TOL-MCH and the DBT-PDBT systems, respectively. However, it is still required to assess how these processes could benefit the export of H_2 in value and supply chain. In particular, the goal is to minimise the final price of imported green H_2 in the Dutch market and the respective infrastructure configuration given different scenarios of future production and demand between 2030-2050, different LOHC technologies and carbon tariffs. As the impact of the LOHC based supply chain infrastructure on the final price of green H_2 remains unclear, as well as its level of competitiveness within the Dutch H_2 market, this research aims to answer the question:

What is the potential of H_2 import to the Netherlands from Portugal using LOHCs via maritime transport and its role in the future energy transition?

Following Carvalho's research (2021), the present study addresses the impact of transportation and storage at port locations. Aside from this, it was also necessary to assess in more detail the costs associated with the dehydrogenation process integrated with the port of Rotterdam. This port was chosen since most future demand for H_2 will be generated by industries in Rotterdam, such as using it as feedstock for ammonia and steel production and as a refining agent for synthetic and bio-based transport fuels. Projected demand of H_2 within the port of Rotterdam is detailed further in sub-section 2.3.2. It is also relevant to mention that Rotterdam is the largest port in Europe and a central location for distributing imported goods and materials, as mentioned in the previous sub-section. Finally, to assess how the imported H_2 could compete within the Dutch market, it is necessary to overview the projected costs and final price of H_2 produced in the Netherlands. With all this in mind, this study focused on answering the following sub-questions:

- *How much does logistics costs increment the supply chain and the final price of renewable H_2?*
- *What are the options and costs of integrating the imported H_2 in the H_2 supply chain, via the port of Rotterdam?*
- *What are the current and future potentials for domestic H_2 supply and demand in the Netherlands?*

- *What are the associated production costs?*
- *What is the GHG footprint of international H_2 supply through LOHCs?*

A significant cost reduction in the long-distance transport of renewable H_2 can create an international market of transport and deployment of this cleaner alternative to natural gas for fuel applications or fossil fuel based H_2 for chemical purposes. The easily dispatchable characteristics of LOHCs as carriers of renewable H_2 make them a promising mean to store green energy, which in the long-term will help to decarbonise multiple sectors, including those where electrification is deemed to be hard or even unfeasible.

2. Methodology and input data

The following sub-sections provide an overview of all the relevant supply chain steps. Furthermore, it infers on the respective input data required and method applied for each of the steps. By firstly introducing the entire supply chain considered for this research, it becomes clearer which topics needed to be addressed. The subsequent sub-sections will individually detail the method and required data for each of the steps, following the logistical order of the supply chain. This encompasses every step from the production of H_2 in Sines to the dehydrogenation process of the LOHCs in Rotterdam. Finally, the last sub-section focuses on methods chosen to assess the sensitivity of the computed results.

2.1. Supply chain steps

For this research, the analysis was performed based on the detailed steps to complete one roundtrip between Sines and Rotterdam. At the export terminal, the first step involves storing the hydrogenated LOHC, i.e., the cargo that will leave Sines to be transported to Rotterdam, in tanks within the port of Sines. The LOHC is transported via a pipeline from the hydrogenation plant to storage tanks in the export terminal before it is loaded into the tanker. Details on the projected schedules for H_2 production are given in sub-section 2.2., and the respective schedule for the hydrogenation process is covered in sub-section 2.6.1. After the hydrogenation process, enough LOHCs are transported to the storage tanks to ensure that these are sufficiently full to load a ship when it arrives at the port of Sines. The storage requirements are detailed in sub-section 2.6.1. At departure, the tanker is loaded with the LOHC, as explained further in sub-section 2.5.3.3. Contrarily, when arriving in Rotterdam, the tanker is unloaded and the hydrogenated LOHC is transported via pipeline to the dehydrogenation facility. Finally, during the dehydrogenation process, the unloaded LOHC is stored in tanks within the port of Rotterdam, where the make-up LOHC is added to replenish the batch. When this process is finished, the remaining dehydrogenated LOHC is loaded into the tanker and transported back to Sines. After arriving in Sines, the dehydrogenated LOHC is transported once again to the hydrogenated plant to restart the cycle. Figure 8 presented below depicts the supply chain, with a dashed line delimiting the relevant processes mentioned for this research. The figure starts with the production of RES in Portugal, which is used to feed the electrolyser in Sines. Following, the produced green H_2 is sent to the hydrogenation unit, where it proceeds to follow the logistical steps detailed above. After dehydrogenation, the extracted H_2 is then applied to several end uses, which are detailed in sub-section 2.3.2.

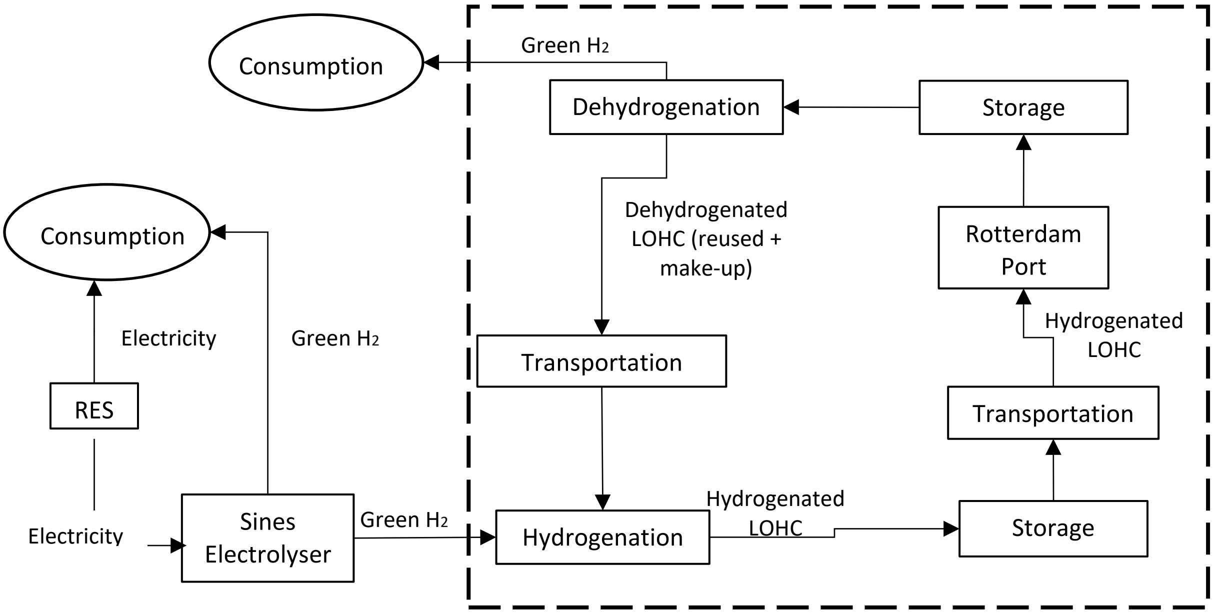

Figure 8 - Flow chart depicting green H_2 supply chain from Sines to Rotterdam. LOHC conversion processes, storage and maritime transportation highlighted.

2.2. H_2 production and price development

To accurately plan the yearly schedule for transportation and storage, it was necessary to infer on how the yearly production of green H_2, in Sines, is projected to be divided throughout one calendar year. Within a personal communication setting with Prof. Rui Castro, from the Instituto Superior Técnico in Lisbon, relevant data on this matter was obtained. This is closely linked with the yearly projected renewable electricity generation in Portugal. Currently, the production of H_2 in Portugal is mainly deemed as a storage solution for excess electricity produced during low demand periods. As a storage solution, H_2 currently competes with both batteries, as well as pumped storage hydropower (PSH) (personal communication, 2021b). Nonetheless, with the increase in the demand of green H_2, it was important to identify the yearly fluctuations in renewably produced electricity, that could be used to feed the electrolyser in Sines. Figure 9 below displays data provided by the DGEG, regarding the production of electricity via RES, in Portugal, between April of 2019 and March of 2021.

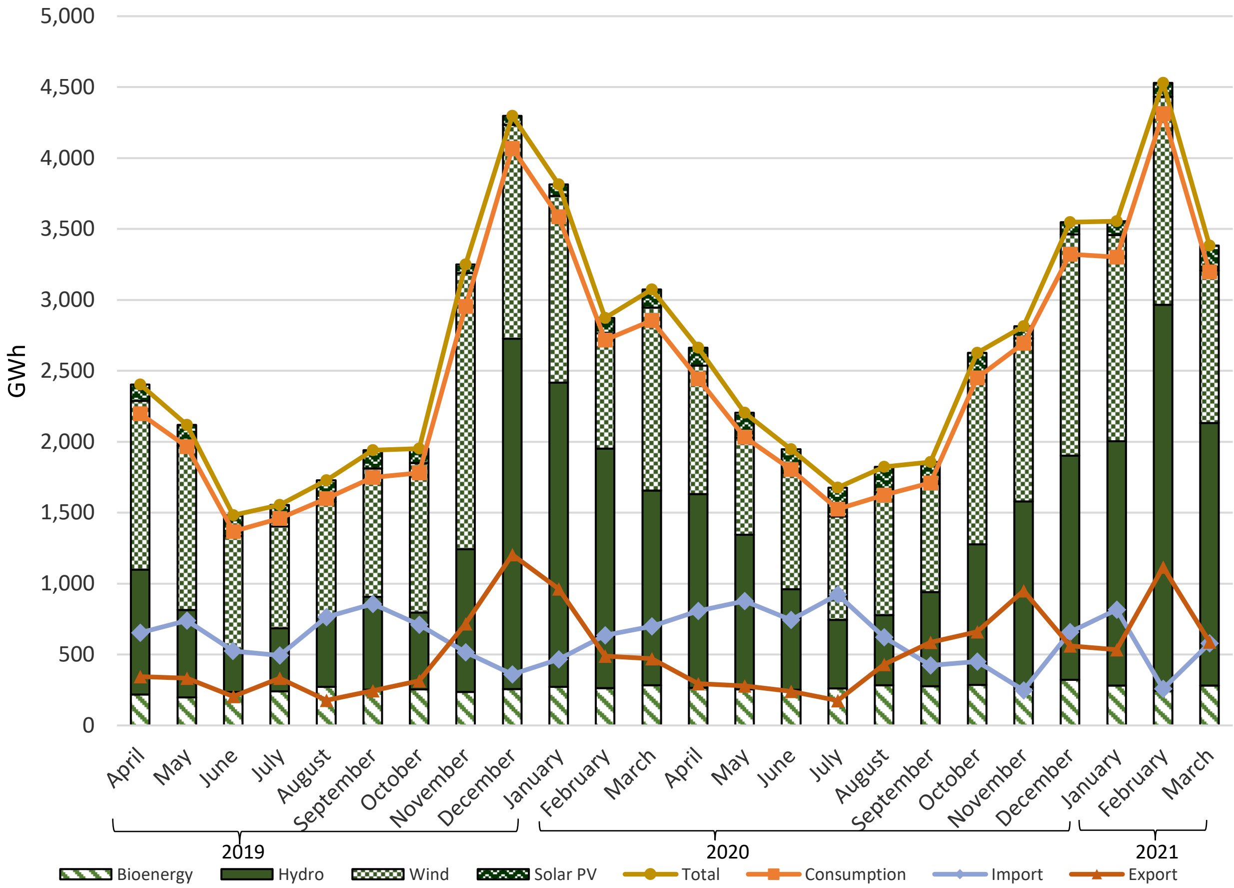

Figure 9 - RES electricity production in Portugal, between April 2019 and March 2021.

As shown in the figure, current renewable electricity generation varies with a consistent trend, depending on the seasons. During the colder months, between October and March, electricity production is substantially higher, mainly due to the contributions of both hydro and wind power. Furthermore, due to the lower installed capacity of solar PV in Portugal, compared with wind turbines, solar PV provides a negligible contribution, throughout the year. This occurs regardless of the climacteric conditions that usually occur – during the warmer months, the amount of insolation is approximately two to three times higher than in the colder months, across the whole country (Cavaco et al., 2016). However, this is projected to be largely balanced out until 2030, as attested by Prof. Rui Castro (personal communication, 2021b), as well as the study published by Leal (2020). Leal modelled the projected mix for electricity generation in Portugal and assessed the projected price for electricity in 2030. The results for electricity generation plus a comparison with the correspondent values for 2019 are presented in Table 1.

Table 1 - Projected energy source mix for electricity production in Portugal, in 2030, in comparison with 2019.

Technology	2019 [TWh]	2030 [TWh]	Relative variation
Hydro	37.162	101.76	174%
Wind	67.64	123.81	83%
Solar	10.273	82.93	707%
Other Renewables	4.673	13.29	184%
Coal	17.845	0	-100%
Natural Gas	109.718	25.14	-77%
Nuclear	55.824	26.21	-53%

Even though all RES options are projected to grow by 2030, solar PV projections surpass the other alternatives substantially as detailed in Leal. With a projected increase of over 700% in installed capacity, solar PV is projected to mitigate the disparity against the available capacity for wind and hydro, allowing for a more homogeneous production of electricity provided by RES, throughout the year. By establishing this conclusion, it was assumed, for this research, that renewable electricity would be fed to the electrolyser in Sines evenly, throughout the year, allowing for a linear production of green H_2. As mentioned in sub-section 1.2, the yearly projected production of green H_2 is expected to reach 465 kt/year. Furthermore, within the context of this research, a nominal yearly capacity of 8,000 h/year was assumed, coinciding with the capacity also used in Carvalho (2021) for operating the hydrogenation and dehydrogenation plants. By equitably dividing the projected yearly production by the nominal yearly capacity, it was calculated an hourly production of roughly 58,125.0 kg-H_2/h. This corresponds to approximately 1.40 kt-H_2/day. Considering the different tankers used for this research, Table 2 below refers to the number of days required to produce the amount of H_2 that can be stored in a full cargo of LOHC. This yearly production plan of green H_2 was also assumed to be linear for the entire duration of the considered timespan between 2030 and 2050.

Table 2 - Number of days required to produce the same amount of green H_2 that each tanker can carry, when carried in each of the LOHC systems considered.

# of days	Small tankers	MR Product Tanker (Handymax)	Supramax	Panamax	Aframax
TOL-MCH	2	2	3	3	4
DBT-PDBT	2	3	3	4	4

Coupled with the requirement for establishing a yearly production plan for green H_2, it was equally necessary to assess the price at which green H_2 is expected to be traded for, between the years of 2030 and 2050. This is closely related to another of the results found in Leal, where it is given a projection for the price of electricity in 2030. Due to the increase in the deployment of RES, and the respective phasing out of fossil-fuels, Leal concludes that the price of electricity is expected to experience a substantial drop, from a reference price of 47.68 €/MWh in 2019, to around 25.00 €/MWh in 2030. This will supply a positive contribution towards the reduction in price for green H_2, which is currently priced at around 4.70 €/kg-H_2, in Portugal (DGES, 2019). However, this will not be the only factor that deserves consideration in this matter. According to the Roadmap for H_2 in Portugal, the potential reduction in electricity price will, in fact, be the most relevant contributor for reducing the levelized cost of green H_2 (LCOH), until 2040. Notwithstanding, it also highlights the impacts of electrolyser efficiency improvement, increase in capacity factors and reduction in CAPEX of electrolysers. Figure 10 below displays the projected cumulative effect of all the mentioned factors, on the LCOH, according to the roadmap for H_2.

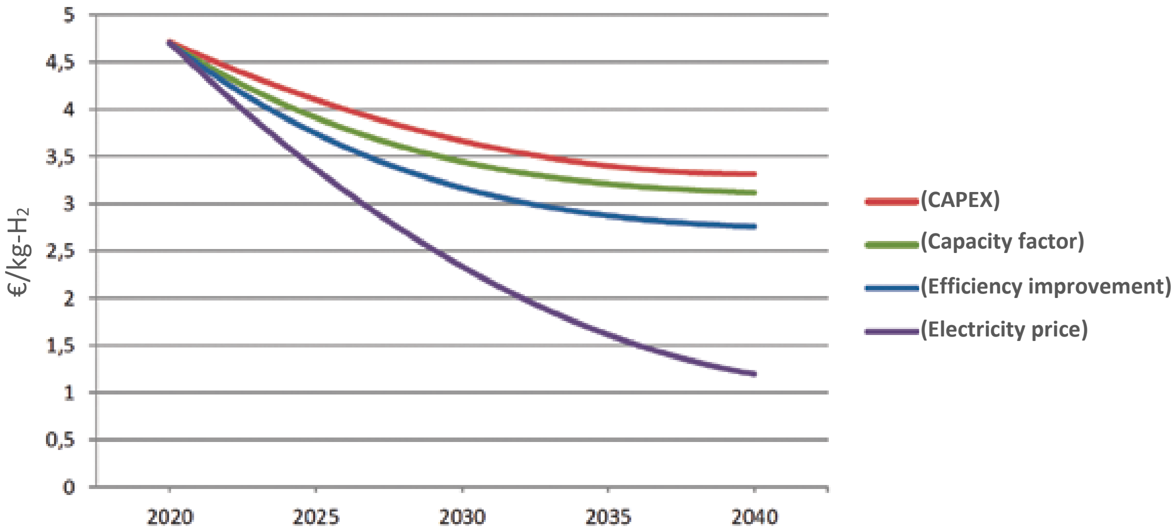

Figure 10 - Projected cumulative effects on the LCOH in Portugal, from 2020 to 2040.

Another analysis was conducted by Bento (2020), who compared the future price projections for both green and blue H_2, in Portugal. In this analysis, two contrasting scenarios (one more optimistic towards the deployment of green H_2 technologies, and another towards blue H_2 technologies) were proposed. In both scenarios, the authors include the effect of economies of scale, regarding CCS technologies to produce blue H_2 as well electrolysers. In their findings, even in the pessimistic scenario, green H_2 is projected to be competitive compared with blue H_2, with prices in 2050 being roughly 1.70 €/kg-H_2 and 1.60 €/kg-H_2, respectively. For the optimistic scenario, green H_2 is projected to be priced at less than half compared with blue H_2, with respective prices being approximately 1.00 €/kg-H_2 and 2.10 €/kg-H_2.

After grouping the relevant data on price projections for green H_2, averages were considered for the years of 2030, 2040 and 2050, respectively. The assumed values are presented in Table 3 below.

Table 3 - Price projections to produce green H_2 in Portugal, for 2030, 2040 and 2050.

		2030	2040	2050
Expected H_2 price	*€/kg-H_2*			
Capital Verde (Bento, 2020)				
LOW		2.50	-	1.80
HIGH		2.00	-	1.00
Roadmap for green H_2 in PT (DGES, 2019)				
CAPEX reduction		3.70	3.30	-
Capacity factor		3.45	3.11	-
Efficiency improvement		3.20	2.75	-
Electricity price		2.12	1.07	-
Average		**2.83**	**2.56**	**1.40**

As verified, the price for green H_2 is projected to decrease considerably from 2030 to 2050. Nonetheless, it is important to emphasize that the decreasing trend in H_2 prices is expected to be much more accentuated between 2040-2050. This can be explained by the increased capacity and higher development of green H_2, compared with blue H_2, coupled with the steeper increase in the production of H_2 that is projected to occur during that decade. Bento mentions that, although blue H_2 might be marginally more competitive that green H_2 under some scenarios, it is noteworthy that the costs for blue H_2, included in this study, do not account for the environmental and public health risks and costs associated with the storage of CO_2.

2.3. Supply and demand scenarios

The focus of this sub-section is to outline the projected scenarios for exporting green H_2 from Portugal to the Netherlands, and the specific role that the ports of Sines and Rotterdam are expected to take. Following this assessment, sub-section 2.3.3. highlights the chosen export scenario for green H_2, within the context of this research.

2.3.1. H_2 supply

Acknowledging the IPCEI project mentioned in sub-section 1.2, Portugal intends to become an exporter of green H_2 in the coming decades, with the Netherlands being one of the projected destinations for export. In fact, the Roadmap and Action Plan for H_2 in Portugal (DGES, 2019) mentions that the port of Sines has been envisioned to be one of the key infrastructures to promote an international supply chain of green H_2. As part of this roadmap, several scenarios were built, considering different levels for H_2 production and export. It also presented projections for the different sources of green H_2 production, with biomass gasification, non-centralized and centralized electrolysers being mentioned. Until 2040, it shows that centralized electrolysers, such as the case for the upcoming 1 GW capacity electrolyser in Sines, are expected to gain substantial momentum, with green H_2 produced this way accounting for around 97% of the total green H_2 production in Portugal. The different scenarios accounted for this research, and their specificities, are the following:

- H_2 base: Considers the investment on green H_2 by electrolysis, with capacity being built for 2 GW of production. This scenario assumes that the electrolysers are fed via solar PV and wind energy sources. It also predicates that the use of green H_2 is equally divided by domestic consumption and export.
- H_2 export +: Based on the previous scenario, it maintains the 2 GW capacity, but prioritizes export over domestic consumption.
- H_2 export -: Contrarily to the H_2 export + scenario, here domestic consumption of green H_2 is prioritized over export.
- H_2 double: Variant of the H_2 base scenario, it projects double the capacity, at 4 GW. Like H_2 base, it assumes that the produced H_2 is equally distributed between domestic consumption and export.

With the assessed scenarios detailed, it is important to quantify the exact amount of export that is projected for each of them. For that purpose, Figure 11 is presented below.

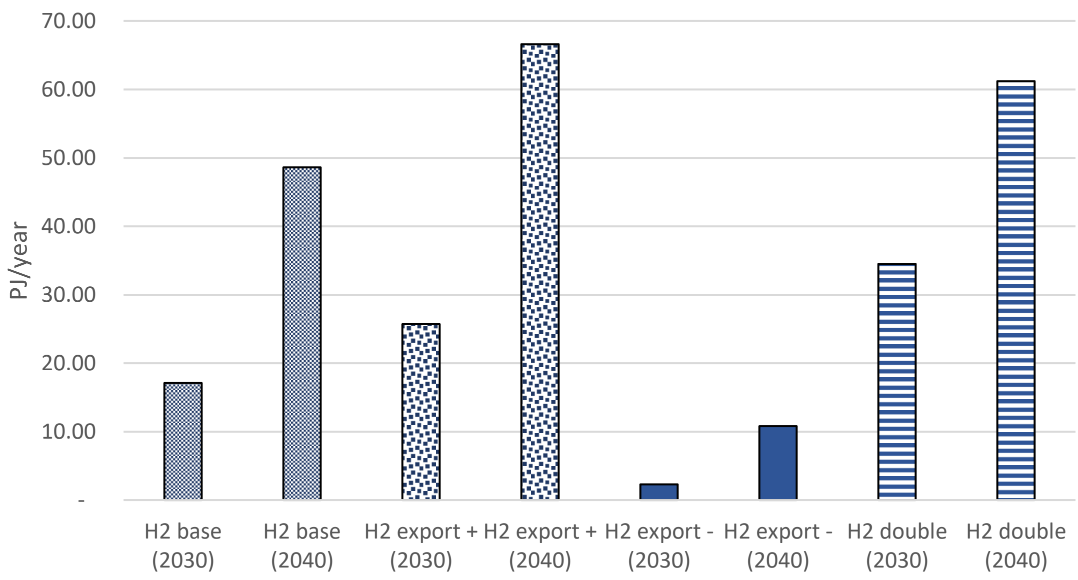

Figure 11 - Values for projected green H_2 export scenarios for Portugal, for 2030 and 2040 (DGES, 2019).

2.3.2. H_2 demand

This sub-section provides a distinct overview of the role that H_2 is expected to play specifically within the port of Rotterdam, thus supplementing the data provided in sub-section 1.2, which presents the general outlook for the Netherlands. The port of Rotterdam holds the position of being the energy port for Northwest Europe, by moving 8,800 PJ annually of incoming and outgoing energy sources. This represents roughly three times the energy demand of the Netherlands (Port of Rotterdam, 2020). However, this energy is currently originating primarily from fossil fuels, and thus the Port of Rotterdam H_2 Roadmap emphasizes the importance of increasing the focus on developing H_2 technologies that can facilitate the energy transition. Despite that some infrastructures projects are expected to contribute towards local production of blue and green H_2, the roadmap states that promoting the import of H_2 from world regions where there is a large potential for cheap renewable electricity and H_2 is of pivotal importance. Until 2030, the port is expected to produce roughly 800 kt of blue H_2 for the feedstock and process heat industries. Apart from this, another 360 kt of green H_2 will also be produced, with 0.5 GW of electrolyser capacity being operational in 2025, and an extra 1.5 GW capacity expected to be added by 2030. Furthermore, extensive plans for offshore wind electricity production are set to be implemented, which will provide approximately 60-72 GW of capacity by 2050. However, according to the presented estimations, only around 18-24 GW capacity is expected to be directed towards producing H_2 for the port of Rotterdam. Table 4 below presents the projected demand for H_2 for the port of Rotterdam, in 2050.

Table 4 - Projected demand for imported H_2 coming through the port of Rotterdam, in 2050. Based on max scenario w/ limited use of biomass (Port of Rotterdam, 2020).

	Share (%)	**H_2 in Rotterdam (Mt)**
Feedstock industry	25%	0.8
Process heat industry	50%	1.1
Build environment, greenhouses	25%	0.1
Mobility over land	50%	0.9
Aviation (H_2 in synthetic fuels)	50%	1.0
Maritime shipping (H_2 in liquid fuels)	75%	3.2
Total demand in the Netherlands		**6.9**
Demand in Germany via Rotterdam	33%	8.0
Other demand in NWE via Rotterdam		5.0
Total potential demand		**19.9**

As seen in the Table, the projected demand of H_2 within the port far exceeds what has been proposed for internal production for 2030. Additionally, the projected complement supplied by offshore wind will not be sufficient, as detailed calculations suggest that a total of 200 GW of offshore wind capacity would be necessary to produce the required 20 Mt of green H_2. This demand will fulfil over half of the total demand for H_2 in the Netherlands, with the main applications being related to renewably produced fuels for aviation, maritime and road transportation, and well as for several industries. Within these industries, the process heat industry is highlighted, with estimations of nearly 50 % of the country's demand being supplied via Rotterdam. Other industries include feedstock, build environment and greenhouses. Apart from this, as shown in Table 4, a further 13 Mt of H_2 will likely come through Rotterdam to supply the German market and other countries in the Northwest European region. These values reflect the current outbound energy flows that fulfil the needs of the neighbouring countries' industries. Germany is stated to currently rely on the port of Rotterdam to supply one third of its oil and coal demand.

2.3.3. Yearly transportation of green H_2

The total amount of green H_2 projected to be transported to Rotterdam, between 2030 and 2050, matches the target established in Carvalho's research (2021). This corresponds to 50 kt/year, which, when using a mass energy density conversion factor for H_2 of 120.0 MJ/kg-H_2 (Fruchart, 2013), yields an equivalent of 6.0 PJ/year. When compared with the projected export scenarios presented in sub-section 2.3.1., the yearly amount of H_2 to be transported to Rotterdam would represent roughly 35.1% and 12.3% of the "H_2 Base" scenario values, for 2030 and 2040, respectively. This is shown in Figure 12, where the considered scenario for this research is labelled as "REF". As explained further in sub-section 2.2, the H_2 is assumed to be delivered across a nominal capacity of 8,000 hours per year, in accordance with the method presented by Carvalho (2021). During this period, the H_2 is projected to, evenly, be fully loaded and unloaded from the selected LOHCs, covered in sub-sections 2.4.1. and 2.4.2. Hence, for the purpose of this research, transportation and storage operations were also assumed to be evenly distributed across a nominal capacity of 8,000 h/year. This was done by firstly computing the relevant cost components per round-trip – as defined is sub-sections 2.5.3. and 2.6. – and subsequently extrapolated to fit the yearly schedule, as detailed in sub-section 2.7.

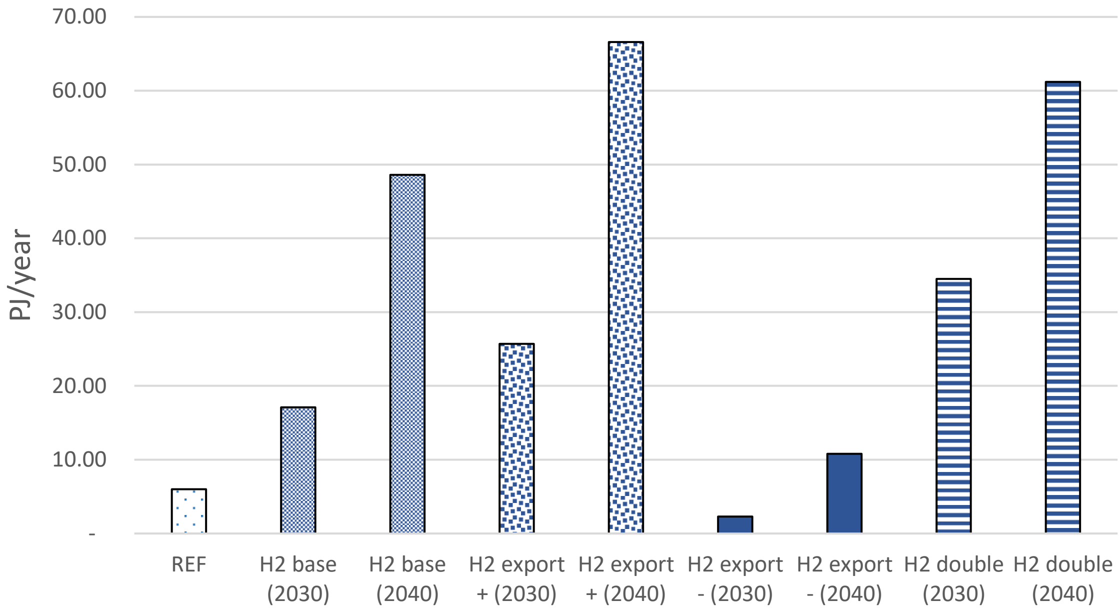

Figure 12 - Values for projected green H_2 export scenarios for Portugal, for 2030 and 2040, compared with "REF" scenario (DGES, 2019).

2.4. LOHC conversion processes

This sub-section focuses on addressing the individual characteristics of each of the selected LOHC systems. Additionally, it also provides insight regarding the chosen locations for both the hydrogenation and the dehydrogenation units, located in Sines and in Rotterdam, respectively. The locations were chosen based on collected data related to each of the ports, previously presented in sub-sections 1.4.3. and 1.4.4.

2.4.1. TOL-MCH system

Starting with the TOL-MCH system, it is one of the most investigated LOHCs, as mentioned before, and Carvalho (2021) also emphasizes that it is one of the most promising LOHCs. Some companies, such as the Chiyoda Corporation (2013), already have hydrogenation and dehydrogenation units in operation for this system. There are, however, some drawbacks such as a highly demanding dehydrogenation process, which occurs due to the high enthalpy of reaction (- 68.3 kJ/mol-H_2). Furthermore, there is a need for an advanced distillation systems to separate the two products because TOL and MCH have a close boiling point. In terms of toxicity, TOL is the second most toxic of all the LOHCs mentioned in sub-section 1.4.1, with a Toxic Potential Indicator (TPI) close to diesel's (Carvalho, 2021). For this research, it was necessary to source several characteristics from both products and their respective conversion processes.

Table 5 presented below gathers all the relevant technical data referent to the TOL-MCH LOHC system. The data in question was necessary to address the research questions stated in sub-section 1.5. In the $C_{s,n} = C_{REF,n} \times (1 + VAR_s)$

$$\forall\, n = 2030, 2040, 2050$$

section, the specific steps that required the data provided are detailed.

Table 5 - Technical data for the TOL-MCH system, concerning each of the system's products and respective conversion processes.

Product	**Unit**	**TOL**	**MCH**	Ref
Volumetric storage density	*kg-H_2/m^3*	48.00	-	(Carvalho, 2021)
Enthalpy of reaction	*kJ/mol-H_2*	- 68.30	-	(Carvalho, 2021)
Molar mass	*g/mol*	92.14	98.19	(PubChem Database, 2017b, 2017a)
Density	*kg/L*	0.88	0.77	(Niermann et al., 2019)
Dynamic viscosity (at 20°C)	*mPa.s*	0.58	0.73	(Jonas et al., 2008; Santos et al., 2006)
Conversion process		**Dehydrogenation**	**Hydrogenation**	(Carvalho, 2021)
Pressure	*Bar*	1.01	30.00	
Temperature	*°C*	450.00	170.00	
Conversion	*%*	97.34%	99.98%	
Energy consumption	*kWh/kg-H_2*			
High-pressure steam		-	3.36	
Fired heat		12.10	-	
Low-pressure steam		3.80	-	
Electricity		1.40	0.12	
TOTAL		17.30	3.48	
LOHC loss per cycle	*%*	1.44%		(Carvalho, 2021)
Global warming potential	*g CO_2-eq/kg-H_2*	29.03		(Carvalho et al., 2021)

2.4.2. DBT-PDBT system

Regarding the second LOHC system for this research, a successfully tested system for the hydrogenation of DBT, to be transported through a natural gas pipeline, is already commercially available by Hydrogenious Technologies (Modisha et al., 2019). Apart from this, DBT is commonly used as a heat transfer oil. When compared with TOL, DBT has a higher volumetric storage density. Table 6 below highlights this value, as well as additional technical data for each individual compound and their respective conversion processes. Moreover, it is also characterised by having a high boiling point – its enthalpy of reaction is -65.4 kJ/mol-H_2 –, which enables it to maintain its liquid state during the hydrogenation process (Carvalho, 2021). This aspect highly simplifies the required purification step and its transportation. Additionally, it is a non-flammable and non-toxic compound. Conversely, there is yet a lack of information regarding the safety of using PDBT.

Table 6 - Technical data for the DBT-PDBT system, concerning each of the system's products and respective conversion processes.

Product	**Unit**	**DBT**	**PDBT**	Ref
Volumetric storage density	*kg-H_2/m^3*	57.00	-	(Carvalho, 2021)
Enthalpy of reaction	*kJ/mol-H_2*	- 65.40	-	(Carvalho, 2021)
Molar mass	*g/mol*	272.40	284.50	(PubChem Database, 2018, 2020)
Density	*kg/L*	1.04	0.91	(Niermann et al., 2019)
Dynamic viscosity (at 20°C)	*mPa.s*	49.0	389.0	(Jorschick et al., 2020)
Conversion process		**Dehydrogenation**	**Hydrogenation**	(Carvalho, 2021)
Pressure	*Bar*	1.00	30.00	
Temperature	*°C*	320.00	260.00	
Conversion	*%*	96.00%	100.00%	
Energy consumption	*kWh/kg-H_2*			
Fired heat		11.50	3.06	
Electricity		1.29	0.11	
TOTAL		12.79	3.17	
LOHC loss per cycle	*%*	4.25%		(Carvalho, 2021)
Global warming potential	*g CO_2-eq/kg-H_2*	23.90		(Carvalho et al., 2021)

2.4.3. Hydrogenation Unit

Here, details are given regarding the costs for building and operating a hydrogenation unit, based on the research performed by Carvalho (2021). As mentioned in sub-section 1.4.1, for the hydrogenation process of both LOHCs, the process reactor is fed with H_2 directly from the electrolyser. For this reason, this unit is assumed to be located in the ZILS, in close proximity to the electrolyser. Following Carvalho's findings, this would prevent the need to invest in a multi-stage compression zone, which occurs when the reactor is fed with H_2 at atmospheric conditions. According to this study, the potential synergies that can be achieved by coupling the electrolyser with the hydrogenation unit can lower the yearly operational costs by roughly 75%, and the total investment in more than 85%. Table 7 below provide the results obtained from Carvalho's research regarding the total CAPEX required, the yearly OPEX and respective breakdowns for the hydrogenation units for the TOL-MCH and the DBT-PDBT systems. Furthermore, the price of each of the LOHCs is also provided. The original results were provided in USD, and an exchange rate of 1.21 USD/EUR was applied to convert the displayed values below to EUR.

Table 7 - Economic data for the hydrogenated process, concerning the individual costs and the price of both LOHC systems (Carvalho, 2021).

		TOL-MCH	DBT-PDBT
Operational costs	*M€/year*		
Electrical		0.49	0.47
Heat		2.50	2.60
Catalyst		0.55	1.01
Maintenance and repair		1.09	1.02
Operating labour		0.24	0.24
Total OPEX		**4.86**	**5.34**
Capital depreciation	*M€*		
Compressors, pumps and drivers		3.45	3.42
Heat-exchangers		1.47	2.21
Towers		1.04	-
Reactors		0.05	0.06
Working capital		0.65	0.65
Total CAPEX		**6.66**	**6.33**
Price	*€/kg-LOHC*	0.30	4.00

2.4.4. Dehydrogenation Unit

Further insights from Vopak (personal communication, 2021a) inferred on the possibility for synergetic processes related to the dehydrogenation process. Referring to the operation conditions and energetic demand mentioned in sub-sections 2.4.1 and 2.4.2, for the respective dehydrogenation processes, the temperature pinch required for the reactors to operate are 450 °C for MCH and 320 °C for PDBT. With such high temperatures, synergetic integration is not sufficient to provide the necessary heat. However, to potentially reduce the process costs for utilities, it is possible – even though it was deemed unlikely (personal communication, 2021a) – to benefit from excess gas resultant from neighbouring processes. For this reason, the dehydrogenation unit is assumed to be located within the petrochemical industrial area. Complementing the data presented in sub-section 2.4.3, Table 8 displayed below show the relevant yearly OPEX, total CAPEX and their different components relative to the construction of a dehydrogenation unit within the port of Rotterdam. The conversion cycle cost per kg-H_2 and the break-even price of using each of the LOHC systems to store H_2 are also provided. As for the values regarding the hydrogenation processes, here an exchange rate of 1.21 USD/EUR was also used to convert the original values. The break-even price, labelled as "H_2 break-even price" in the table below, refers to both LOHC conversion processes i.e., hydrogenation and dehydrogenation, covering a full cycle, as referred in sub-section 2.1. This value was used as a reference for 2030 and adjusted for inflation at a 1% annual growth rate, until 2050.

Table 8 - Economic data for the dehydrogenated process, concerning the individual costs, as well as the respective cost per kg-H_2 and the break-even price of both LOHC systems (Carvalho, 2021).

		TOL-MCH	DBT-PDBT
Operational costs	*M€/year*		
Electrical		5.77	5.28
Heat		11.44	9.70
Catalyst		3.03	2.16
Waste treatment		0.57	0.00
Maintenance and repair		11.69	5.37
Operating labour		0.36	0.24
Total OPEX		**32.87**	**22.76**
Capital depreciation	*M€*		
Compressors, pumps and drivers		21.55	20.06
Heat-exchangers		32.08	9.53
Towers		12.10	0.21
Reactors		0.13	0.12
Working capital		6.85	3.17
Total CAPEX		**72.72**	**33.10**
H_2 cost	*€/kg-H_2*	1.08	0.81
H_2 break-even price	*€/kg-H_2*	1.59	1.14

2.5. Maritime Transportation

The following sub-sections provide an overview of the methods applied to measure the economic and GHG impact of the maritime transportation of LOHCs. A brief description of the shipping route is given in sub-section 2.5.1, followed by the tanker classes that were chosen to fulfil the transportation, in sub-section 2.5.2. Moreover, each of the assessed cost components used for the economic analysis is thoroughly explained, in sub-section 2.5.3. This encompasses the calculation of the GHG footprint, which was also assessed as a cost component.

2.5.1. Shipping route

The maritime route between the ports of Sines and Rotterdam can be calculated through a route calculator, of which several can be accessible for free. Figure 13 below shows the specific maritime route which is crossed for tanker freights. The total distance $(Dist_{Sin2Rott})$between the two ports is approximately 1,112 NM or around 2,600 km.

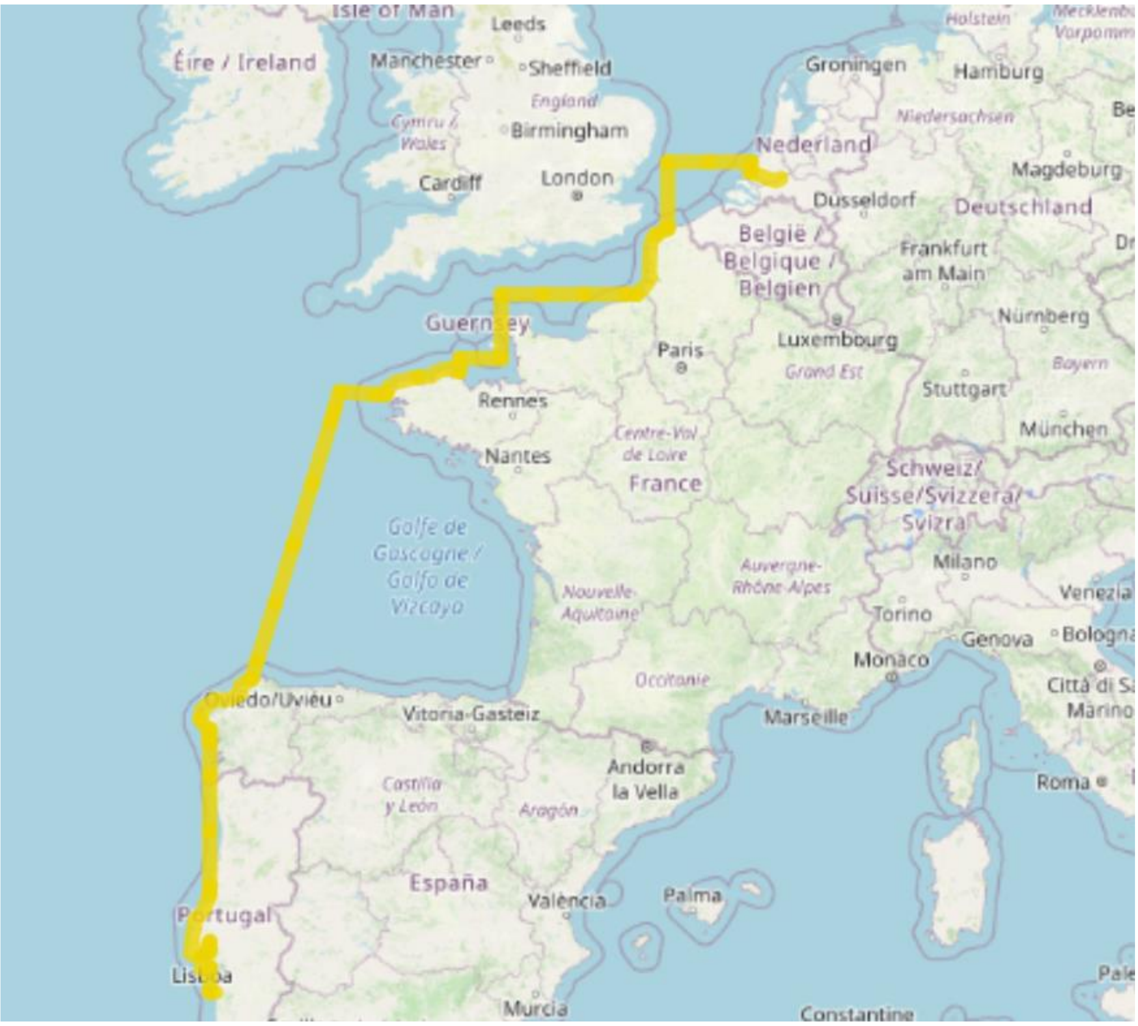

Figure 13 - Depiction of maritime route between the port of Sines and the port of Rotterdam. Extracted from calculator, accessed through www.shiptraffic.net, in June 2021.

2.5.2. Tanker selection

For the purposes of this research, using the two largest classes of tankers – very large crude tankers (VLCC) and ultra large crude tankers (ULCC) – could not be justified, considering that these are exclusively used for the transportation of crude oil. Furthermore, the total annual cargo transported is relatively small, as shown in Table 9 below, when compared to average amounts of cargo yearly transported, either by the Netherlands or Portugal (Amerini, 2008). Hence, ships from the LR2 class – as displayed in Figure 3 from sub-section 1.4.2. – were also disregarded.

Table 9 - Total amount of cargo to be transported yearly, per LOHC system.

Unit	TOL-MCH	DBT-PDBT
kt/year	1,870.50	1,835.75
m^3/year	2,282,521.44	1,897,324.58

Considering the four first tanker classes in Figure 3 and the data provided in Stopford (2013), a set of five different tankers was chosen, each with different DWT capacity. The considered tankers were labelled according to their class or sub-class and are presented below in Table 10. Additionally, the specific DWT and volumetric storage capacity of each vessel is also provided.

Table 10 - DWT and volumetric capacity per tanker class considered. *Note: MR = Medium Range.*

Unit	**Small tankers**	**MR Product Tanker (Handymax)**	**Supramax**	**Panamax**	**Aframax**
DWT	27,300.00	47,000.00	60,000.00	75,000.00	105,000.00
m^3	30,283.29	54,888.47	64,476.01	75,538.54	97,663.62

2.5.3. Transportation

The total costs of maritime transportation of LOHCs were assessed by summing the relevant cost components. In this sub-section, the methods for determining each of the components is detailed. Starting, the steps to account for the daily freight rates is presented. This encompasses all the required OPEX to be considered, as well as insurance and fees. Secondly, all details regarding the incurrence of port costs will be explained. Here, it will be possible to assess two different accounting methods, which depend on the port in question. Thirdly, this sub-section will specify how fuel consumption and the respective emissions were computed, while acknowledging their specific variation throughout the 20-year timespan considered for this research. Also, calculations were primarily made to calculate the cost of a single round-trip, as mentioned in sub-section 2.3.3. Following this assessment, the results were scaled to match the overall yearly cost of transporting the total expected cargo. The methods for scaling the transportation requirements are detailed in sub-section 2.7. All the following sub-sections detail the methods applied to calculate the transportation costs for all considered tanker classes.

2.5.3.1. Daily freight rates

Starting with the relevant expenses related to the operational use of the tankers, it was necessary to source the cost of an intermittent use of the tankers, which is determined by their daily rates (C_{DR}), sourced from the Baltic Exchange (Brazier, 2021). The Baltic Exchange is an independent source of maritime market data. They provide several key figures for assessing the maritime transportation market, including the mentioned daily rates. These daily rates include most of the relevant expenses, more specifically the cost of the crew (C_{crew}), technical costs (C_{tech}) which include maintenance, and a final parcel including insurance and other fees ($C_{insurance\&fees}$). Thus, the daily rates can be calculated as per Equation (1), shown below:

$$C_{DR} = C_{tech} + C_{crew} + C_{insurance\&fees}$$
(1)

Due to the negligible variance of the daily rates across different tanker sizes, the Baltic Exchange platform supplies an average of the daily rates of an Aframax tanker and a Medium Range (MR) Product tanker (also referred to as Handymax tanker). These calculations account for a crew size of 22-24 members. Further details on the calculations are provided in the source reference. Moreover, due to the high volatility of daily tanker freight rates, it was assumed for this research that no specific trend in price would be applied across the considered timespan. Historical data show that, since 2015, for example, crude oil and oil products tankers have earned revenues from around 10,000 to almost 320,000 USD per day, with fluctuations in between far too unpredictable to establish a proper temporal trend (Hellenic Shipping News, 2017; Sand, 2020). Nonetheless, the values sourced, which were respective to 2021, were subject to a 1% annual growth rate, until 2050, to adjust for inflation. To address the unpredictability of the fluctuations, this cost component was included as a variable for the sensitivity analysis, as detailed in sub-section 2.8.

2.5.3.2. Port Costs

The following cost component refers to port costs (C_{PC}). As expected, port tariffs are not shared between the two ports in question, even presenting different charges and methodologies for implementing such charges. Starting with the Port of Rotterdam (Samuels, 2021), it is possible to analyse the general terms and conditions, including port tariffs, since they provide this information. Apart from the tabled values related to the different tariffs, the reference also provides steps for the consumer to calculate the expected costs of entering the port and unloading/loading cargo at any of its terminals. At the entrance point, port dues ($C_{pd_{Rotterdam}}$) are charged based on the ships GT (GT_{ship}). The GT of a ship is calculated by measuring a ship's volume non-linearly (from keel to funnel, to the outside of the hull framing). It is conventionally used to determine several details, such as a ship's manning regulations, safety rules, registration fees, and port dues. Chemical/gas tankers are charged a tariff ($GT_{tariff_{Rotterdam}}$), and this first charge is then calculated using Equation (2):

$$C_{pd_{Rotterdam}} = GT_{ship} \times GT_{tariff_{Rotterdam}}$$
(2)

A second tariff is applicable to account for the transhipped cargo ($C_{cargoin_{Rotterdam}}$). To calculate this parcel, a balance is considered between the maximum port dues related to the cargo based on the ship's GT ($C_{cargo_{MAXGT}}$), and the actual total cargo being transhipped, in mass ($C_{cargoin_{mass}}$). The former is computed by multiplying the GT-size, a switch percentage (SP_{tanker}) which is used as a conversion variable, and the specific cargo tariff ($CargoTariff_{Rott}$), as shown in Equation (3). The switch percentage is dependent on the type of ship, and the cargo tariffs are dependent on the type of cargo. Both are supplied by the tariff statement.

$$C_{cargo_{MAXGT}} = GT_{ship} \times SP_{tanker} \times CargoTariff_{Rott} \tag{3}$$

To calculate $C_{cargoin_{mass}}$, it is necessary to multiply the total cargo being transported ($TotalCargoin_{Rott}$), in mass units, with the same cargo tariff applied for $C_{cargo_{MAXGT}}$, as follows:

$$C_{cargoin_{mass}} = TotalCargoin_{Rott} \times CargoTariff_{Rott} \tag{4}$$

From these two calculations, the lower value is added to the total costs. This method allows each tanker to be charged no more than its total volume capacity, regardless of the density of the cargo. Succinctly, at the entrance point, a tanker must incur the following costs:

$$C_{PC_{Rotterdam_{in}}} = C_{pd_{Rotterdam}} + C_{cargoin_{Rotterdam}} \tag{5}$$

with:

$$C_{cargoin_{Rotterdam}} = MIN(C_{cargo_{MAXGT}}; C_{cargoin_{mass}}) \tag{6}$$

A charge for the transhipped cargo is again applied at the exit point, where the tankers will leave the Port of Rotterdam with the dehydrogenated components. The same method is applied as in $C_{cargoin_{Rotterdam}}$. However, due to the different mass density between the inbound product (hydrogenated compound) and the outbound product (dehydrogenated compound), the value of the charge might not be the same, and thus it is necessary to discriminate between the two, which results in the following set of equations:

$$C_{cargoout_{mass}} = TotalCargoout_{Rott} \times CargoTariff_{Rott} \tag{7}$$

$$C_{cargoout_{Rotterdam}} = MIN(C_{cargo_{MAXGT}}; C_{cargoout_{mass}}) \tag{8}$$

These two equations thus allow for the assessment of the total port costs related to the Port of Rotterdam ($C_{PC_{Rotterdam}}$):

$$C_{PC_{Rotterdam}} = C_{PC_{Rotterdam_{in}}} + C_{PC_{Rotterdam_{out}}} \tag{9}$$

with:

$$C_{PC_{Rotterdam_{out}}} = C_{cargoout_{Rotterdam}} \tag{10}$$

Following with the Port of Sines, two separate expenses are charged. Firstly, when entering the port, a ship harbour fee is due, which is assessed according to the ship's GT and the ratio between the loaded and unloaded cargo quantity combined, in metric tons, and the GT. In case the value of this ratio surpasses a certain threshold, which can vary depending on the type of tanker, then a maximum unitary rate $\left(GT_{tariff_{Sines}}\right)$ is charged per each tanker's GT. This is the case for every considered tanker since both at arrival and departure, the tankers are always fully loaded. The methods of calculation and the respective rates are given by the port's authority tariff regulations (Samuels, 2021). By assessing $GT_{tariff_{Sines}}$, it is possible to calculate the port dues ($C_{pd_{Sines}}$):

$$C_{pd_{Sines}} = GT_{size} \times GT_{tariff_{Sines}} \tag{11}$$

The second expense that is incurred is related to the loading and unloading of the cargo. At the liquid bulk terminal located in the Port of Sines, a monetary rate per ton of moved cargo is enforced ($CargoTariff_{Sines}$) and the overall cost can be easily calculated by multiplying this rate with the amount of metric tons loaded or unloaded. Thus, the following two equations were used:

$$C_{cargoin_{Sines}} = TotalCargoin_{Sines} \times CargoTariff_{Sines} \tag{12}$$

$$C_{cargoout_{Sines}} = TotalCargoout_{Sines} \times CargoTariff_{Sines} \tag{13}$$

with:

TotalCargoinSines = Total cargo unloaded at liquid bulk terminal in the Port of Sines, in metric tons.

TotalCargooutSines = Total cargo loaded at the liquid bulk terminal in the Port of Sines, in metric tons.

Again, the distinction is required between the inbound and outbound cargos, since the products being transported are not identical, and thus have different values for density. Having computed the mentioned separate expenses, it is possible to quantify the total port costs from the Port of Sines ($C_{PC_{Rotterdam}}$):

$$C_{PC_{Sines}} = C_{PC_{Sines_{in}}} + C_{PC_{Sines_{out}}} \tag{14}$$

with:

$$C_{PC_{Sines_{in}}} = C_{pd_{Sines}} + C_{cargoin_{Sines}} \tag{15}$$

$$C_{PC_{Sines_{out}}} = C_{cargoout_{Sines}} \tag{16}$$

Finally, following the historical trends on the variation of port costs implemented by the port of Rotterdam (Liang, 2021), it was assumed that, for all of the mentioned port charges, an annual growth rate of 1% was applied. This also serves to adjust for inflation, as referred to for C_{DR} in the previous sub-section. The original values for Rotterdam (Samuels, 2021) and Sines (Porto de Sines, 2021b) were extracted for 2021 and extrapolated until 2050. C_{PC} was then calculated for 2030, 2040 and 2050, respectively. In sub-section 2.8, it is discussed how C_{PC} was subject to changes from the results obtained for scenario “REF”.

2.5.3.3. Fuel usage and costs

Since the daily rates (C_{DR}) previously mentioned do not include fuel cost, it is necessary to also search for outlooks that could provide the missing information. According to Stopford (2013), the speed ($Speed_{knots}$) at which each considered tanker travels changes slightly to optimize fuel consumption. Smaller tankers travel at a slightly lower speed of 14.7 knots, while the Aframax tankers travel at 15 knots. The same reference also provides the data regarding the daily fuel consumption ($Fuel_{day}$) for each of the considered tankers t referred to in sub-section 2.5.2. Finally, Stopford provides insight on the specific daily fuel consumption of the auxiliary engines, which amounts to roughly 10% of the main engine's fuel consumption.

The auxiliary engines are used to generate electricity onboard the tanker (Jalkanen et al., 2009) and serve a purpose in modelling emissions within the harbour areas. The electricity provided by the auxiliary engines is used, among other ends, to power cargo pumps to unload and load the LOHC from the tankers. In this research, it is assumed that the auxiliary engines are operating at a fixed rate during the time from when the tanker arrives at the port, i.e. after the entrance port dues (C_{pd}) are charged, until it leaves the port fully loaded. This is also known as the turnaround time ($Days_{TA}$) (PPIAF, 2007), and for this research, this is comprised of the total days it takes for one tanker to be fully unloaded and fully loaded, as well as the respective waiting days inside the port, combined for both locations. The relevant data for this matter was obtained during an interview with Vopak (personal communication, 2021a), who detailed the amount of time required to unload and load a tanker, dependent on its size. With this information it was possible to assess the specific duration ($Days_{RT}$) and fuel consumption ($Fuel_{RT}$) of a round-trip between the two ports. Also, for the calculation of $Fuel_{RT}$, it is important to calculate separately the days of navigation ($Days_{nav}$), as well as $Days_{TA}$, seeing that fuel consumption varies depending on whether the main engine is working. Equations (17) and (18) below detail how $Days_{nav}$ and $Days_{RT}$ were calculated.

$$Days_{nav} = \frac{Dist_{Sin2Rott}}{Speed_{knots}} \Big/ 24\ hours \times 2 \tag{17}$$

$$Days_{RT} = \frac{Dist_{Sin2Rott}}{Speed_{knots}} \Big/ 24\ hours \times 2 + Days_{TA} \tag{18}$$

Fuel consumption is given in tons of consumed fuel per day of operation ($Fuel_{day}$). These values are presented for the consumption of Heavy Marine Fuel (HMF), also referred to as Heavy

Fuel Oil (HFO). By establishing reference values for fuel consumption in the current days, it was further necessary to research how the maritime transportation industry is intending on tackling the emissions produced by the global shipping sector. According to Wada et al. (2021), the International Maritime Organization (IMO), has established the goal of cutting the respective emissions from the sector in half by 2050, compared with the values registered for 2008. Notwithstanding, Wada et al. mentions that, under the IMO's GHG emissions studies, there is still room for improvement regarding their estimations. Consequently, research was conducted by developing a system dynamics model that incorporated and evaluated the impact of ship speed reduction, transition to lower emission fuels and the promotion of energy efficiency design index (EEDI) regulations, until 2050. Regarding specifically the introduction and proliferation of lower emission fuels, Wada et al. considers that the shipping sector will experience a phase out from HFO, and gradually increase the share of LNG-fuelled and introduce zero-emissions ships. This has also been expressed by Xing et al. (2021), which states that synthetic fuels such as H_2 and NH_3, when produced with RES, could prove to immensely contribute towards decreasing the emissions produced by short sea shipping. Regarding the introduction of zero-emissions ships, these were modelled to use H_2 fuel, NH_3 fuel, and other alternatives. Also, both "Low" and "High" scenarios were considered to project the market performance of zero-emission fuels, and the increase in usage of LNG-fuelled ships. These scenarios were built to discriminate the percentual share ($Fuel_{share}$) of each type of fuel (f) used, per decade, until 2050. For this research, the projection of used fuels within the modelled supply-chain were based on the average between the two scenarios presented by Wada et al. and are presented in Table 11 below.

Table 11 - Projected fuel mix used by tankers in LOHC supply chain, for 2030, 2040 and 2050, based on Wada et al. (2021).

	%	**HFO**	**LNG**	**Zero-emission fuel**
2030		20%	80%	-
2040		5%	50%	45%
2050		-	20%	80%

Having established the share of used fuels until 2050, it was also necessary to assess how these are currently priced, and what price trajectory each of the fuels is projected to follow. Helgason (2020) addresses this topic by conducting a comprehensive cost-competitiveness comparison between HFO, conventional methanol (NG) and renewably produced methanol (RN). As stated in the reference, RN is produced using CO_2 from a geothermal power plant in Iceland. By using electricity from the Icelandic energy grid, hydrogen is produced by performing water electrolysis, which it then combined with captured CO_2 to produce RN. This CCU process is possible due to the waste stream of CO_2 originating from the geothermal power plant. In this research, RN will be used to refer to renewably produced, or zero-emission fuels. This will serve as a general condition to assess the impact of CO_2 emissions, which is covered in the next sub-section. Furthermore, it is relevant to mention that Helgason's research is conducted within the context of the maritime sector in Iceland. Apart from the previously mentioned established measures by the IMO, Iceland is also aiming to introduce 10% renewable energy into the maritime sector until 2030, while fully phasing out the use of HFO, by 2050. As seen from Table 11, this latter detail is consistent with the considered scenarios from Wada et al. (2021), where HFO is also expected to be fully phased-out by 2050. As of 2018, Helgason states that HFO has a price of 57€/bbl, NG is priced at 380€/tonne, and RN at 921€/tonne. Similarly to Wada et al., Helgason et al. (2020) also proposes different plausible projections for the development of fuel prices (a "Low", a "Medium" and a "High" scenarios). In general, for all three considered fuels, the "Low" scenario can be interpreted as a BAU type of scenario, where current fuel prices are fixed throughout the assessed period, between 2018-2050. This means that, both HFO and NG would continue to benefit from lower prices, compared to RN. However, this would also imply that the process to produce RN is not prone to benefit from cost reductions, and that fossil-fuels could still maintain their price, despite the inevitable shifts on supply and demand balances in fuel markets, which is unreasonable. Both the "Medium" and "High" scenarios propose some annual growth rates, consistent with the possibility of implementing environmental protection legislature, and the respective market responses. In each of these scenarios, both HFO and NG are projected to suffer from price increases, while RN is expected to see its price lower, based on an average annual rate ($FuelPrice_{AR}$). For this research, the "Medium" scenario was chosen as a reference, and the respective annual growth rates for the three fuels are presented in Table 12 below. In the sensitivity analysis detailed in sub-section 2.8, price variations from the values used for 2030, 2040 and 2050 are covered.

Table 12 – Annual growth rates for every considered tanker fuel in mix, assumed from 2018 to 2050.

HFO	1.8%
LNG	0.6%
RN (zero-emission)	-0.7%

To then calculate the price $(Fuel_p)$ of each fuel f, for every year n until 2050, it was necessary to use the following formula, using the reference prices for 2018:

$$Fuel_{p_{f,n}} = Fuel_{p_{f,n-1}} \times FuelPrice_{AR} \qquad \forall f, n \tag{19}$$

Finally, with both the fuel mix and the respective prices, the remaining issue was to correctly calculate the amount of the alternative fuels required to operate the tankers. As mentioned above, the source for fuel consumption provided data in tons of HFO consumed per day. To solve the disparity between the energy contents of the analysed fuels, the daily fuel consumption $(Fuel_{day})$ was converted on an energy basis. By searching the energy content (EC) of both HFO $(11.10\ kWh/kg \approx 39.96\ GJ/t)$ and LNG $(13.33\ kWh/kg \approx 48\ GJ/t)$, it was easier to visualize the amount of each fuel that is needed, per day. Furthermore, since there is no concrete data on the energy content of RN, the value for LNG was used instead. To find the total fuel consumption $(Fuel_{RT})$ needed to cover a round-trip between Sines and Rotterdam, the following Equation (20) was used:

$$Fuel_{RT} = Fuel_{day} \times Days_{nav} + 0.1 \times Fuel_{day} \times Days_{TA} \tag{20}$$

With the relevant data collected regarding both the amount and shares of projected used fuel, as well as their annual price projections, it was possible to calculate the costs of fuel consumption (C_F). However, for the purpose of objectivity and succinctness, only the years 2030, 2040 and 2050 were considered. To do so, Equation (21) below was used.

$$C_{F_n} = Fuel_{RT} \times \sum Fuel_{p_{f,n}} \times Fuel_{share_{f,n}} \tag{21}$$

$$\forall f \quad \wedge \quad \mathrm{n} = 2030, 2040, 2050$$

2.5.3.4. CO_2 emissions costs

Having assessed the full consumption of fuel and the respective fuel mix of the used tankers, until 2050, it remained imperative to quantify and calculate the cost of the resulting CO_2 emissions. For that purpose, it was crucial to source the CO_2 emission factors (EF) of each of the considered fuels f. These were extracted from Agarwal (2021), who covers the fundamentals that are required for marine shipping. For HFO, a factor of 3.114 t-CO_2/t-fuel was considered, whereas for LNG the used factor was 2.750 t-CO_2/t-fuel. Since RN is assumed to be produced from RES, no CO_2 emissions are considered. Even in the specific case mentioned from Iceland, the waste stream of CO_2, which is used to produce fuel, is biogenic CO_2, meaning that it is disregarded from emissions analysis. To fully assess the total CO_2 emissions, in tons ($CO_{2_{RT}}$), resulting from a complete round-trip between the two locations, Equation (22) below was used:

$$CO_{2_{RT}} = \frac{Fuel_{RT}}{3.6\ GJ/MWh} \times \sum \frac{EF_f \times Fuel_{share_{f,n}}}{EC_f} \tag{22}$$

$$f = HFO, LNG \quad \wedge \quad \mathrm{n} = 2030, 2040, 2050$$

Note that, since $Fuel_{RT}$ was calculated based on the energy contents of the used fuels f, it was necessary to convert the correspondent share of each fuel to their respective mass values, using the values for EC mentioned in the section above. The associated CO_2 emissions were calculated for all tanker classes, for 2030, 2040 and 2050. In sub-section 3.2, the results breakdown the relevant results, and provide the associated CO_2 emissions of the LOHC conversion processes. This was done by adding the respective values for GWP for each LOHC, mentioned in sub-sections 2.4.1. and 2.4.2.

With the total amount of CO_2 emissions computed, the missing variable to calculate the cost of emissions was the projected price for CO_2 from 2030 to 2050. According to the European Commission, several emission reduction policies are expected to be implemented, at different points in time, if the established goals referred to in sub-section 1.1. are to be achieved. One of the acting measures was to establish the EU Emissions Trading System (ETS) (Meadows et al., 2019). The EU ETS works as a “cap-and-trade” system, and it is based on the yearly amount of CO_2-eq emitted by all installations covered within the system. The set “cap” will be reduced over time, with the objective of complying with the 55% net reduction target in GHG emissions by 2030. Future projections on the price of CO_2 vary considerably, with some studies estimating more conservative scenarios, where CO_2 could be priced as low as 38.00 €/t-CO_2 in 2030 and 55.00 €/t-CO_2 (Luckow, 2016), and other studies in the opposite spectrum projecting that CO_2 price could reach 400.00 €/t-CO_2 by 2050 (Kitous et al., 2010). Due to the vast disparity in future projections, the method followed in this research was to average a comprehensive amount of gathered estimations and find a fixed value for both 2030 and 2050. To interpolate in between the two values, an exponential trend line was drawn using Excel, and the respective exponential function was used. Thus, the price for CO_2 (CO_{2_p}), in the context of this research, started at

69.67 €/t-CO_2 in 2030, increased to 102.31 €/t-CO_2 in 2040, and finally reached its maximum value at 163.75 €/t-CO_2 in 2050. With this data, with was then possible to calculate the costs (C_{Em}) associated with the CO_2 emitted from covering a roundtrip between the two port locations, by using the Equation (23) presented below.

$$C_{Em_n} = CO_{2_{p_n}} \times CO_{2_{RT_n}}$$

$$with \quad \mathrm{n} = 2030, 2040, 2050 \tag{23}$$

It can be noted that, currently the shipping sector is not included under the ETS. However, the sector is expected to be included in 2022 (Sbraga & Malpas, 2020), and thus the GHG footprint and respective costs were considered in this research.

2.5.3.5. Total transportation costs (roundtrip)

Having assessed all the individual cost components, it was possible to calculate the total transportation costs to fulfil one roundtrip. Hence, for all tankers t, both LOHC systems s and for the years n of 2030, 2040 and 2050, the following Equation (24) was used:

$$C_{RT_{t,s,n}} = C_{DR_v} + C_{PC_{t,s}} + C_{F_{t,n}} + C_{Em_{t,n}} \qquad \forall\ t, s, n \tag{24}$$

2.5.3.6. Transportation requirements

The method to identify the necessary transportation requirements for a full year was designed based on the total amount of H_2 that each tanker was able to carry. Since each of the considered LOHCs provides a different volumetric density – as mentioned in sub-sections 2.4.1. and 2.4.2., TOL can retain 48 kg-H_2/m^3 and DBT retains 57 kg-H_2/m^3 – the yearly transportation requirements will differ accordingly. This portends that for each of the considered tankers, it will be necessary to travel a larger number of roundtrips per year when using the TOL-MCH system, to fully transport the total amount of H_2 from Sines to Rotterdam. Table 13 below shows the amount of H_2 that each tanker can carry, when loaded either with MCH or with PDBT.

Table 13 – H_2 capacity in t, for every considered tanker class and LOHC system.

		Small tankers	MR Product Tanker (Handymax)	Supramax	Panamax	Aframax
TOL-MCH	t-H_2	1,453.60	2,634.65	3,094.85	3,625.85	4,687.85
DBT-PDBT	t-H_2	1,710.00	2,943.96	3,675.13	4,305.70	5,566.83

As observed in table, the discrepancy in H_2 capacity ($H_{2_{CAP}}$) can vary from around 250 t for the Small Tankers class, to nearly 1,000 t for the Aframax class. With the relevant information provided, hence it was possible to calculate the total number of roundtrips per year RT_{year} required to fully transport the projected amount. To this end, since H_2 is only carried from Sines to Rotterdam, for each of the considered tankers t and LOHC systems s, Equation (25) below was used.

$$RT_{year_{t,s}} = ROUNDUP\left(\frac{H_{2_{year}}}{H_{2_{CAP_{t,s}}}}\right) \qquad \forall \;\; t,s$$

(25)

$$w/ \;\; H_{2_{year}} = Total\ amount\ of\ transported\ H_2\ per\ year$$

2.5.3.7. Total transportation costs (year)

Following the method explanation for C_{RT} and RT_{year}, the total yearly transportation costs for all tankers t and LOHC systems s, for the years n 2030, 2040 and 2050 were calculated using the Equation presented below.

$$C_{T_{t,s,n}} = C_{RT_{t,s,n}} \times RT_{year_{t,s}} \quad \forall\, t,s,n$$

(26)

2.6. LOHC storage

The following two sub-sections cover the round-trip requirements and respective costs of storing the LOHCs in each of the ports, as mentioned in sub-section 2.1. It is assumed that, for Sines and Rotterdam, an equal amount of storage space is available for both the hydrogenated and the dehydrogenated forms of the considered LOHCs. The yearly storage schedule was planned contingently on the assumed nominal capacity, referred to in sub-section 2.3.3. Furthermore, for the purpose of ensuring enough capacity is provided, and as general good practice, it was assumed that the available tank capacity always equalled 120% of the tanker's volumetric capacity, regardless of the class used (personal communication, 2021a).

2.6.1. Storage requirements

The requirements for the storage of LOHC for both Sines and Rotterdam were based on the number of days necessary to complete both the hydrogenation process in Sines, as well as the dehydrogenation process in Rotterdam. This information was extracted from Carvalho's research (2021), which provides the mass balance for both process reactions. Starting with the hydrogenation process, the optimized design for the hydrogenation facility, when using TOL, is fed with H_2 at a mass flow rate of 6,332.39 kg/h and with 94,642.9 kg/h of the respective LOHC. This reaction yields a product stream of yields around 102,221 kg/h of MCH. This corresponds to roughly 2,453.30 t or 3,186.11 m^3 of MCH, per day. For the DBT-PDBT system, the H_2 flows into the reactor at a rate of 6,509.12 kg/h, with a debit of 99,811.3 kg/h of DBT. The optimized design for hydrogenation yields PDBT at a mass flow rate of 106,320 kg/h, which corresponds to 2,551.68 t or 2,804.04 m^3 per day of PDBT. These two mass outflows are related with the cargo that is projected to be shipped from Sines, or to put it differently, with the supply side of the considered logistics chain. Regarding the dehydrogenation process, the optimized design proposed by Carvalho yielded results for the outflows of H_2 and the respective dehydrogenated compounds. Within the context of this research, this optimized design is assumed to be used in Rotterdam as a dehydrogenation plant, supplying the projected demand for green H_2. For the TOL-MCH, the dehydrogenation process allows for an extraction of H_2 at a mass flow rate of 6,254.55 kg/h and returns TOL at a rate of approximately 96,028 kg/h, while the DBT-PDBT dehydrogenation process yields 6,252.15 kg/h of H_2 and returns 100,067 kg/h of DBT. This is equivalent to 2,304.68 t/day or 2,618.95 m^3/day for TOL, and to 2,401.61 t/day or 2,309.24 m^3/day for DBT.

With the relevant data gathered, regarding the outflows in t/day ($MassFlow$), the next step was calculating the amount of time, in total number of days, for each of the conversion processes to yield enough amount of LOHC, in both their hydrogenated and dehydrogenated forms, to fully load the considered tankers. The tankers were assumed to be fully loaded for every trip, according to their mass and volumetric cargo boundaries, presented in Table 10. Also, as presented in sub-section 1.4.1, the two assessed LOHCs have different densities. Apart from this, the respective hydrogenation processes convert them into lighter compounds, which occurs disproportionately since their volumetric storage densities also do not match. To solve this problem, the amount that each tanker can carry ($Cargo_{MAX}$) of each of the four transported products p was computed by always meeting either their mass or their volumetric limit. Using the values for density of each of the transported products, i.e., the hydrogenated and dehydrogenated forms of both LOHCs, the volumetric limits (Vol_{MAX}) of the tankers t were converted to mass and compared with the respective mass limits ($Mass_{MAX}$), through Equation (27) below.

$$Cargo_{MAX_{t,p}} = MIN\left(Vol_{MAX_t} \times Density_p; Mass_{MAX_t}\right) \qquad \forall\, t, p$$

(27)

Considering the values for $Cargo_{MAX_{v,p}}$ the total number of days required for the hydrogenation processes to occur, for both TOL and DBT, i.e., the days required for storage in Sines, for one roundtrip was calculated using the following Equation:

$$Storage_{days,Sines_{t,p}} = ROUNDUP\left(\frac{Cargo_{MAX_{t,p}}}{MassFlow_p}\right)$$

(28)

$$\forall\, t \;\wedge\; \mathrm{p = TOL, DBT}$$

Conversely, the days required for storage in the port of Rotterdam, per roundtrip, were calculated as follows:

$$Storage_{days,Rotterdam_{t,p}} = ROUNDUP\left(\frac{Cargo_{MAX_{t,p}}}{MassFlow_p}\right)$$

(29)

$$\forall\, t \;\wedge\; \mathrm{p = MCH, PDBT}$$

By summing the counterparts for both the TOL-MCH and the DBT-PDBT systems, it was possible to assess the total number of storage days ($Storage_{days,RT}$), for all tankers and both LOHC systems, that are required to complete a roundtrip between Sines and Rotterdam. Moreover, data was collected concerning the associated emissions. During the loading of the storage tanks, the tankers' cargo pumps mentioned in sub-section 2.5.3.3. are utilized, and the respective emissions were addressed as detailed in sub-section 2.5.3.4. Conversely, during the unloading of the storage tanks, different pumps belonging to the storage unit are used (personal communication, 2021c). For this research, the emissions associated with the electric pumps are assumed to be included in the consumption of the tanker's auxiliary engines, referred to in sub-section 2.5.3.3.

2.6.2. Storage cost

Converging with the method used to assess the costs of transportation, the storage of LOHC at both ports was likewise calculated based on the requirements for one roundtrip. It was necessary to identify suitable storage tariffs that could apply to the LOHCs considered in this research. For this purpose, the Global Tank Storage Rate Report provided by Insights Global

(2021) served as a reliable source. The report in question was the quarterly edition from April 2021, and the sourced tariffs for storage of LOHCs were 2.00 €/m^3/month for the TOL-MCH system and 3.75 €/m^3/month for the DBT-PDBT system. These tariffs refer to the average that Insights Global highlights and are based on a range of tariffs which are indicative and based on typical tank sizes, throughput allowances and a one-year contract duration. Additionally, for the purpose of this research, the tariffs were adjusted for inflation. Thus, a fixed 1% annual growth rate was applied, assumed for the timespan considered. This assumption was based on data stating that, currently, there is no clear answer regarding the future profitability assessment of the tank storage market in Europe (Insights Global, 2019). This topic is further addressed in sub-section 2.8. The difference between the applied tariffs is grounded on the different chemical characteristics of the considered LOHCs. Firstly, the tariff applied for TOL was the average usually used for the storage of middle distillates like gasoil and diesel (MD). As mentioned in sub-section 2.4, TOL has the lowest boiling between the two chosen LOHCs, and the kinematic viscosity is similar to that of MD products. Conversely, for DBT, which as detailed in sub-section 2.4.2, is a heavier compound than TOL, and has a considerable high boiling point (Carvalho, 2021), the assumed and most suitable tariff was the average used for (residual) fuel oil (FO). Since the sourced tariffs ($Storage_{month}$) were related to monthly charges, a conversion was performed to proportionally calculate the respective daily expense. This was done by following Equation (30) below.

$$Storage_{tariff} = Storage_{month} * \frac{12\ months}{365\ days} \tag{30}$$

With the set daily charges for both LOHCs, it was possible to compute the storage costs associated with one roundtrip between both locations. With the results from $Storage_{days,RT}$ for each of the considered LOHC systems s and tankers t, the total storage costs for one roundtrip ($C_{Storage_{RT}}$) were calculated using the Equation below.

$$C_{Storage_{RT}}{}_{t,s} = Storage_{tariff}{}_{s} \times Storage_{days,RT}{}_{t,s} \quad \forall\, t, s \tag{31}$$

$$w/\ \ s = \ \ TOL - MCH, \qquad DBT - PDBT$$

2.7. Tanker fleet requirements

Having quantified the technical transportation and storage requirements to complete a roundtrip between Sines and Rotterdam, the following step focused on extrapolating these requirements to fit a timeframe of one full year. This was done to ensure that the projected annual amount of green H_2 to be exported to Rotterdam is completely fulfilled. Firstly, accounting for the yearly target of transporting 50 kt of green H_2 the number of necessary roundtrips (RT_{year}) was assessed, as detailed in sub-section 2.5.3.6. The extrapolation for the timeframe of one year was further constrained based on the results of $Storage_{days,RT}$, which encompassed the total days required for the LOHCs to be stored, in tanks, both in Sines and in Rotterdam, to complete one roundtrip. The reason for adopting this approach was because $Storage_{days,RT}$ focuses on the amount of time it requires to perform the hydrogenation and dehydrogenation processes. Since this step takes the longest amount of time – as shown in sub-section 2.2, the electrolyser in Sines produces H_2 at a rate of roughly 1.40 kt-H_2/day, while the hydrogenation and dehydrogenation steps only process H_2 within a range of roughly 150.0 to 152.0 t-H_2/day – this means that the transportation schedules were built around the projected plans for H_2 storage within LOHCs. The method regarding the optimization for the number of tankers used ($Fleet$) was grounded on the criteria that the total number of storage days per year could not surpass the assumed nominal yearly capacity of 8,000 h/year, or roughly 333.33 days/year. Apart from this condition, it was also pivotal to minimize the yearly costs for LOHC storage ($C_{storage_{year}}$). Thus, the values for $Fleet$, for each of the assessed tankers t and LOHC systems s was calculated by satisfying the following equation:

$$MIN\left(C_{storage_{year_{t,s}}}\right) \tag{32}$$

$by\ changing$:

$$Fleet$$

$subject\ to$:

$$RT_{year_{t,s}} \times Storage_{days,RT_{t,s}} \leq 333.33\, days/year \quad \forall\, t,s \tag{33}$$

Furthermore, the values for $Fleet$ were constrained to yield only integers.

2.8. Sensitivity analysis

To assess the sensitivity of each of the mentioned cost components, two contrasting scenarios were considered based on the yearly capacity of green H_2 being transported to Rotterdam ($H2_{year}$). The first alternative scenario, henceforth called the "BEST" scenario, assumes double the amount of H_2 assumed in the "REF" scenario i.e., 100 kt per year. Contrarily, the "WORST" scenario presents a lower yearly capacity of 20 kt of H_2 delivered. A comprehensive set of parameters was chosen for this analysis, each impacting all the regarded cost components from the previous sub-sections. For every parameter, an interval was established based on the values assumed for the "REF" scenario. Each of the elected parameters is detailed in Table 14 below. The table also provides the respective variation that was considered for each of the parameters, compared with the base values in the "REF" scenario. Starting with the "H_2 delivered per year" parameter, this changed the value for $H_{2_{year}}$ mentioned in sub-section 2.5.3.6. Hence, the values for $Fleet$ was also influenced, following the methods presented in sub-section 2.7. However, changing "H_2 delivered per year" impacts not only the transportation and storage costs, but also the hydrogenation and dehydrogenation costs calculated by (Carvalho, 2021). Consequently, the "H_2 break-even price" for each of the LOHC systems, presented in sub-section 2.4.4, is also affected. To account for this variation, scale law was applied to the costs shown in sub-sections 2.4.3 and 2.4.4, as described by Blok & Nieuwlaar (2017). Thus, for each of the alternative scenarios s, Equation (34) below was used.

$$C_s = C_{REF} \times \left(\frac{H_{2_{year_s}}}{H_{2_{year_{REF}}}} \right)^{SF} \tag{34}$$

$With$:
$C_s = cost\ for\ each\ of\ the\ cost\ components, for\ scenarios\ s$ "HIGH" and "LOW"
$C_{REF} = cost\ for\ each\ of\ the\ cost\ components, for\ scenario$ "REF"
$SF = Scale\ factor$

The scale factor SF here is used to account for economies-of-scale. When considering the LOHC costs for raw materials ("Catalyst"), utilities ("Electrical" and "Heat") and "Waste treatment", a scale factor of 1 was used. This implies that these costs vary linearly, according with the assumed value for the "H_2 delivered per year" parameter. The costs for "Maintenance and repair" and "Operating labour", as well as the value for "Total CAPEX" were varied using an SF equal to 2/3. This value is commonly used for costs related to capital investment, and it implies that these costs vary less than proportionally with scale (Blok & Nieuwlaar, 2017).

Table 14 - Range for parameters considered for "BEST" and "WORST" scenarios

		BEST	WORST
H_2 delivered per year	kt	100	20
Daily rates		-75%	+75%
Port costs		-25%	+25%
CO_2 price		-50%	+100%
Fuel price		-50%	+50%
Tank storage rates		-15%	+15%
H_2 production cost		-25%	+25%

Following with the daily rates charged for tankers, as explained in sub-section 2.5.3.1, due to the high volatility found in historical data, no variation trends were assumed across the timespan between 2021 and 2050. When looking at historical data, from 1992 to 2002, for example, daily rates for Handymax class ships recorded no significant variation (Merikas et al., 2013). However, from around 2004 to 2010, these rates experienced abnormal fluctuations, increasing at a rate of over 100%, for repeated years. This was related to the coinciding increase in oil prices, thus after 2010, the daily rates decreased to nearly the same values before 2004 (Başer & Açık, 2018). Since 2015, rates have been steadily increasing once again, with values in April 2021 being the highest since 2005 (Hellenic Shipping News, 2021). By acknowledging the inconsistency of historical data, it was assumed that it would not be unreasonable to consider substantial changes for the assessed years. Thus, for this analysis, the values from 2030, 2040 and 2050 were subject to percentual changes of -75% and +75%, respectively. For the case of the port costs, since historical data is consistent with a 1% increase per year, coinciding with the adjustment for inflation applied for the daily rates, the alternative scenarios were considered with slightly lower variations. The correspondent values for 2030, 2040 and 2050 were varied in -25% and +25%. In respect to the fuel costs (C_F), the respective fuel prices were assessed in terms of their volatility. Data was collected on historical data and the future projections for the prices of bunker fuel (Bradley et al., 2009), crude oil and NG (Knoema, 2021; Kolesnikov, 2014). Due to the lack of historical data, only future projections were used to infer on the price of bioethanol (IRENA, 2020). Firstly, bunker fuel was shown to increase substantially, starting from 1996 to 2006 – at a rate of around 13.5% per year. This rate of increase was more or less consistent until 2018 (Sharples, 2019). However, due to the recent COVID-19 pandemic, and the current price war between Saudi Arabia and Russia, prices have decreased nearly 70% in only one year (Argus, 2020). Since bunker fuel prices are perceived to fluctuate proportionately with crude oil (Brouer et al., 2014), and are expected to be just as volatile, data was also collected on the respective future projections. Accordingly, the price of crude oil is projected to increase between 1.8% and 4.5% every year, from 2020 to 2050 (Kolesnikov, 2014). For NG, the collected data projected an increase in price between approximately 2.3% to 3.9% per year, between 2020 and 2050. Lastly, the price of bioethanol is projected to decrease at a rate of roughly 1.2% per year (IRENA, 2020). To encompass a comprehensive range of possibilities, the individual fuel prices computed for the relevant years were subject to changes of -50% and +50%. It is noteworthy that, based on the fuel mix used in $Fleet$, as referred to in sub-section 2.5.3.3, these impacts will vary considerably between 2030 and 2040. When focusing on the volatility of the emissions costs (C_{Em}), the chosen parameter was the price of CO_2. As detailed in sub-section 2.5.3.4, the projections for the price of CO_2 are highly discordant. For this reason, the respective prices for CO_2 in the “REF” scenario, in 2030, 2040 and 2050, were subject to variations of -50% and +100%. Additionally, as referred in sub-section 2.6.2, the tariffs collected for tank storage of the considered LOHCs were only adjusted for inflation between 2021 and 2050. Since fluctuations in the oil market can have opposite impacts on the tank storage market (Insights Global, 2019), this analysis considered variations of -15% and +15% for the values in 2030, 2040 and 2050. Finally, the projected price for H_2 produced in Portugal, mentioned in sub-section 2.2, was also considered in this analysis. The assumed prices for 2030, 2040 and 2050 were subject to -25% and +25% variation rates. All the parameters were varied using Equation (35) below, with the respective interval variations (VAR) for each scenario s. The results for this analysis were extracted to assess the impact of individually changing each of the mentioned parameters, for the alternative scenarios. Furthermore, the cumulative effect was also calculated, allowing to analyse the potential impact of changing every parameter, simultaneously, on the final price of H_2. Additionally, as highlighted in Table 14, the results for the “BEST” scenario were aggregated based on the respective interval variations that yielded a decrease in the final price of H_2. Conversely, for the “WORST” scenario, all the impacts that resulted in an increase of the final price of H_2 were allocated. As a note, it is relevant to refer that the assumed fuel mix for $Fleet$ mentioned in sub-section 2.5.3.3. was considered for the sensitivity analysis. However, even for the most extreme variations in this parameter, the observed results were negligible.

$$C_{s,n} = C_{REF,n} \times (1 + VAR_s)$$
$$\forall\, n = 2030, 2040, 2050 \tag{35}$$

3. Results

The extracted results here shown focus on the economic and GHG emissions impact for 2030, 2040 and 2050. The economic results are shown first, in sub-section 3.1, followed by the results regarding the GHG emissions in sub-section 3.2. A macro analysis of the economic results is firstly showed for the most viable combination for the supply chain of green H_2 i.e., the cheapest option. Secondly, a detailed breakdown of the transportation and tank storage costs is provided, for all tanker classes. The results for the GHG footprint here shown are related to the cheapest option assessed in the economic analysis, and include the LOHC conversion processes, as well as the transportation and tank storage. Finally, the results for the performed sensitivity analysis are provided in sub-section 3.3.

3.1. Economic analysis

This sub-section focuses on the economic results from the methods presented in sub-sections 2.5.3. through 2.7. Firstly, a detailed look is provided into the cheapest options to transport each of the LOHC systems from Sines to Rotterdam. This will focus on the entire supply chain, covering the methodology in section 2. The following sub-sections allow for a more in-depth analysis, showing the general results for both transportation and storage of LOHCs, across all the tanker classes considered. The final sub-section highlights the combined impacts of both transportation and storage, which was vital to assess how these two components balance between each other.

3.1.1. Total supply chain cost

The results for the total supply chain costs, which help to identify the potential price of green H_2, after the dehydrogenation process in Rotterdam, are presented below in Figure 14 and Figure 15. Furthermore, Table 15 provides the approximated values and the respective relative shares of each of the cost components. Apart from the costs for transportation and tank storage, assessed in this research, here are also included the "H_2 break-even price" mentioned in sub-section 2.4.4, and the cost of producing H_2, addressed in sub-section 2.2. The first notable aspect is that the Small Tankers class was deemed as the cheapest option, for both LOHC systems. This was determined by the transportation and tank storage costs, further detailed in the following sub-sections. Starting with the TOL-MCH system, the "LOHC supply chain" – as referred to in Table 15 is projected to increment in roughly 1.872 to 2.290 €/kg-H_2, between 2030 and 2050, for the TOL-MCH system. This amounts to a share of around 39.8% of the final price of H_2 in 2030, increasing to approximately 62.1% in 2050. This considerable leap in the associated share can be explained partly from the increase in transportation costs. Additionally, the price associated with the production of H_2 is assumed to decrease over time, as explained in sub-section 2.2. Apart from this, it is also relevant to mention that the transportation and tank storage costs account for less than 20% of the "LOHC supply chain". The total supply chain costs for TOL-MCH are projected to decrease 1.43% between 2030 and 2040. Between 2040 the 2050 the costs are expected to drop roughly 20.34%. The disparity in this fluctuation is explained by the substantial decrease in the production costs of H_2 from 2040 to 2050.

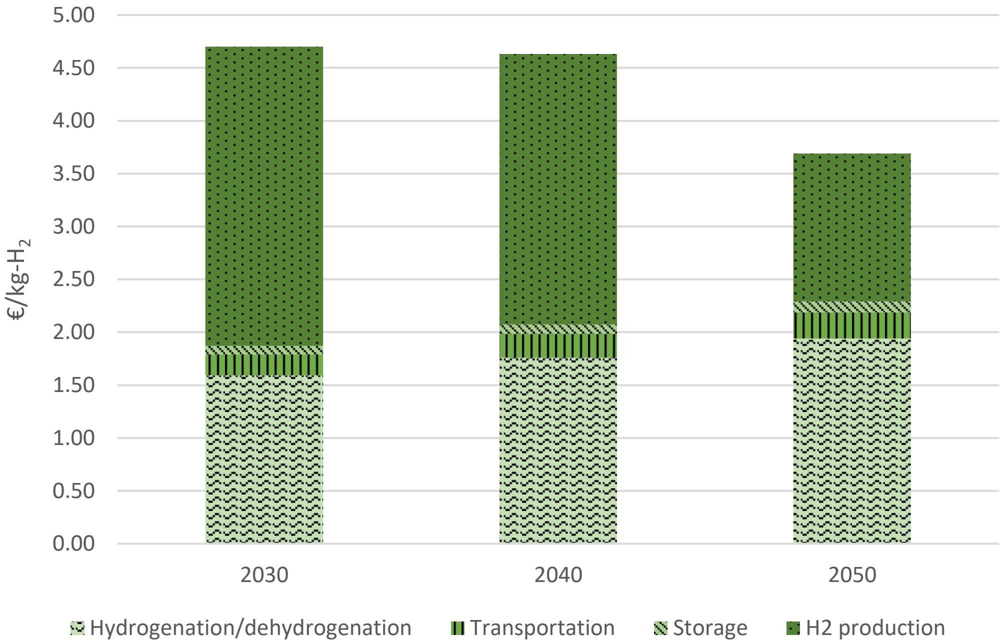

Figure 14 - Total supply chain costs for the TOL-MCH system, in € per kg of H_2 delivered. Results shown for Small Tankers in 2030, 2040 and 2050.

For the DBT-PDBT system, the "LOHC supply chain" varies from 1.447 €/kg-H_2 in 2030, to 1.772 €/kg-H_2 in 2050. Accordingly, the relative shares are also lower compared to TOL-MCH, since the assumed costs for H_2 production are the same. Overall, using the DBT-PDBT system and the Small tankers class to transport green H_2 is the most viable option, with H_2 supply chain costs projected to be 4.276 €/kg-H_2 in 2030, 4.163 €/kg-H_2 in 2040, and finally at 3.172 €/kg-H_2 in 2050. This expresses a relative decrease of approximately 2.64% between 2030 and 2040, and of 23.81% between 2040 and 2050. The relevance of the obtained results was inferred on, and further discussed in section 4. Based on the parameters considered for the sensitivity analysis, presented in sub-section 2.8, the results here shown were assessed on their volatility. The relevant results for this analysis are shown further in sub-section 3.3.

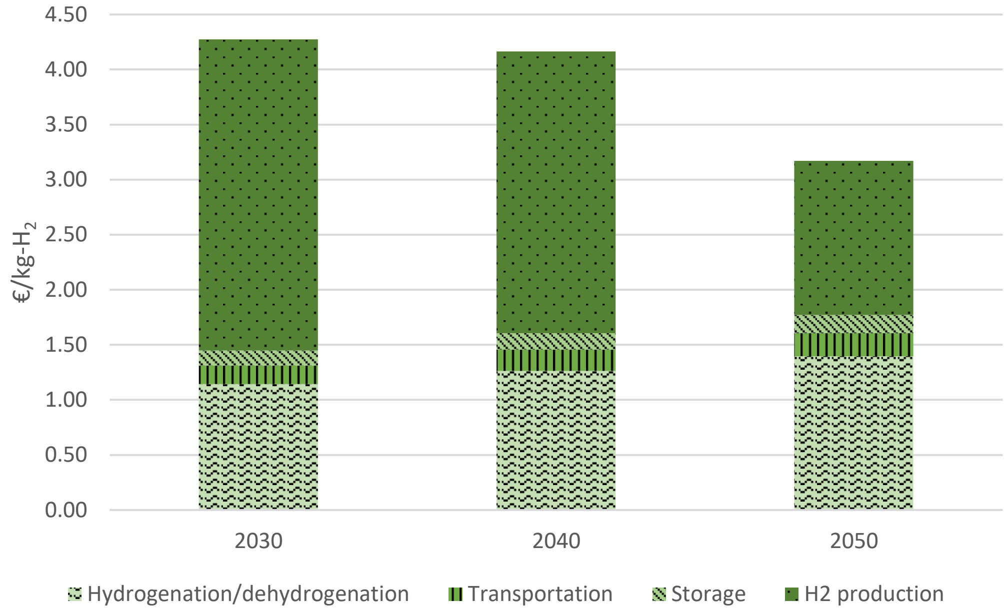

Figure 15 - Total supply chain costs for the DBT-PDBT system, in € per kg of H_2 delivered. Results shown for Small Tankers in 2030, 2040 and 2050.

Table 15 – Total cost for the green H_2 supply chain, for 2030, 2040 and 2050. Results shown for TOL-MCH and DBT-PDBT using Small tankers, in €/kg-H_2 and the respective relative share.

€/kg-H_2	**2030**		**2040**		**2050**	
TOL-MCH – Small Tankers		share of H_2 final price		share of H_2 final price		share of H_2 final price
Transportation	0.197	4.2%	0.225	4.9%	0.247	6.7%
Storage	0.083	1.8%	0.091	2.0%	0.101	2.7%
H_2 break-even price	1.592	33.9%	1.758	38.0%	1.942	52.6%
LOHC supply chain	**1.872**	**39.8%**	**2.075**	**44.8%**	**2.290**	**62.1%**
H_2 production	2.828	60.2%	2.558	55.2%	1.400	37.9%
Total supply chain cost	**4.700**		**4.633**		**3.690**	
DBT-PDBT - Small Tankers						
Transportation	0.168	3.9%	0.192	4.6%	0.211	6.6%
Storage	0.135	3.2%	0.149	3.6%	0.165	5.2%
H_2 break-even price	1.144	26.8%	1.264	30.4%	1.396	44.0%
LOHC supply chain	**1.447**	**33.9%**	**1.605**	**38.6%**	**1.772**	**55.9%**
H_2 production	2.828	66.1%	2.558	61.4%	1.400	44.1%
Total supply chain cost	**4.276**		**4.163**		**3.172**	

3.1.2. Transport

Results for the economic assessment of transporting LOHCs from the port of Sines to the port of Rotterdam are presented in this sub-section. As mentioned in the methodology section, the transportation expenses were calculated for a roundtrip between the two locations, and further extrapolated to a full year, while fulfilling the targeted export amount. Also, the computation included all considered tankers, and spanned the years between 2030 and 2050. Nonetheless, this sub-section will focus on the values calculated for the years 2030, 2040 and 2050, which allows to better compare the temporal variations of the results obtained.

3.1.2.1. Costs per roundtrip

Figure 16 shown below displays the total projected costs, in M€, for a roundtrip between Sines and Rotterdam. For each of the tankers represented, the pair of stacked columns refers to the two assessed LOHC systems, with each of the cost components discriminated. Also, for easier visualization, the values here presented were averaged for all cost components, across the results for 2030, 2040 and 2050.

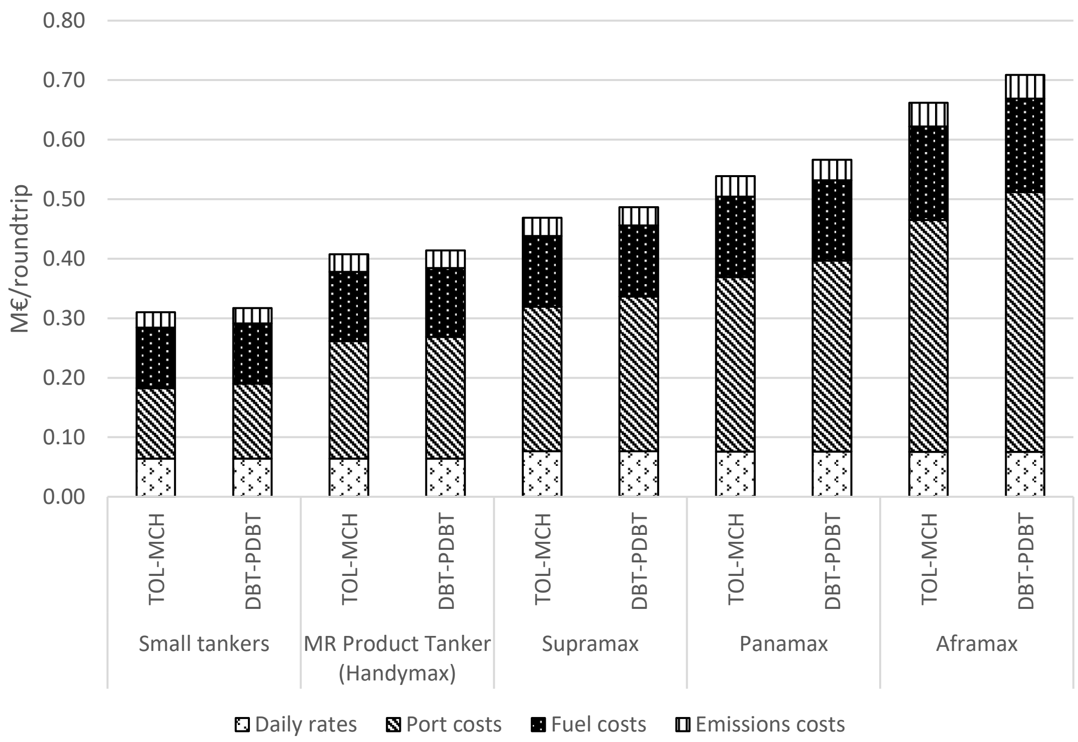

Figure 16 - Total costs per roundtrip and per cost component, in M€, for all considered tankers and LOHC systems. All costs components were averaged for the entire timespan, between 2030 and 2050.

Firstly, it can be observed that the transportation costs for a roundtrip increase as the size of the tanker also increases. Using Small tankers would cost approximately 310,176 €/roundtrip for the TOL-MCH system, and around 317,308 €/roundtrip for the DBT-PDBT system. On the opposite extreme, using the Aframax class would cost roughly 662,130 and 708,879 €/roundtrip, for the TOL-MCH and the DBT-PDBT systems, respectively. Looking closely at the individual cost components, it is clear that the port costs C_{PC} have the highest variation across the considered tankers, with the Aframax class being charged more than three times the amount charged for the Small tankers class. This can be explained from the fact that C_{PC} is directly related with the amount of cargo, in weight, that each tanker carries. Regarding the daily rates C_{DR}, it is notable that the Supramax class yielded the highest value for all tankers. This result is explained since the Supramax class is assumed to travel at the same cruising speed as the lowest two tanker classes i.e., to have a high value for $Days_{nav}$. Additionally, being over 50,000 DWT capacity, it is considered to have the same value for $Days_{TA}$ as the biggest two tanker classes, thus having the highest value for $Days_{RT}$ of all the considered tankers. Seeing that the values for all cost components were averaged for the assessed period, the Figure above does not allow for a relevant analysis of how these cost components will vary, as well as their overall impact on the total transportation costs for a roundtrip. For this purpose, Figure 17 and Figure 18 are provided below. Here it is possible to see how the respective roundtrip costs will vary between 2030, 2040 and 2050, for both LOHC systems and all considered tankers. The first figure here shown corresponds to the TOL-MCH system. Each of the tanker classes is identified by a different marker. Furthermore, the temporal variation is highlighted across the horizontal axis, with the values shown in M€/roundtrip. The second figure shows the respective results for the DBT-PDBT system.

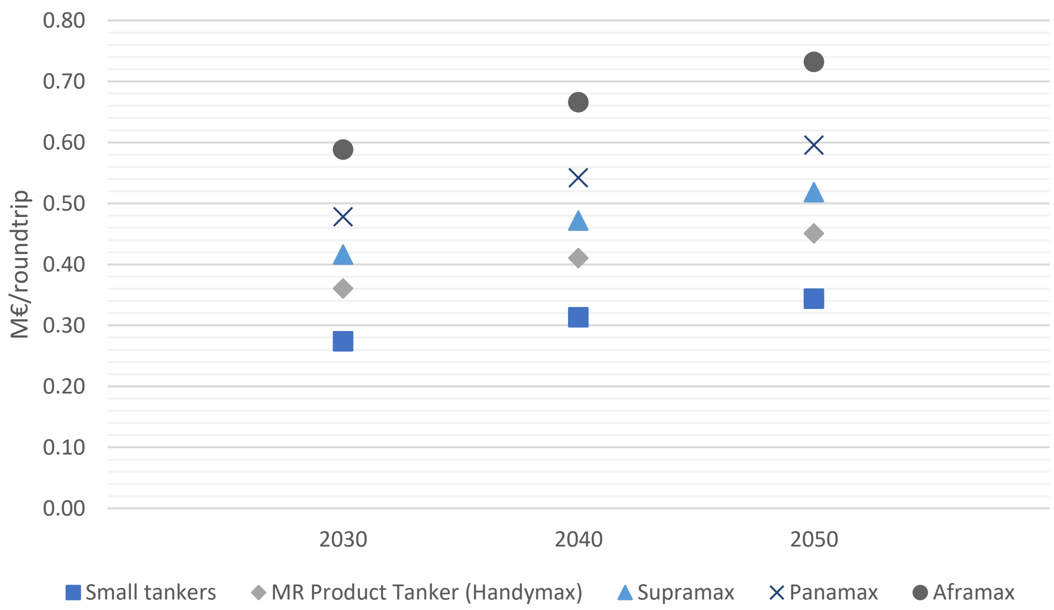

Figure 17 – Transport costs per roundtrip for the TOL-MCH system. Results shown for all tanker classes, in 2030, 2040 and 2050.

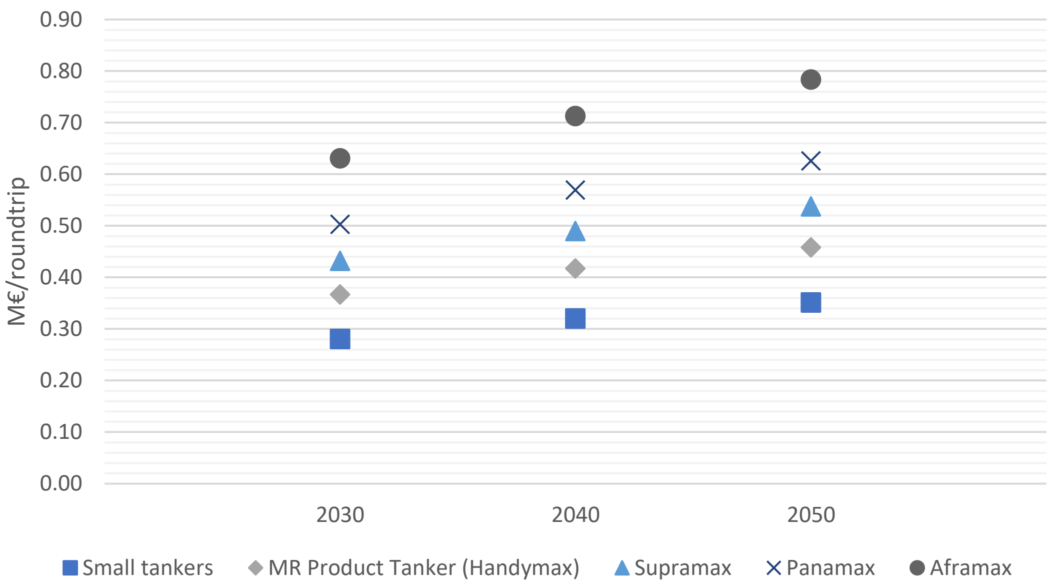

Figure 18 - Transport costs per roundtrip for the DBT-PDBT system. Results shown for all tanker classes in 2030, 2040 and 2050.

The results show that, for both LOHC systems, and across all tanker classes, the total transportation cost per roundtrip C_{RT} increases from 2030 to 2050. Apart from this, it can also be stated that the respective increase from 2030 to 2040 is higher than the leap from 2040 to 2050. On average, costs increase around 13.2-14.3% between 2030 and 2040, and approximately 9.7-9.9% between 2040 and 2050. Finally, when comparing the smaller and the bigger tanker classes, it can be noted that the difference between the assessed years is more accentuated for the bigger tanker classes. All these impacts are fully caused by the variation in both the fuel costs C_F and the respective emissions costs C_{Em}. Firstly, due to the gradual change of used fuels $Fuel_{share}$, shown in Table 11, from sub-section 2.5.3.3, as well as the respective price variation rate $FuelPrice_{AR}$, the fuel prices $Fuel_p$ increase considerably between 2030, 2040 and 2050. The average fuel price considered for 2030 is 9.27 €/GJ-fuel, increasing to 12.65 €/GJ-fuel in 2040 and finally to 14.18 €/GJ in 2050. Secondly, regarding the emissions costs C_{Em}, two relevant aspects contribute towards a balance between a positive and a negative effect. As mentioned in sub-section 2.5.3.3, the shift in fuels used contribute towards a lower level of CO_2 emissions. This impacts the transportation cost by lowering C_{Em}. However, as referred to in sub-section 2.5.3.4, CO_2 emissions are assumed to be priced at an increasing rate, with the respective price in 2050 being around 53.36 % higher than in 2040, and around 135.05 % higher than in 2030. As such, this attenuates the previous decrease in C_{Em}. Figure 19 shown below displays how both C_F and C_{Em} are projected to vary across the considered timespan.

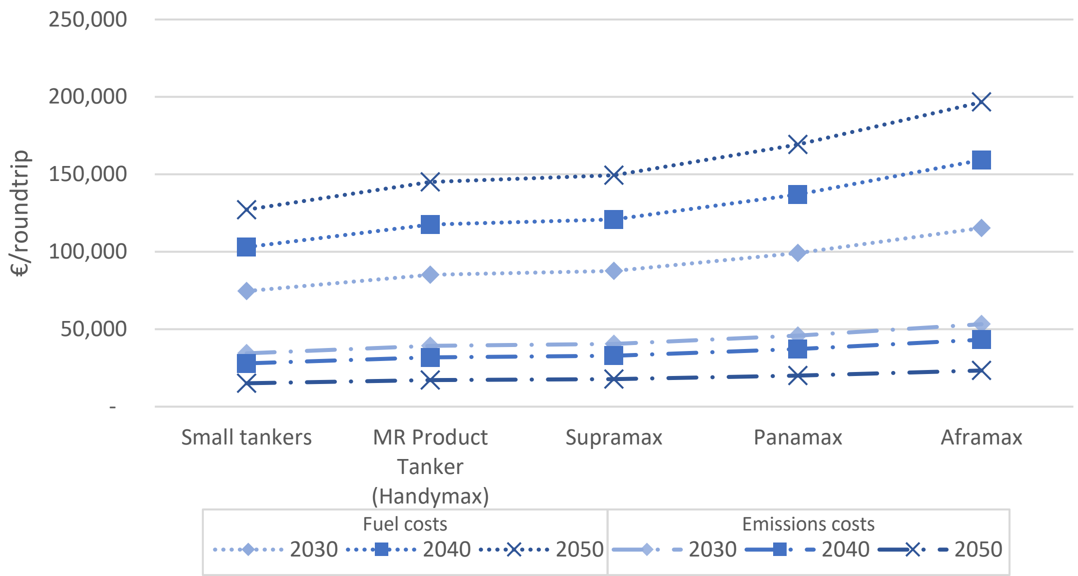

Figure 19 - Comparison between fuel costs and emissions costs, per roundtrip, in €, for all considered tankers, for 2030, 2040 and 2050

As it can be observed, fuel costs C_F have a slightly higher variation from 2030 to 2040, while the emissions costs C_{Em} have the respective lowest variation between the same period. It is due to these two reasons that the increase from 2030 to 2040 is higher than the respective increase from 2040 to 2050, as shown in Figure 17.

3.1.2.2. Costs per year

As detailed in sub-section 2.5.3.6, following the calculation for the transportation costs related to one roundtrip, it was necessary to extrapolate these costs to comply with one full year of green H_2 transport. Considering the method explained in sub-section 2.7. regarding the necessary number of tankers $(Fleet)$ required to comply with the determined conditions, it was assessed that $Fleet$ was equal to three tankers, when $H_{2_{year}}$ is equal to 50 kt. The results are firstly shown in total costs per year, both in Figure 20 and the respective Table 16 below. From the figure, it is easily observable how the total yearly costs are projected to have a downward trend, when looking at the tankers from smallest to largest. This is mainly explained since, for the smaller tankers, the total number of required roundtrips that are necessary per year (RT_{year}) is higher, which in turn substantially boosts the amount of port costs C_{PC} that are due. Moreover, the expenses related to fuel C_F and respective emissions C_{Em} are also higher for the smaller tankers. Even though the larger tankers consume more fuel per day, due to their size, the difference in daily fuel consumption $(Fuel_{day})$ only amounts to an increase of roughly 53.85 % when comparing the Aframax class with the Small tankers class. Conversely, the amount of total cargo, per volume unit, that the Aframax tanker can carry is around 222.50 % more than the respective capacity for the Small tankers. This implies that, for the same amount of cargo, the smaller tankers required a relatively higher amount of fuel to transport it. Looking closely at the values contained in the table, the lowest transportation costs could be expected in 2030, when using the Aframax class to transport green H_2 stored in DBT, with around 5.67 M€ required in that year. These costs are projected to rise to 6.41 M€ in 2040 and to 7.05 M€ in 2050. On the opposite side, transporting TOL-MCH in 2050 would be the most expensive option, with the highest expense related to Small tankers, at approximately 12.37 M€ for that year.

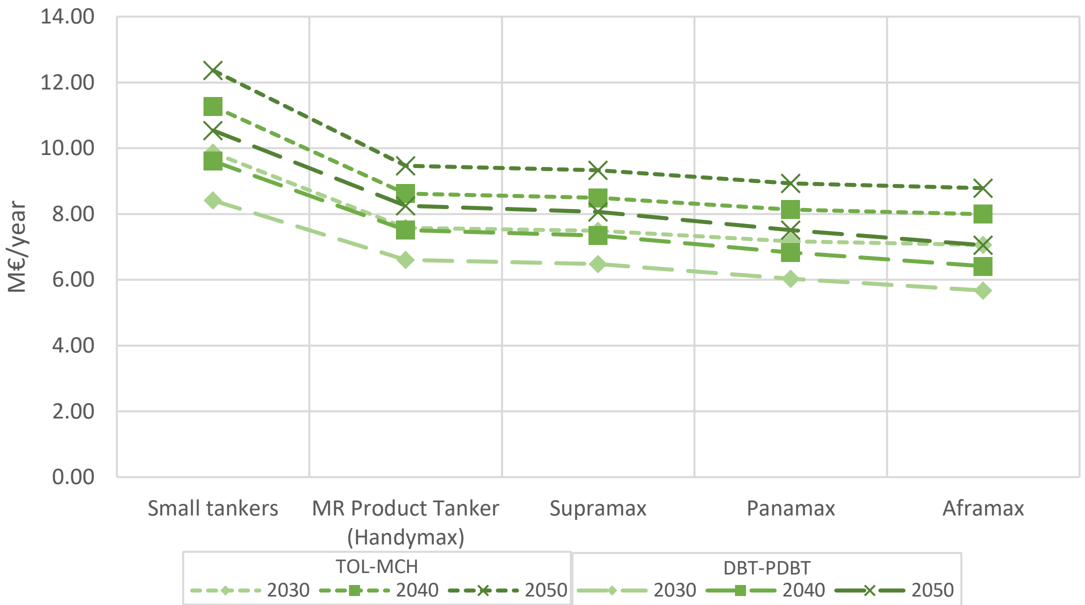

Figure 20 - Total transportation costs in M€/year, for all considered tankers and LOHC systems, for 2030, 2040 and 2050.

Table 16 - Total transportation costs in M€/year, for all considered tankers and LOHC systems, for 2030, 2040 and 2050.

M€/year	**2030**		**2040**		**2050**	
	TOL-MCH	**DBT-PDBT**	**TOL-MCH**	**DBT-PDBT**	**TOL-MCH**	**DBT-PDBT**
Small tankers	9.86	8.41	11.27	9.61	12.37	10.54
MR Product Tanker (Handymax)	7.57	6.60	8.62	7.51	9.46	8.25
Supramax	7.49	6.48	8.49	7.34	9.33	8.07
Panamax	7.17	6.03	8.13	6.83	8.94	7.51
Aframax	7.06	5.67	7.99	6.41	8.78	7.05

3.1.2.3. Costs per kg-H_2 transported

The results shown below in Figure 21 and Table 17 refer to the relative transportation costs per kg of H_2 delivered to the port of Rotterdam. As seen in the figure, the same trend as with the total yearly costs occurs here, with the Small tankers class having the highest relative costs, and the Aframax class yielding the lowest relative costs. However, it can be noted that, unlike what was stated for the results presented in Figure 20, the variations are not proportionally related with the total costs. For example, Table 17 shows that between the Handymax and the Supramax class, the relative costs regarding the TOL-MCH system are projected to be relatively closer, thus contrasting with the results found for the total yearly costs. This can be explained with a few key aspects. Firstly, as mentioned in sub-section 3.1.2.1., the Supramax class yielded the highest results for C_{DR}. Furthermore, as explained in sub-section 2.4, TOL has a lower density when compared with DBT. This, of course, translates to an equivalent relation between the correspondent hydrogenated forms. Following Equation (27), it was assessed that the Supramax class can carry 18.18 % more cargo, in mass terms, when transporting PDBT instead of MCH. Finally, since the H_2 volumetric storage density is also higher for DBT than for TOL, this results in an extra 18.75 % of H_2 being transported, in mass units, by the Supramax class. This last aspect also helps to explain why the convergence in costs from the Handymax to the Supramax classes only occurs for the TOL-MCH system.

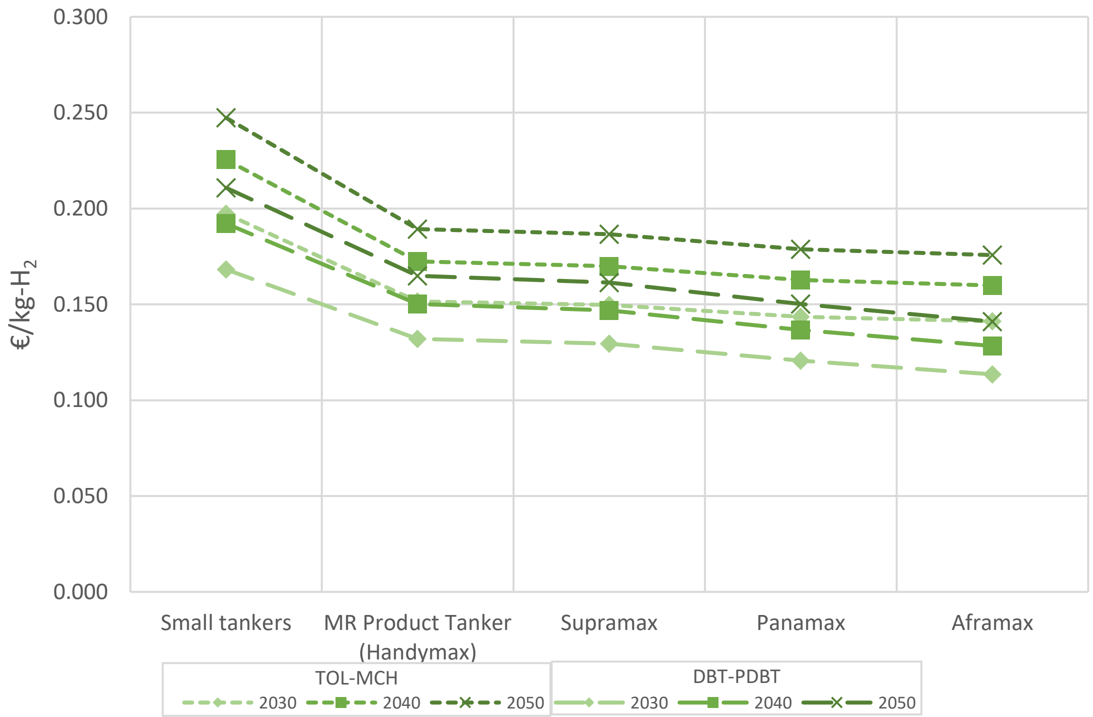

Figure 21 - Transportation costs in €/kg-H_2, for all considered tanker classes and LOHC systems, for 2030, 2040 and 2050

When analysing the results presented in Table 17, the lowest value matches the findings for the total yearly costs, with transportation incrementing the final price of H_2 in 0.113 €/kg-H_2 in 2030, when using the Aframax class and the DBT-PDBT system. For 2050, the homologous result increases slightly, to 0.141 €/kg-H_2. Also, similarly to the previous results, the highest costs correspond to 0.247 €/kg-H_2, when using Small tankers in 2050, carrying the TOL-MCH system to transport H_2. When considering the tanker class options for the TOL-MCH system, using Small tankers is, on average, 40.5% more expensive than using the Aframax class. For the DBT-PDBT system, the same comparison showed a 49.2% decrease from the Small tankers to the Aframax.

Table 17 - Transportation costs in €/kg-H_2, for all considered tankers and LOHC systems, for 2030, 2040 and 2050

€/kg-H₂	2030		2040		2050	
	TOL-MCH	**DBT-PDBT**	**TOL-MCH**	**DBT-PDBT**	**TOL-MCH**	**DBT-PDBT**
Small tankers	0.197	0.168	0.225	0.192	0.247	0.211
MR Product Tanker (Handymax)	0.151	0.132	0.172	0.150	0.189	0.165
Supramax	0.150	0.130	0.170	0.147	0.187	0.161
Panamax	0.143	0.121	0.163	0.137	0.179	0.150
Aframax	0.141	0.113	0.160	0.128	0.176	0.141

Figure 22 shown below shows the share of each individual cost component, relative to the total transportation costs. To simplify the observation of the results, the values were averaged for the period between 2030 and 2050. As seen, C_{PC} is projected to have the highest impact, accounting for around 40% of the total transportation costs of the Small tankers class. For the Aframax class, this component is nearly 70% of the total costs, on average. C_F is the second most impactful component, followed by the daily rates C_{DR} and CO_2 emissions costs C_{Em}.

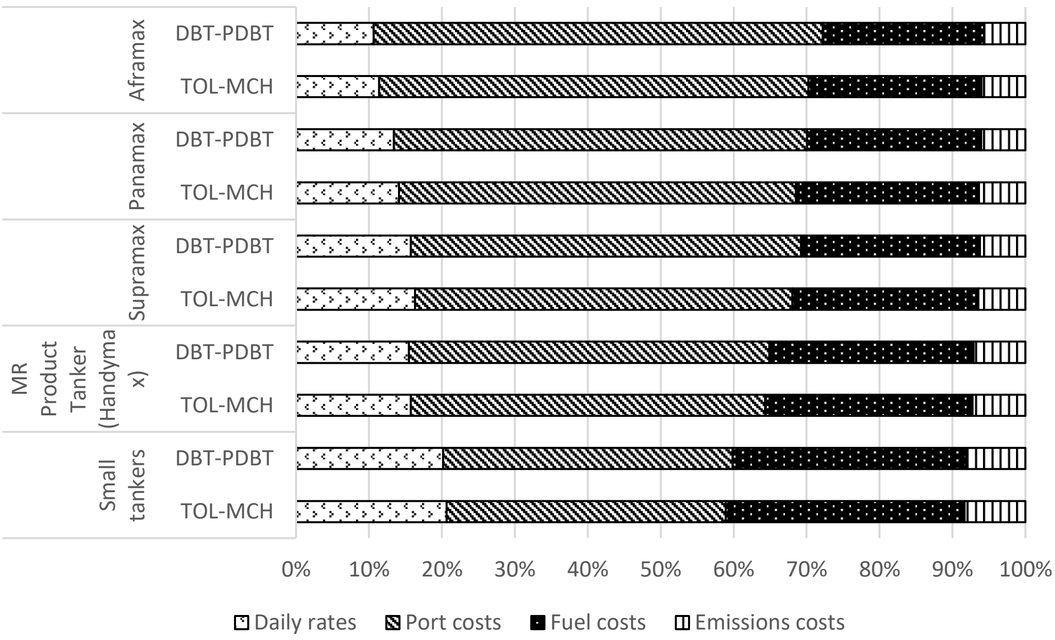

Figure 22 - Relative share of each cost component from the transportation costs, relative to the amount of H_2 delivered per year. Values shown for all tanker classes and averaged between 2030-2050.

Apart from the costs per kg-H_2, results are also shown for the costs per cargo transported i.e., the hydrogenated and dehydrogenated LOHCs. It is noteworthy that, since the tankers are projected to always travel at maximum capacity, – the respective method on $Cargo_{MAX}$ is explained in sub-section 2.6.1. – the costs in €/t-LOHC were calculated based on the total amount of LOHCs transported, of both the hydrogenated and dehydrogenated products. On this basis, Figure 23 given below displays the same relative distribution as the previous shown results. Accordingly, the lowest yielded result was 3.09-3.84 €/t-LOHC, when using the Aframax tanker class to transport DBT-PDBT, from 2030 to 2050. Conversely, the most expensive option was the Small tanker class when transporting TOL-MCH. In this case, the costs varied between 5.27-6.61 €/t-LOHC, from 2030 to 2050.

Figure 23 - Transportation costs in €/t-LOHC, for all considered tankers and LOHC systems, for 2030, 2040 and 2050

3.1.3. Storage

Concerning the results for the costs of storing the LOHCs at the ports of Sines and Rotterdam, the following sub-sections detail how they vary from a single roundtrip to the expected yearly requirements. Furthermore, insight is given on how these yearly expenses are projected to be split, between the tank farms present in both ports, in sub-section 3.1.3.2. Finally, as it was presented for the transportation costs, the unitary costs are shown in sub-section 3.1.3.3, relative to both the units of H_2 delivered, and the units of LOHC transported.

3.1.3.1. Costs per roundtrip

Figure 24 and Figure 25 shown below depict the tank storage costs, per roundtrip, for TOL-MCH and DBT-PDBT, respectively. Since $Storage_{tariff}$ was adjusted for inflation with a 1% annual growth rate, an upward trend in costs can be observed. Moreover, resembling the results highlighted in sub-section 3.1.2.1., the costs of storing the LOHCs during the respective processes of hydrogenation and dehydrogenation are in ascending order, from the smallest to the biggest tankers. This was expected, since the storage expenses are based on the number of days required for the usage of the tanks ($Storage_{days,RT}$). As explained in sub-section 2.6.2., this variable is related to the total number of days necessary to load/unload the amount of LOHC each tanker can carry, thus explaining the ascending order of the results in the figure below. Also similar to the findings from sub-section 3.1.2.1. is the fact that the DBT-PDBT system yielded higher costs, compared with the TOL-MCH system, when considering the costs per roundtrip of LOHC storage. For this case, two key aspects clarify the yielded outcomes. Firstly, $Storage_{days,RT}$ is higher when processing the DBT-PDBT system. Even though, as detailed in sub-section 2.6., the flow rates of the processes associated with the DBT-PDBT system are faster, the respective densities are also higher than for the TOL-MCH system. Thus, the total cargo of DBT-PDBT, in mass units, transported by the considered tankers ($Cargo_{MAX}$), is larger than the respective TOL-MCH cargo. Secondly, the incurred tariff ($Storage_{tariff}$) for the DBT-PDBT system is roughly 87.5 % higher than the correspondent tariff for TOL-MCH. These two aspects contribute for an increasing disparity in costs per roundtrip, between the two LOHC systems, as the size of the tankers also increases. For Small Tankers, the TOL-MCH yielded a roundtrip storage cost of 114,987 €/roundtrip in 2030, increasing to 127,017 €/roundtrip in 2040, and finally to 140,306 €/roundtrip in 2050. Conversely, the DBT-PDBT value was approximately 96.0% higher across the entire timespan, at 225,400 €/roundtrip in 2030, 248,982 €/roundtrip in 2040, and 275,031 €/roundtrip in 2050. For the Aframax class, the difference between the two LOHC systems was approximately 112.0% from 2030 to 2050.

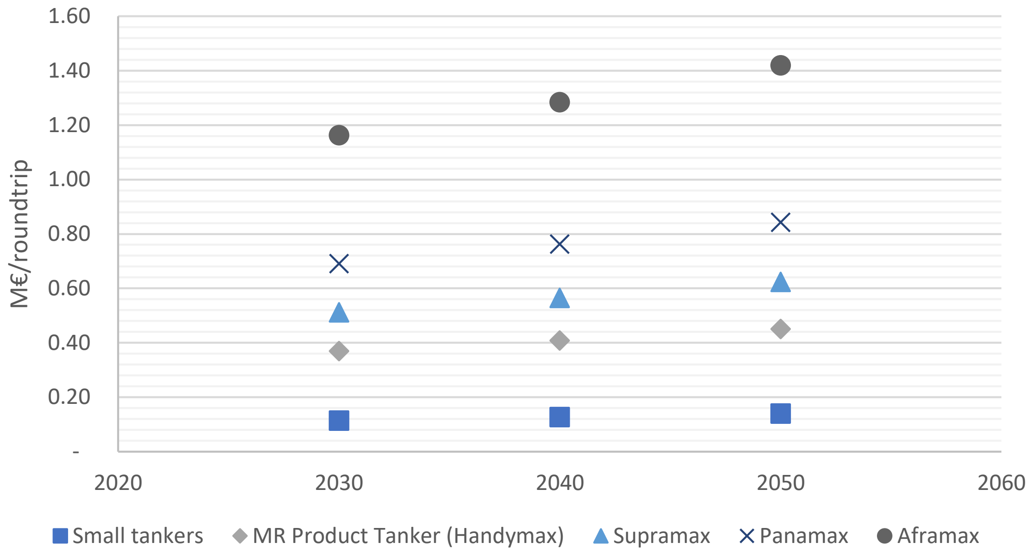

Figure 24 - Storage costs per roundtrip, in M€, for the TOL-MCH system. Results shown for all tanker classes in 2030, 2040 and 2050.

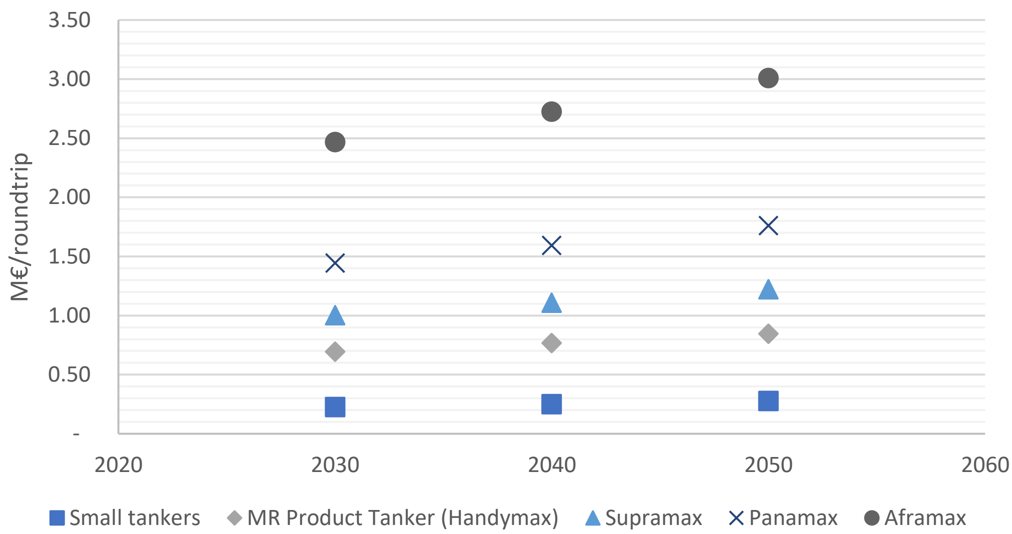

Figure 25 - Storage costs per roundtrip, in M€, for the DBT-PDBT system. Results shown for all tanker classes in 2030, 2040 and 2050.

3.1.3.2. Costs per year

When extrapolating the results for one roundtrip, to match the yearly requirements of the H_2 supply chain, the results shown in Table 18 below were calculated. Furthermore, Figure 26 helps to highlight how the difference in storage costs between the two LOHC systems is slightly harmonized when extrapolating the roundtrip costs to a full year. In contrast to what was observed in the previous sub-section, the results below show that the disparity in costs between LOHC systems has a downward trend, when analysing the tankers from smallest to largest. For

Small Tankers, storing DBT-PDBT for the total number of days required in one year is roughly 63.4% more expensive than storing TOL-MCH. Conversely, the difference between the two LOHC systems for the Aframax class is approximately 59.0%. Nonetheless, storing DBT-PDBT for the Aframax tanker class is the most expensive option, with yearly costs of roughly 22.19 M€ in 2030, 24.51 M€ in 2040, and 27.07 M€ in 2050.

Table 18 – LOHC storage costs in M€/year, for all considered tankers and LOHC systems

	TOL-MCH			DBT-PDBT		
M€/year	**2030**	**2040**	**2050**	**2030**	**2040**	**2050**
Small tankers	4.14	4.57	5.05	6.76	7.47	8.25
MR Product Tanker (Handymax)	7.76	8.57	9.47	12.47	13.77	15.21
Supramax	9.21	10.18	11.24	15.02	16.59	18.33
Panamax	10.36	11.45	12.65	17.31	19.12	21.12
Aframax	13.96	15.42	17.03	22.19	24.51	27.07

As explained in sub-section 2.7., the yearly extrapolation of costs was based on the calculations for $Fleet$. In sub-section 3.1.2.2. it was assessed that the tanker fleet was composed of three tankers, per class. Since this calculation encompasses the total number of yearly roundtrips projected for each LOHC system (RT_{year}), it justifies the relatively closer results – seeing that the TOL-MCH system yielded a higher value for RT_{year}, it was expected that $C_{Storage_{RT}}$ was charged a larger number of times.

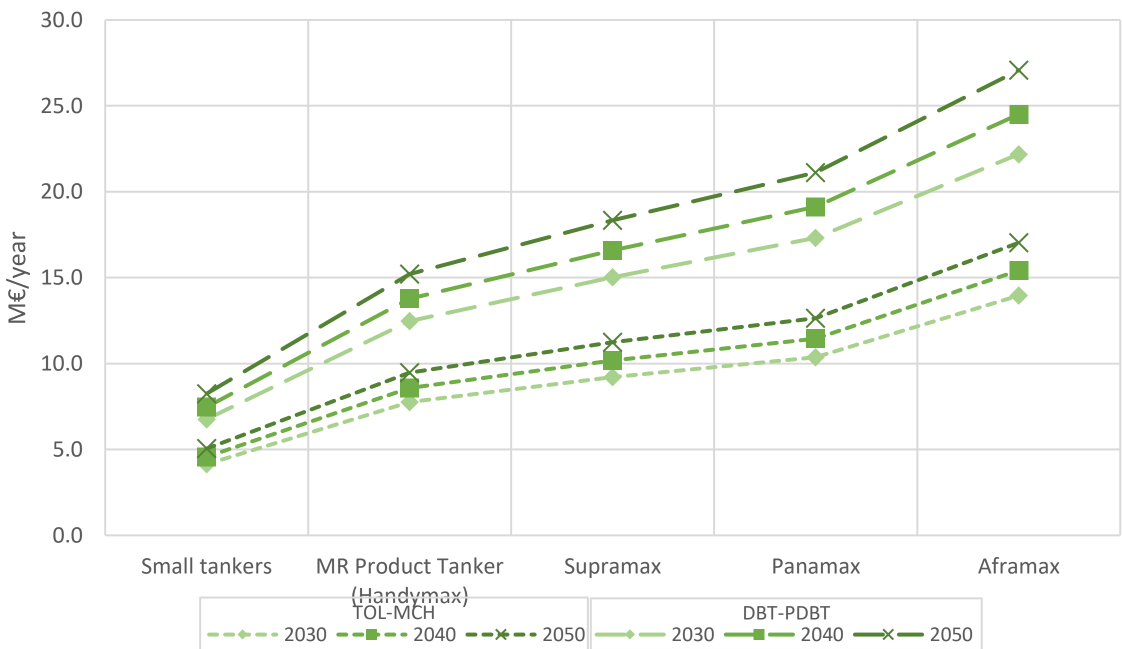

Figure 26 - Total LOHC storage costs in M€/year, for all considered tanker classes and LOHC systems, for 2030, 2040, and 2050.

Finally, a quick analysis was conducted to quantifying the share of the yearly LOHC storage costs, between Sines and Rotterdam. Figure 27 presented below is showing the respective results. As it can be seen, on average, the LOHC storage expenses are expected to be higher within the port of Rotterdam – between 51-56 % of the total projected LOHC storage costs. Considering that $Storage_{tariff}$ only varied according to the type of LOHC stored, and was not dependent on location, this implies that the difference in projected cost shares between the two ports is only related to the respective amount of time for the hydrogenation and dehydrogenations processes. As mentioned in sub-section 2.6.1., the dehydrogenation process takes longer than the hydrogenation process. As the port of Rotterdam is assumed to be where the dehydrogenation unit will be located, hence the projected share of storage costs is higher for this location.

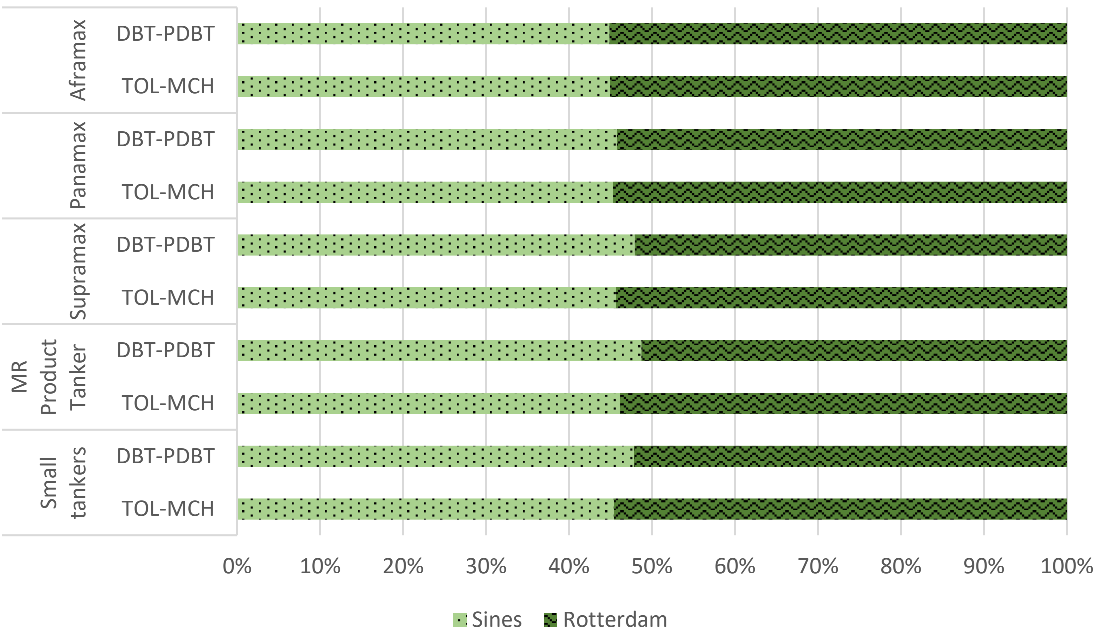

Figure 27 - Share of yearly LOHC storage costs, between Sines and Rotterdam, for all considered tankers and LOHC systems

3.1.3.3. Costs per kg-H_2 stored

When considering the costs per kg of H_2 of storing each of the LOHC systems in tanks, the TOL-MCH system is projected to increment 0.083 €/kg-H_2 in 2030, 0.091 €/kg-H_2 in 2040 and between 2030 and 0.101 €/kg-H_2 in 2050, when using Small tankers. For the Aframax class, the respective increment varies from 0.279-0.341 €/kg-H_2, from 2030 to 2050. This can be seen in Figure 28 below. Conversely, the DBT-PDBT system yielded results of 0.135 €/kg-H_2 for 2030, 0.149 €/kg-H_2 in 2040 and 0.165 €/kg-H_2 in 2050, when using Small tankers. During the same period, the costs for the Aframax class are projected to vary between 0.444-0.541 €/kg-H_2. Regarding the costs per cargo transported, Figure 29 highlights the yearly costs in € per ton of LOHC stored.

Again, the cheapest option was assessed to be the TOL-MCH system, with results spanning between 2.21-2.70 €/t-LOHC, when using Small tankers, from 2030 to 2050. The DBT-PDBT yielded slightly higher values between 3.68-4.49 €/t-LOHC, for the same class. It is noteworthy that, since the relative storage costs yielded an inverse trend when compared with the relative transportation costs – as shown in sub-section 3.1.2.3., the transportation costs per kg-H_2 are projected to be lower for each ascending tanker class – it was necessary to address the balance between these two cost components, before assessing which tanker class would be the cheapest option.

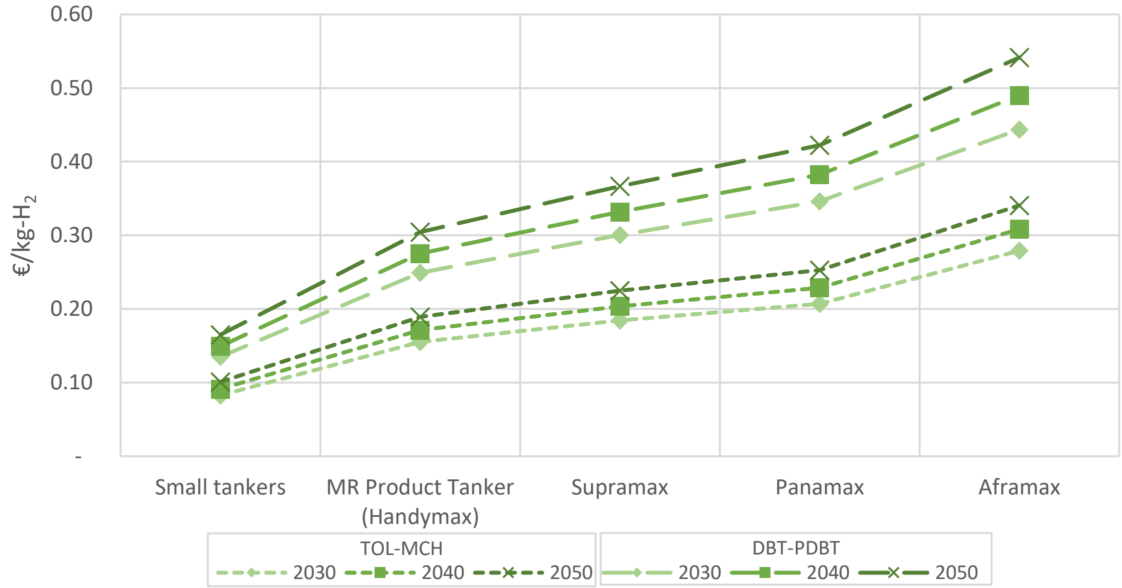

Figure 28 - Storage costs in €/kg-H_2, for all considered tankers and LOHC systems. Results for 2030, 2040 and 2050.

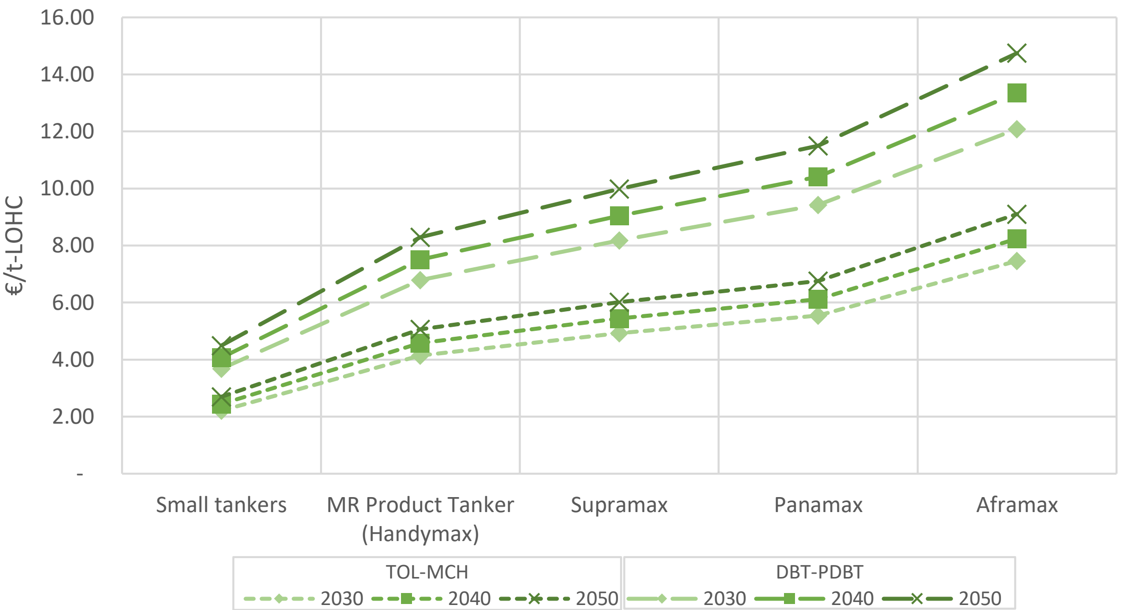

Figure 29 - Storage costs in €/t-LOHC, for all considered tankers and LOHC systems

3.1.4. Transport + storage

When combining the results from sub-sections 3.1.2.3. and 3.1.3.3., a more dynamic set of results was obtained. Figure 30 presented first, displays the combined results for transportation and storage, in € per kg of H_2 delivered. The first overall observation is that, for both LOHC systems, using the smaller class considered i.e., the Small tankers, is the cheapest option to use in the established supply chain mentioned in sub-section 2.1. Additionally, as seen from the figure, the relative costs are relatively more homogeneous, with the values between the Small tankers class and the Aframax class increasing, on average 41.6% and 82.0%, for the TOL-MCH and the DBT-PDBT systems, respectively. When looking closely at the different tanker classes, it can be seen that the Small tankers class is the cheapest option for the TOL-MCH and the DBT-PDBT systems. It can be noted that, when balancing the results from sub-sections 3.1.2.3. and 3.1.3.3, DBT-PDBT is the most expensive option. This occurs despite that the assessed costs for transportation were lower for DBT. The contrast in the tank storage costs between the two LOHCs supersedes the respective contrast for the transportation costs, thus reverting the findings from 3.1.2.3. On average, transportation costs were 18.0% higher for TOL-MCH, or around 0.033 €/kg-H_2 higher for the Small tankers. Contrarily, tank storage costs were, on average 38.4% lower for TOL-MCH, or around 0.052 €/kg-H_2, for the Small tankers.

Figure 31 displays the storage costs in €/t-LOHC. For the Small tankers, the respective costs for TOL-MCH increased from 7.49 €/t in 2030 to 8.47 €/t in 2040, and finally to 9.31 €/t in 2050. The correspondent results for the DBT-PDBT systems were 8.27 €/t, 9.30 €/t and 10.24 €/t, for the respective years. To highlight the cheapest options that were assessed for the accounted LOHC systems, Table 19 below provides the breakdown of all the computed cost components, in € per kg of H_2 delivered.

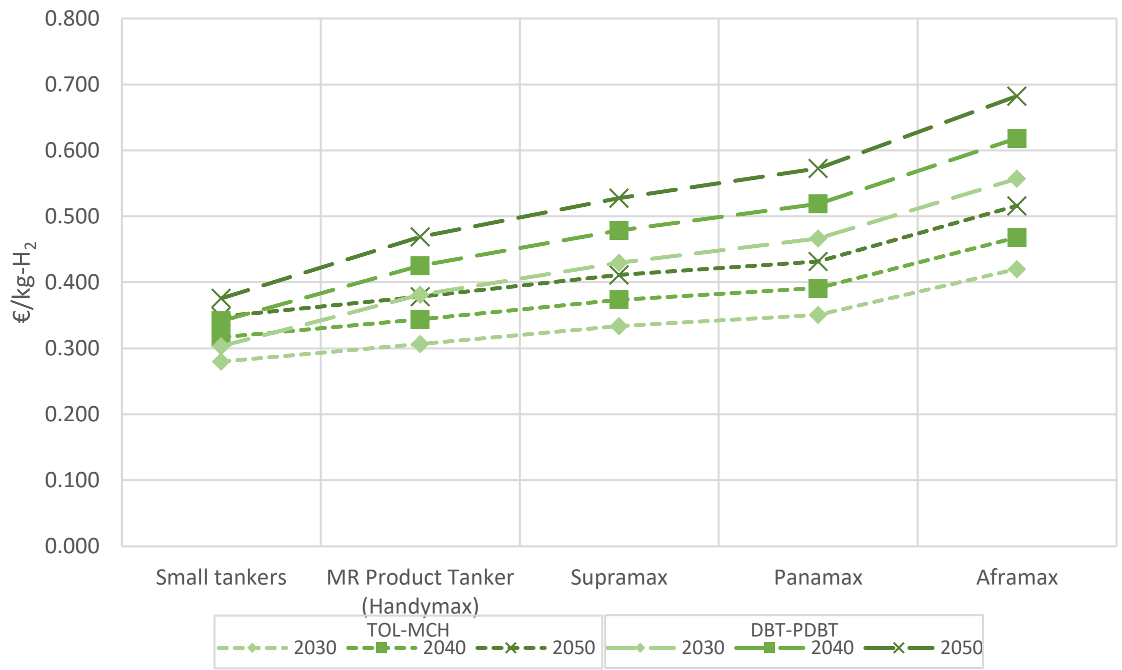

Figure 30 - Transport and storage costs in €/kg-H_2, for all considered tankers and LOHC systems, for 2030, 2040 and 2050

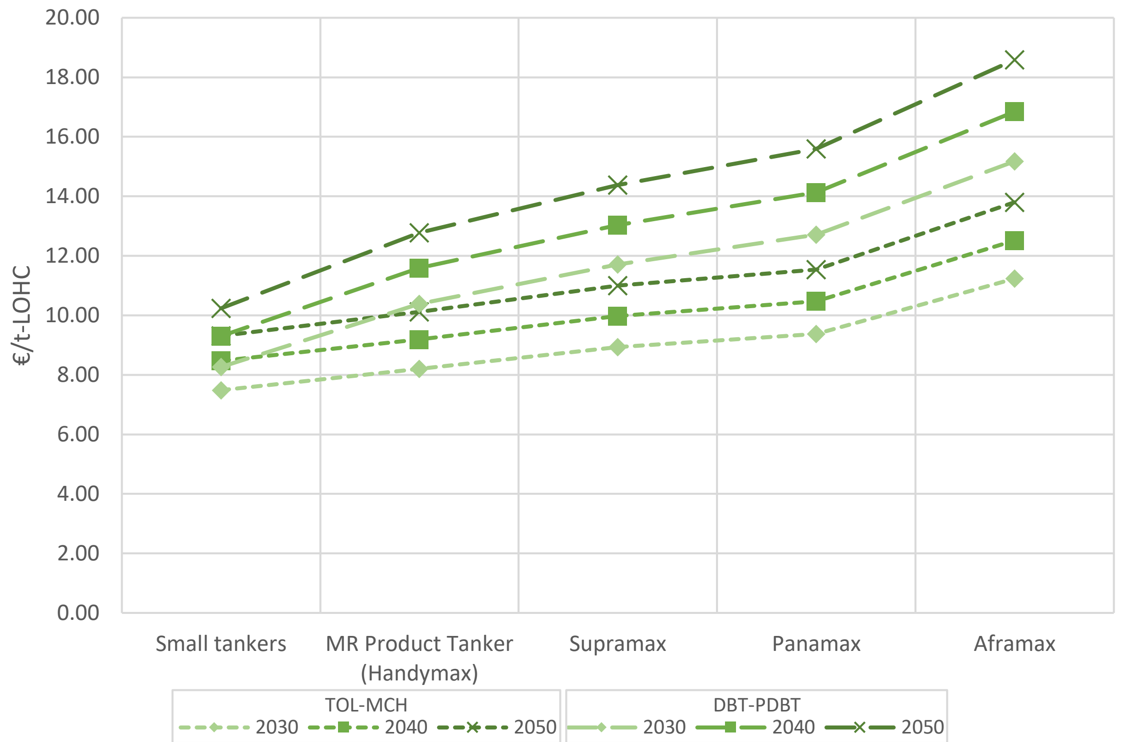

Figure 31 - Transport and storage costs in €/t-LOHC, for all considered tankers and LOHC systems, for 2030, 2040 and 2050

Table 19 - Transport and storage costs, per cost component, in €/kg-H_2, for 2030, 2040 and 2050. Results for TOL-MCH system using the Handymax class, and for the DBT-PDBT system using the Small Tankers class.

€/kg-H_2	**2030**	**2040**	**2050**
TOL-MCH – MR Product Tanker (Handymax)			
Daily rates	0.022	0.022	0.022
Port costs	0.075	0.083	0.091
Fuel costs	0.036	0.049	0.061
Emissions costs	0.016	0.013	0.007
Transportation	**0.149**	**0.168**	**0.182**
Storage	0.071	0.071	0.071
Total	**0.220**	**0.239**	**0.253**
DBT-PDBT – Small Tankers			
Daily rates	0.032	0.032	0.032
Port costs	0.068	0.075	0.083
Fuel costs	0.045	0.062	0.076
Emissions costs	0.021	0.017	0.009
Total Transportation	**0.165**	**0.186**	**0.200**
Storage	0.062	0.062	0.062
Total	**0.227**	**0.247**	**0.262**

3.2. LOHC supply chain GHG footprint analysis

The results presented in Table 20, shown below, highlight the GHG impact of transporting either LOHC system with the Small tankers class. This focus is based on the findings from the economic analysis, which concluded that using the smaller class of tanker would be the most financially viable option. These values, however, do not include the potential GHG emissions of the production of H_2, described in sub-section 2.2. Additionally, it is important to mention that the GHG emissions associated with the LOHC conversion processes i.e., hydrogenation and dehydrogenation, are assumed to be fixed from 2030 to 2050. In sub-section 4.2, a further discussion on these matters is provided. Looking at the presented results, it is reported that using DBT-PDBT is projected to have a lower overall GHG footprint. Apart from having a lower GWP, as mentioned in sub-section 2.4, DBT also has a higher volumetric storage capacity for H_2. This contributes to lower the relative GWP of the transportation and tank storage operations. Furthermore, due to the alternating fuel mix, assumed from sub-section 2.5.3.3, the associated GHG emissions are projected to have a downward trend. Overall, emissions are expected to decrease roughly 43.5% from 2030 to 2040, and 56.2% from 2040 to 2050, for the two LOHC systems considered.

Table 20 - CO_2 emissions generated, per each step of LOHC supply-chain, in kg-CO_2/GJ-H_2(LHV), for 2030, 2040 and 2050. Results for Small Tankers with DBT-PDBT system, and for Handymax with TOL-MCH system

kg-CO_2/GJ-H_2(LHV)	**2030**	**2040**	**2050**
TOL-MCH - Small Tankers			
Travel days	2.789	1.478	0.520
Within port	0.176	0.093	0.033
Transport + storage	**2.965**	**1.571**	**0.553**
Hydrogenation/dehydrogenation	0.242	0.242	0.242
Total	**3.207**	**1.813**	**0.795**
DBT-PDBT - Small Tankers			
Travel days	2.324	1.231	0.434
Within port	0.147	0.078	0.027
Transport + storage	**2.471**	**1.309**	**0.461**
Hydrogenation/dehydrogenation	0.199	0.199	0.199
Total	**2.670**	**1.508**	**0.660**

3.3. Sensitivity analysis

The following results here shown reflect the sensitivity of the total supply chain costs assessed for the Small tankers class, for both TOL-MCH and DBT-PDBT. The selected parameters and the respective variation intervals are detailed in sub-section 2.8. For both figures shown below, the individual results for 2030, 2040 and 2050 are presented. Additionally, the effects of the impacts from transportation and tank storage are aggregated. A cumulative effect for the entire supply chain is also reported, including the variations for “H2 break-even price” and for “H2 production costs”. Figure 32 shown first, highlights the volatility of the supply chain costs for TOL-MCH. As seen from the charts in the figure, overall, the most impactful variations for the “BEST” and “WORST” scenarios were caused by varying the parameters “H2 delivered per year” and “H2 production costs”. This was expected, since these parameters influenced the cost level of the two components that contributed the most to the supply chain, according to the results found in sub-section 3.1.1. However, it is notable that for the “WORST” scenario in 2050, the aggregate effects of transportation and tank storage are the most impactful variation. This can be explained solely from the variations applied to the daily rates, which influence C_{DR} calculated based on the methods from sub-section 2.5.3.1. As seen from the results in sub-section 3.1.2.3, C_{DR} is projected to represent, on average, around 20% of the total transportation costs. This implies that the relative changes to C_{DR} a higher potential of impacting the total supply chain costs under the “WORST” scenario, compared with the “BEST”. Figure 33 focuses on the respective results for DBT-PDBT. The same conclusions from the previous LOHC system can be drawn here.

2030

€/kg-H_2	BEST	REF 4.70	WORST
H_2 delivered per year	4.537		4.990
Daily rates	4.669		4.731
Port costs	4.681		4.719
CO_2 price	4.688		4.725
Fuel price	4.673		4.727
Tank storage rates	4.688		4.712
Transportation + storage	4.598		4.814
H_2 production costs	3.993		5.407
Cumulative effect	3.728		5.808

-0.972 0 +1.108

2040

€/kg-H_2	BEST	REF 4.63	WORST
H_2 delivered per year	4.453		4.953
Daily rates	4.589		4.727
Port costs	4.595		4.680
CO_2 price	4.622		4.653
Fuel price	4.595		4.670
Tank storage rates	4.607		4.662
Transportation + storage	4.480		4.862
H_2 production costs	3.993		5.272
Cumulative effect	3.661		5.815

-0.969 0 +1.185

2050

€/kg-H_2	BEST	REF 3.69	WORST
H_2 delivered per year	3.492		4.044
Daily rates	3.640		3.912
Port costs	3.636		3.780
CO_2 price	3.685		3.701
Fuel price	3.645		3.736
Tank storage rates	3.651		3.743
Transportation + storage	3.496		4.111
H_2 production costs	3.340		4.040
Cumulative effect	2.948		4.803

-0.742 0 +1.113

Figure 32 - Tornado chart with sensitivity results for the total supply chain costs using the TOL-MCH system and the Small tankers class, for 2030, 2040 and 2050.

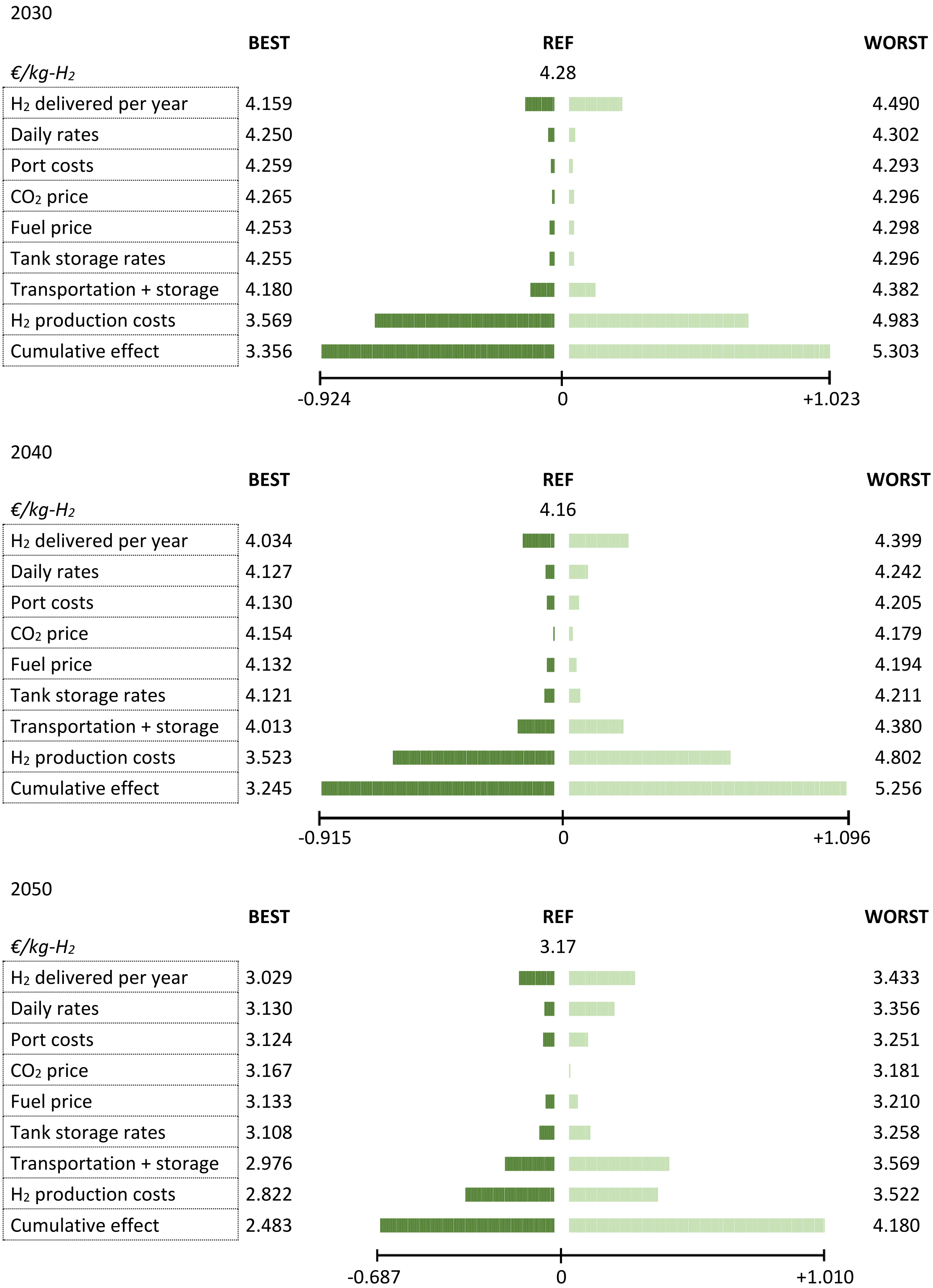

Figure 33 - Tornado chart with sensitivity results for the total supply chain costs using the DBT-PDBT system and the Small tankers class, for 2030, 2040 and 2050.

When comparing the two systems, it can also be observed that TOL-MCH is projected to be more volatile regarding the "H_2 break-even price" associated with the LOHC conversion processes. This can be explained due to the relatively higher operational and investment costs, as presented in sub-section 2.4. Conversely, the results for DBT-PDBT are more sensitive to the variations applied to the "H_2 production cost", since this component holds a higher relative of the total supply chain costs, as detailed in sub-section 3.1.1. The highest value for the total supply chain costs, obtained from the sensitivity analysis, was 5.82 €/kg-H_2 for the "WORST" scenario of TOL-MCH, in 2040. Contrarily, the "BEST" scenario yielded the lowest value, with 2.48 €/kg-H_2, for DBT-PDBT in 2050.

4. Discussion

This section focuses on addressing the relevance of the obtained results from the economic analysis by comparing these results with comparable studies. Additionally, an assessment is provided regarding the level of compliance of the results found in the analysis of the GHG emissions, according to the regulations enforced through the RED II directive (Commission Delegated Regulation (EU) 2021/4987, 2021). Lastly, sub-section 4.3. provides insight into how the LOHC conversion processes can potentially be improved from 2030 to 2050 and suggestions on how this research can be complemented.

4.1. Comparison of results from economic analysis

The computed results were challenged regarding their validity by comparing them with the results found in similar research. As addressed in sub-sections 1.2. and 2.3.2, the supply chain considered for this research will primarily compete with other sources of imported H_2 in the Netherlands. Firstly, a comparison was made with the results found in Lanphen (2019). As referred to in sub-section 1.3, Lanphen assessed the cost price of importing H_2 through the port of Rotterdam, using different carriers, as well as transportation of liquid and gaseous H_2. This cost price includes the production of green H_2 as well as the costs of the supply chain, which is fulfilled by maritime transportation. Furthermore, several importing locations were considered, providing a range of different sources for comparison. However, for that study, the investment costs for each supply chain component were also included, encompassing the construction of the H_2 production units, the conversion plants, the transportation modes, and the necessary port infrastructures. Finally, the lifetime of each supply chain component was accounted for in a WACC discount-based model, allowing for the cost price to be diluted throughout the entire lifetime. Lanphen also performs this analysis for an import rate of 800 kt of green H_2 per year. To adjust for this last aspect, the total supply chain costs assessed for this research were converted, based on the methods detailed in sub-section 2.8, regarding the parameter "H_2 delivered per year". Even though the assumed methods between the two studies diverge regarding the mentioned aspects, it can be seen from Figure 34 that the results are relatively within the same range. Note that the presented results for scenario "REF" are the average of the total supply chain costs for 2030, 2040, and 2050. Apart from this, it is reported that, since the useful lifetime assumed for most of the components for CAPEX, the considered timespan for Lanphen is substantially longer – as is the with the storage tanks for MCH, for example, a useful lifetime of 50 years is considered.

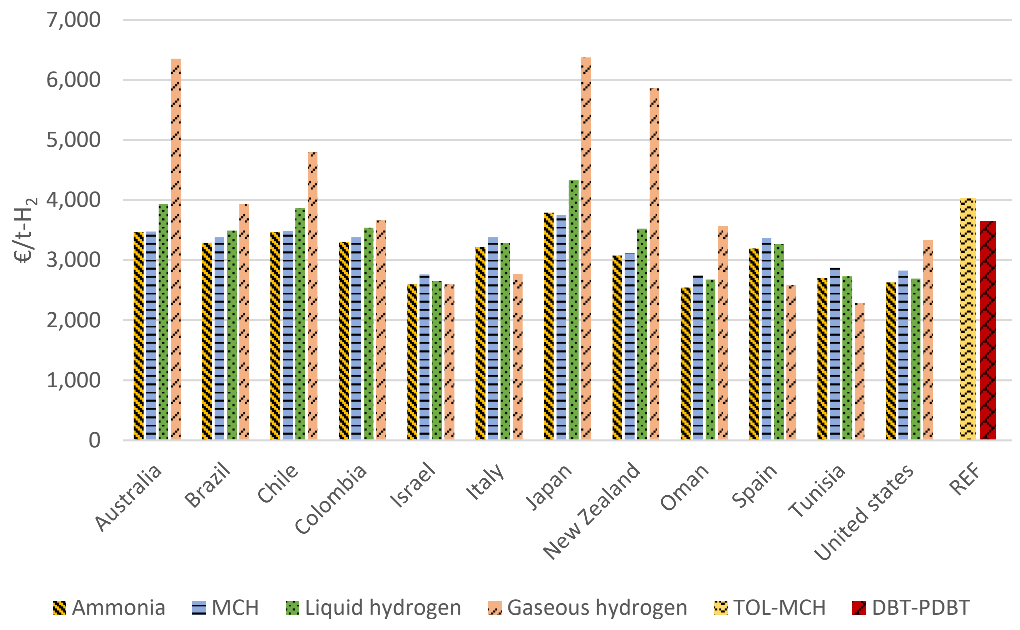

Figure 34 - Comparison between results from "REF" scenario and from Lanphen (2019), for the total supply chain of green H_2, in € per tonne of H_2 delivered.

A second comparison was made with the study from Teichman (2012), which focuses on the transportation of liquefied H_2 and LOHC. The main differences considered for this study are related to the LOHC, which in Teichman is assumed to use the NEC-DNEC system, mentioned in sub-section 1.5. Additionally, Teichman also considers that the ships used for each of the carriers are purchased, accounting for capital depreciation. Conversely, it does not account for port costs, nor does it assume a cost for the associated GHG emissions. The input data for the NEC-DNEC system assumed tankers with 10,000-45,000 DWT capacity. For this reason, the comparison shown in Figure 35 below only highlights the results for the “Small Tankers” and “Handymax” classes. Similarly, the results from both studies are within the same range, with the values from “REF” being closer for those assessed for the NEC-DNEC system. As presented in the study, liquefied H_2 is the most expensive alternative. This is mainly due to the conditions required for the transportation of liquefied H_2, as referred to in sub-section 1.4.1. It can also be reported that, even though the “Handymax” class here shows a lower transportation cost compared with the “Small Tankers”, this does not imply that using the “Handymax” would be the best option. As shown in the Economic analysis, the aggregate balance between the transportation and the respective tank storage costs favours the “Small Tankers”. Notwithstanding, both this study and the one from Teichman focus on short-distance transportation. As mentioned in sub-section 1.4.2, short-distance routes are usually performed by the smaller classes of tankers, due to economic viability.

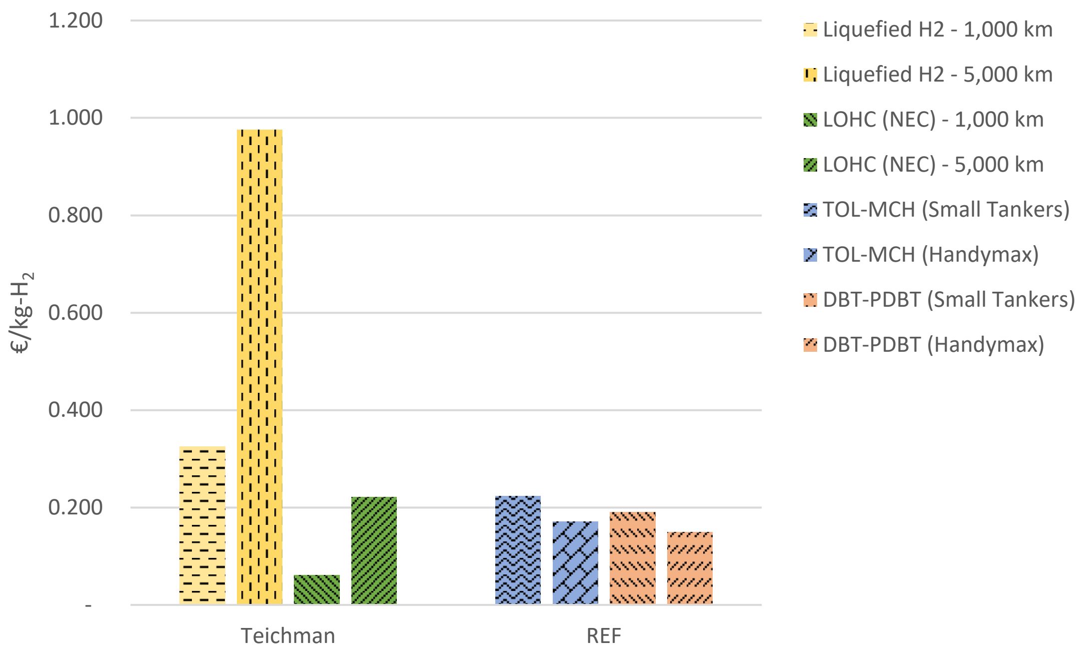

Figure 35 - Comparison between results from "REF" scenario and Teichman (2012), for the transportation costs in €/kg-H_2.

4.2. Compliance of GHG emissions from LOHC supply chain

The results obtained from the GHG footprint analysis report that the associated GHG emissions from the LOHC conversion processes, as well as from the respective transportation and tank storage of the LOHCs, are projected to have a downward trend. By focusing on the highest value for GHG emissions, in 2030, the respective emissions for the TOL-MCH and the DBT-PDBT systems are 3.207 and 2.670 kg-CO_2/GJ-H_2 (LHV), respectively. This is equivalent to 0.38 tCO_2-eq/tH_2 for TOL-MCH, and 0.32 tCO_2/tH_2 for DBT-PDBT. Assuming a GWP of 8.08 tCO_2-eq/tH_2 for conventional steam methane reforming (SMR) (Naterer et al., 2010), this reflects total savings of 95.2% and 96.0% for the respective LOHC systems. These values comply with the targets set by the RED II directives (Commission Delegated Regulation (EU) 2021/4987, 2021). This can potentially allow the LOHC systems to be eligible for investment subsidies. However, as further referred in the following sub-section, performing a full life-cycle assessment (LCA) could provide insightful data regarding the GHG emissions associated with the production of H_2. As referred in Leal (2020), the production of H_2 via electrolysis is expected to be mainly fed by surplus electricity from RES. Nonetheless, accounting for the electricity mix in Portugal, the electrolyser in Sines may not be fed with electricity produced 100% from RES. Apart from this, the production of H_2 via electrolysis is prone to generate additional net CO_2 emissions (Rijksoverheid, 2020). When comparing with the GHG emissions from the production of electricity in the Netherlands, the results from sub-section 3.2. express savings of over 95%, for both LOHC systems. This is based on a GHG impact of 118.81 kg-CO_2/GJp, corresponding to the values from 2019 (IEA, 2021), and a conversion efficiency of 55% (Blok & Nieuwlaar, 2017) for H_2 powered turbines.

4.3. Potential improvements and further suggestions

This sub-section will highlight some aspects that could improve the economic and GHG impact of the LOHC supply chain. Additionally, it will also emphasize relevant steps that can be implemented to complement this research. Focusing first on the LOHC conversion processes, it is necessary to mention that the "H_2 break-even price" from sub-section 2.4.4. is assumed to be fixed throughout the considered timespan. As mentioned, this value was only adjusted for inflation, and any potential improvements in its operational conditions were disregarded. More specifically, considering the hydrogenation process of either LOHC system, the inherent reaction is exothermic i.e., heat is released when the LOHC is loaded. For the research performed in Carvalho (2021), the released heat was regarded as waste. This neglects the potential economic savings of the hydrogenation unit, which could benefit from selling the surplus heat to neighbouring industries. This refers to another focal aspect towards improving the assessment of the LOHC supply chain, which is process integration. Similarly, the dehydrogenation unit in Rotterdam could also benefit from process integration. For this reaction, high-temperature heat is required, as mentioned in sub-sections 2.4.1 and 2.4.2. Within the nearby industrial cluster, any process that might yield surplus heat – or, alternatively, compostable by-product that could be processed as biomass – could potentially contribute to decrease the respective costs and GHG emissions.

It can also be noted that "H_2 break-even price" was computed by assuming that all energy requirements were fulfilled by using NG (Carvalho, 2021). Changing this assumption could also be and improvement towards accurately assessing the temporal variation of the GHG emissions impact, until 2050. By considering alternative sources of energy, the results regarding the LOHC conversion processes, shown in sub-sections 3.1.1. and 3.2. could be further complemented. As referred in Carvalho, relatively small changes in the "H_2 break-even price" can substantially impact the profitability of the LOHC processes. The results from the sensitivity analysis showed that, for both LOHC systems, an increase in price between 15-25% to increase the level of profitability in 50%. Further progress could also be applied to the fuel efficiency assumed for C_F, detailed in sub-section 2.5.3.3. Based on Stopford (2013), the values for fuel consumption reflect the efficiency of roughly 45-48%, characteristic of an engine powered by HFO. Primarily, this approach neglects potential improvements in efficiency of HFO-powered engines. Furthermore, $Fleet$ is assumed to use a variable mix of fuels, and fuel consumption was computed on an energy basis. This implies that different levels of fuel efficiency, corresponding to each of the fuels, could also complement the accuracy of the results found. To properly address the issues mentioned, a complete LCA for the entire supply chain is recommended, following the guidelines from ISO 14040 (2006). Finally, regarding the performed sensitivity analysis for this research, it is important to highlight that, the proposed alternative scenarios, were selected to evaluate the impact of extreme variations in the cost parameters. This suggests that there is a relatively low probability that the computed results can occur. To mitigate this matter, a Monte-Carlo assessment could be considered to infer on the best possible combination for the cost parameters. Apart from this, a more dynamic approach could be taken, by considering a combination of multiple classes of tankers for each scenario. This would further allow to identify the impacts of scheduling the yearly transportation and tank storage in a non-homogeneous way.

5. Conclusion

This section focuses on the research questions presented in sub-section 1.5, and highlights the respective answers provided from this study. Starting with the main research question:

> *What is the potential of H_2 import to the Netherlands from Portugal using LOHCs via maritime transport and its role in the future energy transition?*

The methods for this study aimed to assess this question by inferring on different quantitative and qualitative impacts of choosing LOHCs as the carrier to transport green H_2, via maritime shipping. Firstly, and economic analysis was performed to assess the cost increment of establishing a supply chain which included maritime transportation, using tankers, as well as tank storage in port locations. This analysis concluded that, for both LOHC systems considered, using the Small tankers class – with 27,300 DWT capacity – is the most financially viable option. The respective cost increment was added to the associated costs of converting the LOHCs i.e., the hydrogenation and dehydrogenation processes required before the H_2 is delivered for final use. By encompassing all the relevant supply chain costs, it was possible to address the first sub-question of "*How much does logistics costs increment the supply chain and the final price of renewable H_2?*" Firstly, regarding the TOL-MCH systems, the total supply chain costs are projected to vary from 4.70 €/kg-H_2 in 2030, to 4.63 €/kg-H_2 in 2040, and finally to 3.69 €/kg-H_2 in 2050. In this instance, transportation and tank storage account for 6.0% or 0.28 €/kg-H_2, for the total supply chain, in 2030, 6.8% or 0.32 €/kg-H_2 in 2040, and finally 9.4% or 0.35 €/kg-H_2 in 2050. This increase in share is explained since transportation and tank storage costs are projected to increase, whereas the cost referring to the production of H_2, is projected to decrease during the same period. When looking closely at the DBT-PDBT systems, it can be concluded that using this system is cheaper, with the total supply chain costs decrease from 4.28 €/kg-H_2 in 2030, to 4.16 €/kg-H_2 in 2040, and finally to 3.17 €/kg-H_2 in 2050. However, the lower supply chain costs are related to the respective LOHC conversion processes, assessed in Carvalho (2021). Regarding transportation and tank storage, it is reported that these expenses are expected to be higher for DBT-PDBT, accounting for an increment of 0.30 €/kg-H_2 in 2030, or roughly 7.1% of the total supply chain costs. This value increases to 8.2%, or 0.34 €/kg-H_2 in 2040. Finally, in 2050, these components represent 11.8% of the total supply chain costs, adding 0.38 €/kg-H_2. The assessed costs can potentially be reduced by considering the integration of the LOHC conversion processes, in both port locations. However, process integration is currently deemed unlikely, and thus was disregarded for this study.

The imported H_2 is expected to provide a major contribution regarding the projected demand for the Netherlands. The port of Rotterdam has reported that future demand of H_2 will far surpass the projected capacity for domestic production of H_2. Regarding the second sub-question "*What are the options and costs of integrating the imported H_2 in the H_2 supply chain, via the port of Rotterdam?*", it was assessed that demand for the imported H_2 in the port of Rotterdam will mainly be associated with the process heating industry, and the synthetization of renewably produced fuels, for the aviation and maritime sectors. The associated costs are related to the dehydrogenation process, which represent roughly 90.2% for TOL-MCH, and around 82.7% for DBT-PDBT, from the LOHC conversion processes (Carvalho, 2021). However, as referred, this process could benefit from process integration, potentially halving the respective costs. Demand for these three applications is projected to reach 5.2 Mt of H_2 in 2050, over 100 times the assumed amount to be transported from Sines. Data collected to answer the sub-questions "*What are the current and future potentials for domestic H_2 supply and demand in the Netherlands?*", "*What are the associated production costs?*", reported that, by 2030, the Netherlands is expecting to have the capacity to produce 1 Mt of climate neutral H_2 – including blue and green H_2. These processes will likely converge to the same cost range, between 2.00-3.00 €/kg-H_2, by 2030. Furthermore, increase in capacity of wind energy is projected to feed around 10-20% of the H_2 demand requirements, in 2050. This can potentially decrease the cost range of green H_2 to 0.80-1.60 €/kg-H_2, by 2050, which would be between 49.5-74.8% cheaper than the reported costs for DBT-PDBT. Nonetheless, accounting for a total demand of 20 Mt of H_2 in the Netherlands, in 2050 (Port of Rotterdam, 2020), the import of H_2 is deemed as an indispensable source, until 2050. Finally, regarding the last sub-question "*What is the GHG footprint of international H_2 supply through LOHCs?*" the results found that the total supply chain using DBT-PDBT and Small tankers would produce around 2.67 kg-CO_2/GJ-H_2 (LHV), in 2030. This value decreases to 1.51 kg-CO_2/GJ-H_2 (LHV) in 2040, and to 0.66 kg-CO_2/GJ-H_2 (LHV) in 2050. When comparing with conventional SMR, this allows for savings of roughly 96.0% in 2030, and of over 99.0% in 2050.

When analysing the results obtained from sub-section 3.1., the low increment implies that it will be relatively easy to establish LOHC supply chains, allowing for these products to become tradeable commodities. Apart from the comparison provided in sub-section 4.1, a subsequent analysis was made to assess the energetic efficiency of the LOHC supply chain. From the research performed by Carvalho (2021), it was assessed that the energy requirements for the TOL-MCH cycle was around 21 kWh/kg-H_2, while for DBT-PDBT the requirements were approximately 16 kWh/kg-H_2. These values are considerably close to the energy requirements for liquefaction of H_2, reported at roughly 15 kWh/kg-H_2 (Krasae-in et al., 2010). Table 21 provides the comparative values between the LOHC supply chain, and liquefied H_2. The values for the LOHC supply chain include the energy requirements presented in sub-sections 2.4.1. and 2.4.2, as well as for transportation and tank storage. The respective energy requirements for the transportation of liquefied H_2 were sourced from Teichmann et al. (2012). When considering process integration for the dehydrogenation process, as mentioned in sub-section 4.3, the total energy efficiency of the LOHC supply chain can potentially be more competitive than liquefied H_2.

Table 21 - Energy efficiency of the LOHC supply chain, compared with liquefaction of H_2. Values for liquefaction of H_2 sourced from Teichmann, et al. (2012) and Krasae-in, et al. (2010).

	GJ-fuel/GJ-H_2 (LHV)
LOHCs	
TOL-MCH	67.16%
DBT-PDBT	51.91%
Liquefied H_2	
Liquefaction + 1,000 km transport	50.20%
Liquefaction + 5,000 km transport	71.10%

Finally, it is important to mention that, due to the possibility of long-term storage in tanks, LOHCs can be pivotal for periods of high peak demand of energy, allowing not only for the safe and cheap storage of H_2, but also ensuring relatively lower losses, compared with gaseous H_2 (through permeation), and liquefied H_2 (through evaporation).

6. References

Aakko-Saksa, P. T., Cook, C., Kiviaho, J., & Repo, T. (2018). Liquid organic hydrogen carriers for transportation and storing of renewable energy – Review and discussion. *Journal of Power Sources*, *396*(April), 803–823. https://doi.org/10.1016/j.jpowsour.2018.04.011

Abas, N., Kalair, A., & Khan, N. (2015). Review of fossil fuels and future energy technologies. *Futures*, *69*, 31–49. https://doi.org/10.1016/j.futures.2015.03.003

Afnor certification. (2006). Management environnemental- Analyse du cycle de Vie- Principes et cadre. *Nf EN ISO 14040*. https://www.iso.org/fr/standard/37456.html

Agbossou, K., Chahine, R., Hamelin, J., Laurencelle, F., Anouar, A., St-Arnaud, J. M., & Bose, T. K. (2001). Renewable energy systems based on hydrogen for remote applications. *Journal of Power Sources*, *96*(1), 168–172. https://doi.org/10.1016/S0378-7753(01)00495-5

AICEP. (2021). *ZILS Características*. AICEP Global Parques. https://globalparques.pt/zils/zils-caracteristicas/

Amerini, G. (2008). Short Sea Shipping of goods 2000-2006. In *Statistics*. https://ec.europa.eu/eurostat/statistics-explained/index.php?title=Maritime_transport_statistics_-_short_sea_shipping_of_goods

Andersson, J., & Grönkvist, S. (2019). Large-scale storage of hydrogen. In *International Journal of Hydrogen Energy* (Vol. 44, Issue 23, pp. 11901–11919). Elsevier Ltd. https://doi.org/10.1016/j.ijhydene.2019.03.063

Argus. (2020). *Crises may push down VLSFO and HSFO prices even further*. Lloyd's List. https://lloydslist.maritimeintelligence.informa.com/LL1131755/Crises-may-push-down-VLSFO-and-HSFO-prices-even-further

Arutyunov, V. S., & Lisichkin, G. V. (2017). Energy resources of the 21st century: problems and forecasts. Can renewable energy sources replace fossil fuels? *Russian Chemical Reviews*, *86*(8), 777–804. https://doi.org/10.1070/rcr4723

Başer, S. Ö., & Açık, A. (2018). Efficiency in Dirty Tanker Market. *Journal of ETA Maritime Science*, *6*(3), 275–287. https://doi.org/10.5505/jems.2018.17136

Benndorf, R., Bernicke, M., Bertram, A., Butz, W., Dettling, F., Drotleff, J., Elsner, C., Fee, E., Gabler, C., Galander, C., Hargita, Y., Herbener, R., Hermann, T., Jäger, F., Kanthak, J., Kessler, H., Koch, Y., Kuntze, D., Lambrecht, M., … Zietlow, B. (2014). *Germany in 2050-a greenhouse gas-neutral country*. http://www.umweltbundesamt.de/publikationen/germany-in-2050-a-greenhouse-gas-neutral-

Bento, A. M. (2020). *Qual é a melhor opção para Portugal: hidrogénio verde ou azul?* Capital Verde. https://eco.sapo.pt/especiais/qual-e-a-melhor-opcao-para-portugal-hidrogenio-verde-ou-azul/

Blok, K., & Nieuwlaar, E. (2017). Introduction to Energy Analysis. In *Nature* (Second, Vol. 1, Issue 26). Earthscan. https://doi.org/10.1038/001647a0

Bradley, D., Diesenreiter, F., Wild, M., & Tromborg, E. (2009). World Biofuel Maritime Shipping Study. *IEA Bioenergy Task*, *40*, 1–45. https://www.researchgate.net/publication/235704249_World_Biofuel_Maritime_Shippi ng_Study

Brazier, G. (2021). 'Market information.' In *Insider Dealing* (pp. 179–184). https://doi.org/10.4324/9781843142270-39

Britannica, T. (2019). *Tonnage.* Encyclopedia Britannica. https://www.britannica.com/technology/tonnage

Brouer, B. D., Alvarez, J. F., Plum, C. E. M., Pisinger, D., & Sigurd, M. M. (2014). A base integer programming model and benchmark suite for liner-shipping network design. *Transportation Science*, *48*(2), 281–312. https://doi.org/10.1287/trsc.2013.0471

Brynolf, S., Taljegard, M., Grahn, M., & Hansson, J. (2018). Electrofuels for the transport sector: A review of production costs. In *Renewable and Sustainable Energy Reviews* (Vol. 81, pp. 1887–1905). Elsevier Ltd. https://doi.org/10.1016/j.rser.2017.05.288

Carvalho, M. (2021). *Liquid Organic Hydrogen Carriers (LOHCs): A review and techno-economic analysis*. *April*.

Carvalho, M., Braz, C., Marques, J., Matos, H., & Granjo, J. (2021). LONG-DISTANCE HYDROGEN DELIVERY WITH A DIBENZYLTOLUENE-BASED LIQUID ORGANIC HYDROGEN CARRIER SYSTEM. *Instituto Superior Técnico, Universidade de Lisboa*, 1–50.

Cavaco, A., Silva, H., Canhoto, P., Neves, S., Neto, J., Collares Pereira, M., & Monteiro, A. (2016). *Radiação Solar Global em Portugal e a sua variabilidade, mensal e anual*. http://www.ipes.pt/ipes/wp-content/uploads/2017/10/Radiação-Solar-Global-em-Portugal-e-a-sua-variabilidade.pdf

Céu, N. (2021). Central fecha em Sines. "Que garantissem o trabalho, tudo menos o desemprego". *Diário de Notícias*. https://www.dn.pt/sociedade/central-fecha-em-sines-que-garantissem-o-trabalho-tudo-menos-o-desemprego-13223929.html

CHIYODA CORPORATION. (2013). *Chiyoda Verified "Large-Scale Hydrogen Storage and Transportation System."* https://www.chiyodacorp.com/en/media/2013/post-77.html

Dawood, F., Anda, M., & Shafiullah, G. M. (2020). Hydrogen production for energy: An overview. In *International Journal of Hydrogen Energy* (Vol. 45, Issue 7, pp. 3847–3869). Elsevier Ltd. https://doi.org/10.1016/j.ijhydene.2019.12.059

Dehghani-Sanij, A. R., Tharumalingam, E., Dusseault, M. B., & Fraser, R. (2019). Study of energy storage systems and environmental challenges of batteries. In *Renewable and Sustainable Energy Reviews* (Vol. 104, pp. 192–208). Elsevier Ltd. https://doi.org/10.1016/j.rser.2019.01.023

Detz, R. J., Lenzmann, F. O., & Weeda, M. (2019). *Future Role of Hydrogen in the Netherlands: A meta-analysis based on a review of recent scenario studies*. 36. www.tno.nl

DGEG. (2019). Plano Nacional Energia e Clima 2021-2030 (PNEC 2030). In *Relatório Técnico* (p. 200). https://apambiente.pt/_zdata/Alteracoes_Climaticas/Mitigacao/PNEC/PNEC PT_Template Final 2019 30122019.pdf

DGES. (2019). *Roteiro e plano de ação para o hidrogénio em portugal*.

Dogan, B., & Erol, D. (2019, October 1). The Future of Fossil and Alternative Fuels Used in Automotive Industry. *3rd International Symposium on Multidisciplinary Studies and Innovative Technologies, ISMSIT 2019 - Proceedings*. https://doi.org/10.1109/ISMSIT.2019.8932925

Domingos, T. (2013). *Terminal XXI - Porto de Sines*. https://es.slideshare.net/Tania_Domingos/terminal-xxi-porto-de-sines/3

Durand, B. (2018). Petroleum, natural gas and coal. Les Ulis. *EDP Sciences*. https://doi.org/https://doi.org/10.1051/978-2-7598-2232-4

European Comission. (2018). *Hydrogen Supply and Transportation using liquid Organic Hydrogen Carriers | HySTOC Project | H2020 | CORDIS*. 2–5. https://cordis.europa.eu/project/id/779694

European Commission. (2018). A Clean Planet for all. A European long-term strategic vision for a prosperous, modern, competitive and climate neutral economy. *COM(2018) 773*, 25. https://eur-lex.europa.eu/legal-content/EN/TXT/PDF/?uri=CELEX:52018DC0773&from=EN

European Commission. (2019). *EUR-Lex - 52019DC0640 - EN - EUR-Lex*. https://eur-lex.europa.eu/legal-content/EN/TXT/?qid=1596443911913&uri=CELEX:52019DC0640#document2

European Commission. (2020a). A hydrogen strategy for a climate-neutral Europe. In *Communication from the commission to the European Parliament, the Council, the European Economic and Social Committee and the Committee of the Regions*. https://www.eu2018.at/calendar-events/political-events/BMNT-

European Commission. (2020b). *European Clean Hydrogen Alliance | Internal Market, Industry, Entrepreneurship and SMEs*. 1–2. https://ec.europa.eu/growth/industry/policy/european-clean-hydrogen-alliance_en

European Commission. (2020c). *Hydrogenious LOHC Technologies GmbH | FUTURIUM |*. https://ec.europa.eu/futurium/en/tech-society-2020/hydrogenious-lohc-technologies-gmbh

Commission Delegated Regulation (EU) 2021/4987, EUR-Lex - Access to European Law 60 (2021). https://ec.europa.eu/info/law/sustainable-finance-taxonomy-regulation-eu-

EuropeanCouncil. (2018). *2030 climate & energy framework | Climate Action*. 2030 Climate & Energy Framework. https://ec.europa.eu/clima/policies/strategies/2030_en

Eypasch, M., Schimpe, M., Kanwar, A., Hartmann, T., Herzog, S., Frank, T., & Hamacher, T. (2017). Model-based techno-economic evaluation of an electricity storage system based on Liquid Organic Hydrogen Carriers. *Applied Energy*, *185*, 320–330. https://doi.org/10.1016/j.apenergy.2016.10.068

Foran, J. (2016). The Paris agreement scam. In *Nation* (Vol. 302, Issue 6). https://unfccc.int/process-and-meetings/the-paris-agreement/the-paris-agreement

Fruchart, D. (2013). *Hydrogen Storage*. Energy Storage. https://doi.org/10.1002/9781118557808.ch5

Gahleitner, G. (2013). Hydrogen from renewable electricity: An international review of power-to-gas pilot plants for stationary applications. In *International Journal of Hydrogen Energy* (Vol. 38, Issue 5, pp. 2039–2061). Elsevier Ltd. https://doi.org/10.1016/j.ijhydene.2012.12.010

Gigler, J., & Marcel, W. (2018). Outlines of a Hydrogen Roadmap. *TKI Nieuw Gas*, 1–105. https://www.topsectorenergie.nl/sites/default/files/uploads/TKI Gas/publicaties/20180514 Roadmap Hydrogen TKI Nieuw Gas May 2018.pdf

Government of Netherlands. (2020). *Portugal and the Netherlands strengthen bilateral cooperation on green hydrogen*. https://www.government.nl/latest/news/2020/09/23/portugal-and-the-netherlands-strengthen-bilateral-cooperation-on-green-hydrogen

Gretz, J., Baselt, J. P., Ullmann, O., & Wendt, H. (1990). The 100 MW euro-Quebec hydro-hydrogen pilot project. *International Journal of Hydrogen Energy*, *15*(6), 419–424. https://doi.org/10.1016/0360-3199(90)90199-9

Helgason, R., Cook, D., & Davíðsdóttir, B. (2020). An evaluation of the cost-competitiveness of maritime fuels – a comparison of heavy fuel oil and methanol (renewable and natural gas) in Iceland. *Sustainable Production and Consumption*, *23*, 236–248.

Hellenic Shipping News. (2017). *Tanker shipping: A strong season lifts crude oil tankers before it is expected to hit the fan in 2017*. http://www.bunkerportsnews.com/News.aspx?ElementId=81b15a88-47cb-4379-a07e-cbf77f6402e9

Hellenic Shipping News. (2021). *'Sky's the limit' for already lofty container-ship charter rates*. International Shipping News. https://www.hellenicshippingnews.com/skys-the-limit-for-already-lofty-container-ship-charter-rates/

IEA. (2021). *The Netherlands - Countries & Regions*. https://www.iea.org/countries/the-netherlands

Insights Global. (2019). *Outlook for European Tank Terminal Sector*. www.insights-global.com

Insights Global. (2021). *INSIGHTS GLOBAL GLOBAL OIL STORAGE RATE SAMPLE REPORT COPYRIGHTS GLOBAL TANK STORAGE RATE REPORT*. www.insights-global.com

IRENA. (2020). *Innovation Outlook: Thermal Energy Storage, International Renewable Energy Agency, Abu Dhabi [Online].* www.irena.org

Jalkanen, J. P., Brink, A., Kalli, J., Pettersson, H., Kukkonen, J., & Stipa, T. (2009). A modelling system for the exhaust emissions of marine traffic and its application in the Baltic Sea area. *Atmospheric Chemistry and Physics*, *9*(23), 9209–9223. https://doi.org/10.5194/acp-9-9209-2009

Jonas, J., Hasha, D., & Huang, S. G. (2008). Self-diffusion and viscosity of methylcyclohexane in the dense liquid region. *Journal of Chemical Physics*, *71*(10), 3996–4000. https://doi.org/10.1063/1.438155

Jorschick, H., Geißelbrecht, M., Eßl, M., Preuster, P., Bösmann, A., & Wasserscheid, P. (2020). Benzyltoluene/dibenzyltoluene-based mixtures as suitable liquid organic hydrogen carrier systems for low temperature applications. *International Journal of Hydrogen Energy*, *45*(29), 14897–14906. https://doi.org/10.1016/j.ijhydene.2020.03.210

Kitous, A., Criqui, P., Bellevrat, E., & Chateau, B. (2010). Transformation patterns of the worldwide energy system - Scenarios for the century with the POLES model. *Energy Journal*, *31*(SPECIAL ISSUE), 49–82. https://doi.org/10.5547/issn0195-6574-ej-vol31-nosi-3

Knoema. (2021). *Natural Gas Price Forecast: 2020, 2021 and Long Term to 2030*. https://knoema.com/infographics/ncszerf/natural-gas-price-forecast-2021-2022-and-long-term-to-2050

Kolesnikov, I. (2014). *Crude Oil Price Forecast: Long Term to 2025 | Data and Charts*.

https://knoema.com/infographics/yxptpab/crude-oil-price-forecast-2021-2022-and-long-term-to-2050

Krasae-in, S., Stang, J. H., & Neksa, P. (2010). Development of large-scale hydrogen liquefaction processes from 1898 to 2009. In *International Journal of Hydrogen Energy* (Vol. 35, Issue 10, pp. 4524–4533). Pergamon. https://doi.org/10.1016/j.ijhydene.2010.02.109

Krauss, C., Fernandez, M., Penn, I., & Rojas, R. (2021). Texas Power Grid Run by ERCOT Set Up the State for Disaster. *The New York Times*. https://www.nytimes.com/2021/02/21/us/texas-electricity-ercot-blackouts.html

Lanphen, S. (2019). *Hydrogen Import Terminal*. 126.

Leal, P. C. (2020). *Influence of Increasing Renewable Power Penetration on the Future Electricity Spot Prices*. *December*.

Li, C. H., Zhu, X. J., Cao, G. Y., Sui, S., & Hu, M. R. (2009). Dynamic modeling and sizing optimization of stand-alone photovoltaic power systems using hybrid energy storage technology. *Renewable Energy*, *34*(3), 815–826. https://doi.org/10.1016/j.renene.2008.04.018

Liang, L. H. (2021). *Rotterdam makes moderate 1% increase in port tariffs for 2021*. https://www.seatrade-maritime.com/ports-logistics/rotterdam-makes-moderate-1-increase-port-tariffs-2021

Luckow, P. (2016). *Synapse's 2016 CO2 Price Forecast Is Out*. Synapse - Energy Economics, Inc. https://www.synapse-energy.com/about-us/blog/synapse's-2016-co2-price-forecast-out

Mayur Agarwal. (2021). *Fuel Oil Consumption Calculations For Ships: What Seafarers Should Know*. Marine Insight. https://www.marineinsight.com/guidelines/fuel-oil-consumption-calculations-for-ships-what-seafarers-should-know/

McDonald, R. I., Green, P., Balk, D., Fekete, B. M., Revenga, C., Todd, M., & Montgomery, M. (2011). Urban growth, climate change, and freshwater availability. *Proceedings of the National Academy of Sciences of the United States of America*, *108*(15), 6312–6317. https://doi.org/10.1073/pnas.1011615108

Meadows, D., Vis, P., & Zapfel, P. (2019). The eu emissions trading system. In *Towards a Climate-Neutral Europe: Curbing the Trend* (pp. 66–94). https://doi.org/10.4324/9789276082569-4

Merikas, A., Merika, A., & Penikas, H. (2013). Dry bulk time charter rates joint return distribution modeling: Copula-approach. *Procedia Computer Science*, *17*, 1125–1133. https://doi.org/10.1016/j.procs.2013.05.144

Minister of Environment and Climate Action of the Portuguese Republic, & Minister of Economic Affairs and Climate Policy of the Netherlands. (2020). *Memorandum of Understanding in the field of Energy - Hydrogen*.

Modisha, P., Gqogqa, P., Garidzirai, R., Ouma, C. N. M., & Bessarabov, D. (2019). Evaluation of catalyst activity for release of hydrogen from liquid organic hydrogen carriers. *International Journal of Hydrogen Energy*, *44*(39), 21926–21935. https://doi.org/10.1016/j.ijhydene.2019.06.212

Mover DB. (2020). *The Largest Seaport In Europe: Port of Rotterdam Map*. https://moverdb.com/port-of-rotterdam/

Müller, B., Müller, K., Teichmann, D., & Arlt, W. (2011). Energiespeicherung mittels Methan und energietragenden Stoffen ein thermodynamischer Vergleich. *Chemie-Ingenieur-Technik*, *83*(11), 2002–2013. https://doi.org/10.1002/cite.201100113

Naterer, G. F., Jaber, O., & Dincer, I. (2010). Environmental Impact Comparison of Steam Methane Ref- ormation and Thermochemical Processes of Hydrogen Pro- duction Environmental Impact Comparison of Steam Methane Reformation and Thermochemical Processes of Hydrogen Production. *Essen Schriften Des Forschungszentrums Jülich / Energy & Environment*, *78*. http://juser.fz-juelich.de/record/135464/files/HP4a_3_Naterer_rev0601.pdf

Niermann, M., Beckendorff, A., Kaltschmitt, M., & Bonhoff, K. (2019). Liquid Organic Hydrogen Carrier (LOHC) – Assessment based on chemical and economic properties. *International Journal of Hydrogen Energy*, *44*(13), 6631–6654. https://doi.org/10.1016/j.ijhydene.2019.01.199

Parliament, E., Union, E., & Vienna, C. A. (2019). *Integrated National Energy and Climate Plan for Austria*. 268.

Port of Rotterdam. (2020). *Port of Rotterdam Becomes Internation Hydrogen Hub - Vision Port of Rotterdam Authority*.

Porto de Sines. (2021a). *Características Gerais*. http://www.portodesines.pt/o-porto/características-gerais/

Porto de Sines. (2021b). *Concessão do terminal de granéis líquidos e da gestão integrada de resíduos do porto de Sines*. Companhia Logística de Terminais Marítimos S.A. http://www.portodesines.pt/media/3663/tarifário-do-concessionário-do-tgls-e-gru-2021-clt.pdf

Porto de Sines. (2021c). *Localização*. http://www.portodesines.pt/o-porto/localização/

PPIAF. (2007). *Glossary of Port and Shipping terms*. 365–376. https://ppiaf.org/sites/ppiaf.org/files/documents/toolkits/Portoolkit/Toolkit/pdf/modules/09_TOOLKIT_Glossary.pdf

PubChem Database. (2017a). *Methylcyclohexane | C6H11CH3 - PubChem*. National Center for Biotechnology Information. https://pubchem.ncbi.nlm.nih.gov/compound/7962

PubChem Database. (2017b). toluene _ C6H5CH3 - PubChem. In *National Center for Biotechnology Information*. https://pubchem.ncbi.nlm.nih.gov/compound/Toluene

PubChem Database. (2018). *Perhydrodibenzo[a,i]fluorene | C21H34 - PubChem*. National Center for Biotechnology Information. https://pubchem.ncbi.nlm.nih.gov/compound/282804

PubChem Database. (2020). *2,3-Dibenzyltoluene | C21H20 - PubChem*. National Center for Biotechnology Information. https://pubchem.ncbi.nlm.nih.gov/compound/3034397

Reuß, M., Grube, T., Robinius, M., Preuster, P., Wasserscheid, P., & Stolten, D. (2017). Seasonal storage and alternative carriers: A flexible hydrogen supply chain model. *Applied Energy*, *200*, 290–302. https://doi.org/10.1016/j.apenergy.2017.05.050

Rijksoverheid. (2020). Government Strategy on Hydrogen. *Report*, *387*, 1–14. https://www.government.nl/documents/publications/2020/04/06/government-strategy-on-hydrogen

Samuels, M. (2021). General Terms and Conditions. In *Commercial Contracts for UK Companies: Formation to Exit* (p. 40). https://doi.org/10.5040/9781526511980.precedent6

Sand, P. (2020). *Tanker shipping: sky high freight rates replaced by reality of falling global oil demand*. BIMCO. https://www.bimco.org/news/market_analysis/2020/20200525_tanker_shipping

Santos, F. J. V., Nieto De Castro, C. A., Dymond, J. H., Dalaouti, N. K., Assael, M. J., & Nagashima, A. (2006). Standard reference data for the viscosity of toluene. *Journal of Physical and Chemical Reference Data*, *35*(1), 1–8. https://doi.org/10.1063/1.1928233

Satterthwaite, D. (2009). The implications of population growth and urbanization for climate change. *Environment and Urbanization*, *21*(2), 545–567. https://doi.org/10.1177/0956247809344361

Sbraga, A., & Malpas, J. (2020). *Inclusion of Shipping Industry in the EU Emissions Trading System: Current Landscape, Perspective and Potential Impact*. HFW - Shipping. https://www.hfw.com/Inclusion-of-shipping-in-the-EU-Emissions-Trading-System-current-landscape-perspective-and-potential-impact

Sharples, J. (2019). LNG as a Shipping Fuel in Northern Fuel. *LNG as a Shipping Fuel in Northern Fuel*. https://globalmaritimehub.com/report-presentation/lng-as-a-shipping-fuel-in-northern-europe

Shell. (2018). *Shell Scenarios: Sky - Meeting the goals of the Paris agreement*. 72. https://www.shell.com/promos/meeting-the-goals-of-the-paris-agreement/_jcr_content.stream/1521983847468/5f624b9260ef2625f319558cbb652f8b23d331933439435d7a0fc7003f346f94/shell-scenarios-sky.pdf

Sherif, S. A., Barbir, F., & Veziroglu, T. N. (2005). Wind energy and the hydrogen economy-review of the technology. *Solar Energy*, *78*(5), 647–660. https://doi.org/10.1016/j.solener.2005.01.002

Ship Technology. (2019). *Port of Rotterdam*. https://www.ship-technology.com/projects/portofrotterdam/

Stopford, M. (2013). Maritime Economics. In *Maritime Economics*. https://doi.org/10.4324/9780203442661

Sugawara, E., & Nikaido, H. (2014). Properties of AdeABC and AdeIJK efflux systems of Acinetobacter baumannii compared with those of the AcrAB-TolC system of Escherichia coli. *Antimicrobial Agents and Chemotherapy*, *58*(12), 7250–7257. https://doi.org/10.1128/AAC.03728-14

Teichmann, D., Arlt, W., & Wasserscheid, P. (2012). Liquid Organic Hydrogen Carriers as an efficient vector for the transport and storage of renewable energy. *International Journal of Hydrogen Energy*, *37*(23), 18118–18132. https://doi.org/10.1016/j.ijhydene.2012.08.066

Teichmann, D., Stark, K., Müller, K., Zöttl, G., Wasserscheid, P., & Arlt, W. (2012). Energy storage in residential and commercial buildings via Liquid Organic Hydrogen Carriers (LOHC). *Energy and Environmental Science*, *5*(10), 9044–9054. https://doi.org/10.1039/c2ee22070a

Tso, W. W., Demirhan, C. D., Lee, S., Song, H., Powell, J. B., & Pistikopoulos, E. N. (2019). Energy

Carrier Supply Chain Optimization: A Texas Case Study. *Computer Aided Chemical Engineering*, *47*, 1–6. https://doi.org/10.1016/B978-0-12-818597-1.50001-1

U.S. Energy Information Administration. (2014). Oil Tanker Sizes Range from General Purpose to Ultra-Large Crude Carriers on Afra Scale. In *U.S. Energy Information Administration*. https://www.eia.gov/todayinenergy/detail.php?id=17991

Wada, Y., Yamamura, T., Hamada, K., & Wanaka, S. (2021). Evaluation of ghg emission measures based on shipping and shipbuilding market forecasting. *Sustainability (Switzerland)*, *13*(5), 1–23. https://doi.org/10.3390/su13052760

Xing, H., Stuart, C., Spence, S., & Chen, H. (2021). Alternative fuel options for low carbon maritime transportation: Pathways to 2050. *Journal of Cleaner Production*, *297*, 126651. https://doi.org/10.1016/j.jclepro.2021.126651

Zhang, C., Wei, Y. L., Cao, P. F., & Lin, M. C. (2018). Energy storage system: Current studies on batteries and power condition system. In *Renewable and Sustainable Energy Reviews* (Vol. 82, pp. 3091–3106). Elsevier Ltd. https://doi.org/10.1016/j.rser.2017.10.030